Fakultät für Medizin

Combining Oncolytic Virotherapy with Target Therapy in Bladder Cancer

Jana Annika Koch

Vollständiger Abdruck der von der Fakultät für Medizin der Technischen Universität München zur Erlangung des akademischen Grades einer
Doktorin der Naturwissenschaften (Dr. rer. nat.)
genehmigten Dissertation.

Vorsitz: Prof. Dr. Andreas Pichlmair, PhD
Prüfer der Dissertation:
1: Priv.-Doz. Dr. Roman Nawroth
2: Prof. Dr. Michael Sattler

Die Dissertation wurde am 24.06.2021 bei der Fakultät für Medizin der Technischen Universität München eingereicht und durch die Fakultät für Medizin am 12.10.2021 angenommen.

"In biology, nothing is clear, everything is too complicated, everything is a mess, and just when you think you understand something, you peel off a layer and find deeper complications beneath.
Nature is anything but simple."
Richard Preston

Abstract

The aim of this study was to improve oncolytic virotherapy in BC by combining the oncolytic Adenovirus XVir-N-31 with small molecule inhibitors (target therapy) and to examine the molecular mechanisms underlying these combination therapies.

It was shown before that the Chk1 inhibitor UCN-01 could enhance the effects of oncolytic virotherapy by ingreasing cellular DNA damage and viral over-replication thereby leading to enhanced cytotoxicity in the combination therapy [21]. Based on these results, we combined the two Chk1 inhibitors UCN-01 and AZD7762 with XVir-N-31 to see whether these combinations could also improve virus induced cell death in BC. Analysis of cell viability upon combination with Chk1 inhibitors showed that UCN-01 but not AZD7762 could enhance virus induced cell death in BC cell lines. Molecular analysis of the mechanism responsible for these differences revealed that the enhanced virus induced cell death upon combination with UCN-01 was probably due to the effects of UCN-01 on cell cycle arrest in G1-phase and downregulation of Rb and pRb expression which were associated with the inhibition of other targets such as CDK4/6 [2]. AZD7762 in contrast, did not arrest cells in G1-phase nor affect Rb or pRb expression.

In a next step, we combined the specific CDK4/6 inhibitors palbociclib (PD-0332991), abemaciclib (LY-2835219) or ribociclib (LEE011) with XVir-N-31. Interestingly, CDK4/6 inhibitors which are known to arrest cells in G1-phase and to downregulate Rb, pRb, and E2F1 expression greatly improved oncolytic virotherapy leading to enhanced virus induced cell death, viral replication, and viral particle formation. So far, it is well established that Adenoviruses rely on the cellular transcription factor E2F1 and S-phase induction for proper DNA replication. Thus, in contrast to the common view G1-arrest as well as downregulation of E2F1 were associated with increased viral replication upon combination with CDK4/6 inhibition in this study.

In the following, we investigated the molecular mechanisms underlying the combination therapy with CDK4/6 inhibitors. Here we showed that CDK4/6 inhibition could only enhance oncolytc virotherapy in Rb positive but not in Rb negative cell lines which are resistant to CDK4/6 inhibition [26, 47]. Furthermore, viral replication was enhanced upon siRNA mediated knockdown of E2F1 although the enhanced effects upon CDK4/6 inhibition were not solely attributable to downregulation of E2F1. In addition, we analysed the effects of CDK4/6 inhibition on viral protein and gene expression using different viral mutants. Theses results showed that CDK4/6 inhibition greatly enhanced viral protein and gene expression independent of the viral E1 region nor the two E2F1 binding sites in the viral E2 early promoter.

In summary, our results showed that CDK4/6 inhibition greatly enhanced oncolytic virotherapy thereby providing a new therapy approach for patients with BC and probably also other malignancies. Additionally, our data showed that viral replication was enhanced upon G1-arrest and E2F1 downregulation which is in stark contrast to what has been shown before. Thus, we do not only provide evidence for a rational to improve oncolytic virotherapy in combination with CDK4/6 inhibitors but also shed light into the mechanisms of Adenovirus biology and replication which in previous studies have not been investigated that deeply.

Kurzfassung

Ziel dieser Arbeit war die Entwicklung einer Kombinationstherapie zur Verbesserung einer onkolytischen Virotherapie im Blasenkarzinom. Hierzu wurde das onkolytische Adenovirus XVir-N-31 mit small molecule Inhibitoren kombiniert und die molekularen Mechanismen, die diesen Kombinationstherapien zugrunde liegen, untersucht.

Es wurde bereits gezeigt, dass der Chk1 Inhibitor UCN-01 durch eine erhöhte zelluläre DNA Beschädigung sowie eine vermehrte virale Überreplikation zu einer verstärkten Zytotoxizität führen und somit die Effekte einer onkolytischen Virotherapie verbessern kann [21]. Basierend auf diesen Ergebnissen kombinierten wir die Chk1 Inhibitoren UCN-01 und AZD7762 mit XVir-N-31, um zu sehen, ob diese Kombinationen den Virus-induzierten Zelltod auch im Blasenkarzinom verbessern könnten. Die Analyse der Zellviabilität in Kombination mit Chk1 Inhibitoren zeigte, dass UCN-01, aber nicht AZD7762, den Virus-induzierten Zelltod in Blasenkarzinomzelllinien verbessern konnte. Die molekulare Analyse der zugrunde liegenden Mechanismen für diese Unterschiede zeigte, dass der verbesserte Virus-induzierten Zelltod in Kombination mit UCN-01 vermutlich auf die durch UCN-01 hervorgerufene Inhibitierung des Zellzyklus in der G1-Phase sowie der Herunterregulation von Rb und pRb zurück zu führen war. Diese Effekte waren bereits zuvor mit der Inhibition von anderen Molekülen, wie CDK4/6, assoziiert worden [2]. AZD7762 dagegen zeigte weder Effekte auf den Zellzyklus, noch auf die Rb und pRb Expression.

In einem nächsten Schritt kombinierten wir die spezifischen CDK4/6 Inhibitoren Palbociclib (PD-0332991), Abemaciclib (LY-2835219) oder Ribociclib (LEE011) mit XVir-N-31. Interessanterweise konnten CDK4/6 Inhibitoren, die zu einem G1-Arrest des Zellzyklus und zu einer Herunterregulation der Rb, pRb und E2F1 Expression führten, die onkolytische Virotherapie deutlich verbessern, was mit einem erhöhten Virus-induziertem Zelltod und damit einhergehender verbesserter viraler Replikation und Partikelbildung assoziiert war. Nach bisherigem Wissensstand jedoch, benötigen Adenoviren den zellulären Transkriptionsfaktor E2F1 sowie die Induktion der S-Phase für eine erfolgreiche DNA Replikation. Dennoch war in dieser Arbeit, im Gegensatz zum bisherigen Wissensstand, ein G1-Arrest des Zellzyklus und eine Herunterregulation der E2F1 Expression durch CDK4/6 Inhibitoren mit einer deutlich verbesserten Replikation assoziiert.

Im Folgenden wurde der zugrunde liegende molekulare Mechanismus der Kombinationstherapie mit CDK4/6 Inhibitoren untersucht. Dabei konnten wir zeigen, dass CDK4/6 Inhibitoren die Effekte der onkolytischen Virotherapie nur in Rb positiven und nicht in Rb negativen Zellen, welche resistent gegen CDK4/6 Inhibition sind, verbessern konnten [26, 47]. Des Weiteren konnte die virale Replikation durch eine siRNA vermittelte Herunterregulation von E2F1 verbessert werden, wenn auch die Effekte in Kombination mit CDK4/6 Inhibitoren nicht auf die alleinige Herunterregulation von E2F1 zurück geführt werden konnten. Als nächstes analysierten wir, mittels verschiedener Virusmutanten, die Effekte von CDK4/6 Inhibition auf die virale Gen- und Proteinexpression. Diese Ergebnisse zeigten, dass CDK4/6 Inhibitoren die virale Gen- und Proteinexpression deutlich erhöhten, unabhängig von der viralen E1-Region oder den E2F1 Bindestellen im viralen E2 early Promoter.

Zusammenfassend zeigten unsere Ergebnisse, dass CDK4/6 Inhibitoren die onkolytische Virotherapie deutlich verbessern konnten, was als Anhaltspunkt für einen neuen Therapieansatz für Patienten mit Blasenkarzinom, und vermutlich auch anderen Tumoren, gesehen werden kann. Des Weiteren zeigten unsere Daten, dass die virale Replikation in G1-arretierten Zellen mit herunterregulierter E2F1 Expression verbessert wird. Dies steht in starkem Gegensatz zu dem, was in früheren Studien gezeigt wurde. Aus diesem Grund liefern unsere Ergebnisse nicht nur die Grundlage für einen neuen Therapieansatz zur Kombination von onkolytischen Viren mit

CDK4/6 Inhibitoren, sondern tragen auch zu einem besseren Verständnis der Adenovirusbiologie und der viralen Replikation bei, was in bisherigen Studien nicht in dieser Tiefe analysiert wurde.

Acknowledgements

This thesis would not have been possible without the help of many people. First and foremost, I would like to thank Prof. Dr. Gschwend for giving me the great opportunity to work in the department of Molecular Uro-Oncology. Many thanks also to Prof. Dr. Sattler for his support in my thesis committee.

I would like to express my sincere gratitute to my thesis supervisor PD Dr. Roman Nawroth for giving me the opportunity to perform this very interesting and promising project in his group. Without his great supervision and all the helpful comments and advises, this project would not have been possible. His well planned and prescient manner as well as his thoroughly analysis of scientific questions helped me to learn a lot about troubleshooting, scientific methodology, and the critical thinking and analysis of data. I am very thankful for the many discussions we had which widened my scientific horizon immensely. He has been an excellent mentor who was always approachable for the planning and discussion of my work. I am very grateful that he always encouraged me to think objectively and independently, to generate scientific hypotheses, and to help me in planning experiments to proof these hypotheses. Thank you for all the support and opportunities you gave me.

I extend my gratitude to Prof. Dr. Per Sonne Holm for all his helpful advises, comments, and interesting discussions which widened my scientific horizon immensely. Through him, I gained deep insights into the very interesting field of Adenovirus biology and oncolytic virotherapy for which I am very thankful.

Moreover, I would like to thank the DFG for financial support of this project.

I would also like to thank Pan Qi, Eva Lichtenegger, and Lisa Kreutzer for their experimental support. Many thanks also to Judith Schäfers and Klaus Mantwill for their excellent technical assistance, their helpful advices, and useful discussions. I extend my regards to all the past and present members of the AG Nawroth and AG Holm. The atmosphere in the lab has always been very friendly and co-operative thus making it an excellent place to work.

Lastly, I want to thank my family, especially my parents and Peter, for all their love and support and for always encouraging me to pursue my goals. Thank you for always beeing there for me.

Contents

List of Abbreviations

aa	Amino acid
AB	Antibody
ADP	Adenovirus death protein
AdV	Adenovirus
APS	Ammonium persulfate
ATF	Activating transcription factor
ATM	Ataxia telangiectesia mutated
ATR	ATM and Rad3 related
BC	Bladder cancer
BCG	Bacillus Calmette-Guerin
bcl-2	B-cell lymphoma 2
bp	Base pair
BSA	Bovine serum albumin
CaCl	Calcium chloride
CAR	Coxsackie adenovirus receptor
Cdc25 A/B/C	Cell division cycle 25 A/B/C
CDK	Cyclin-dependent kinase
Chk 1/2	Checkpoint kinase 1/2
CI	Combination index
CIS	Carcinoma in situ
CMV	Cytomegalie virus
CPE	Cytopathic effect
CR	Conserved region
CRAd	Conditionally-replicative Adenovirus
CTLA4	Cytotoxic T-lymphocyte associated protein 4
Ctrl	Control
$\triangle 24$	24 nucleotide deletion in CR2 domain of E1A region
DAB	3,3-Diaminobenzidine
dai	Day(s) antes (before) infection
DBP	DNA binding protein
dH_2O	Distilled water
DMEM	Dulbecco's modified eagle's medium
DMSO	Dimethylsulfoxid
DNA	Deoxyribonucleic acid
dNTP	Deoxynucleoside triphosphate
dpi	Day(s) post infection
ds	Double-strand
DTT	Dithiothreitol
ECL	Enhanced chemiluminescent substrate
EDTA	Ethylenediaminetetraacetic acid
EGFP	Enhanced green fluorescent protein

EMSA	Electrophoretic mobility shift assay
EtOH	Ethanol
FBS	Fetal bovine serum
FDA	Food and Drugs Administration
FISH	Fluorescence in situ hybridisation
5-FU	5-Fluorouracil
fw	Forwards
GAPDH	Glyceraldehyde 3-phosphate dehydrogenase
GFP	Green fluorescent protein
GM-CSF	Granulocyte-macrophage colony-stimulating factor
H_2O	Water
H_2O_2	Hydrogen peroxide
hai	Hour(s) antes (before) infection
HCl	Hydrochloric acid
HER2	Human epidermal growth factor receptor 2
hpi	Hour(s) post infection
HRP	Horseradish peroxidase
HSV	Herpes simplex virus
IFU	Infectious units
IgG	Immune globulin G
IHC	Immuno-histo-chemistry
IP	Immuno-precipitation
IVE	Intravesical
kb	Kilobase
KCl	Potassium chloride
kDa	Kilo Dalton
LEE	LEE011
LY	LY2835219
MDM2	Mouse double minute 2 homologue
MDR1	Multi drug resistance gene 1
MgCl	Magnesium chloride
MGMT	O-6-methylguanine-DNA methyltransferase
MHCI	Major histocompatibility complex I
MIBC	Muscle invasive bladder cancer
ml	Millilitre
MLP	Major late promoter
MOI	Multiplicity of infection
mRNA	Messenger ribonucleic acid
MRP1	Multi drug resistance associated protein 1
mTOR	Mammalian target of rapamycin
μl	Microlitre
NaCl	Sodium chloride

NEAA	Non-essential amino acids
nm	Nanometre
NMIBC	Non-muscle invasive bladder cancer
NMP22	Nuclear mitotic apparatus protein 22
PBS	Phosphate buffered saline
PCR	Polymerase chain reaction
PD	PD-0332991
PD-1	Programmed cell death protein 1
PD-L1	Programmed cell death ligand 1
PP2A	Protein phosphatase 2A
pRb	Phospho retinoblastoma protein
PS	Penicillin Streptomycin
PVDF	Polyvinylidene difluoride
qPCR	quantitative PCR
Rb	Retinoblastoma protein
rcf	Relative centrifugal force
rev	Reverse
RGD	Arginyl-glycyl-aspartic acid
RNA	Ribonucleic acid
rpm	Rotations per minute
RPMI	Roswell park memorial institute medium
RSV	Respiratory syncytial virus
RT	Room temperature, Reverse transcription
S.D.	Standard deviation
SDS	Sodium dodecyl sulfate
S.E.	Standard error
Ser	Serin
SI	Single instillation
SRB	Sulforhodamine B
TBP	TATA-Box binding protein
TCA	Trichloroacetic acid
TE	Tris-EDTA
TEMED	Tetramethylethylenediamine
TMZ	Temozolomide
TNF-α	Tumour-necrosis factor alpha
TNM	Tumour-node-metastases
TURB	Transurethral resection of bladder tumours
WB	Westernblot
WT	Wild type
XVir	XVir-N-31
YB-1	Y-box binding protein 1

1. Introduction

1.1. Bladder Cancer

Worldwide, Bladder cancer (BC) is the seventh most common cancer in men and the 17th most common cancer in women [13] with an incidence of 570.000 (2015) and a mortality of 165.000 (2012) cases per year [25, 60]. Two thirds of all cases are diagnosed in the Western world, thus making BC more common in developed countries where it is the fourth and ninth most common cancer in men and women, respectively [13, 25]. Approximately 75% of newly diagnosed BCs are non-invasive (NMIBC) with the other 25% being muscle invasive BC (MIBC) [13]. Despite local therapy, patients with NMIBC have a high rate of recurrence and progression and once advanced to MIBC, patients face a poor outcome even with systemic therapy, radical surgery, and/or radiotherapy, thus causing an enormous burden on global health care systems [13].

1.1.1. Histopathology

The most widely used and accepted staging system is the tumour-node-metastases (TNM) system. According to this classification, NMIBCs confined to the epithelial mucosa are called carcinoma in situ (CIS) or, if the tumour exhibits a papillary structure, Ta tumours. As shown in Fig. 1.1, NMIBCs invading subepithelial tissues such as the lamina propria are called T1 tumours, whereas MIBCs invading muscle layers, perivesical tissues or other organs are referred to as T2, T3, and T4 tumours, respectively [20]. Furthermore, tumours are classified according to lymph nodes affected: tumours without regional lymph node metastases are categorised as N0, whereas tumours with a single lymph node metastasis whithin <2cm distance from the tumour side are categorised as N1. Tumours with a single lymph node metastasis within 2-5cm or multiple lymph node metastases within <5cm from the tumour lesion are categorised as N2, whereas N3 tumours show lymph node metastases within >5cm distance from the lesion [20]. Lastly, tumours are categorised according to their metastasis status: tumours without distant metastases are called M0, whereas M1 tumours exhibit distant metastases at other organs [20]. Besides, BCs can be graded into well differentiated (G1), moderately differentiated (G2) or poorly differentiated (G3) tumours [20].

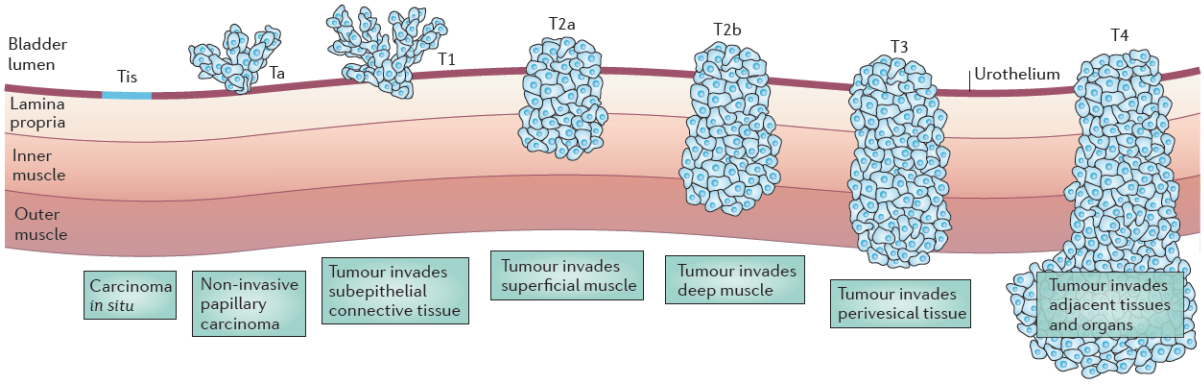

Figure 1.1.: **Bladder Cancer Staging and Grading.** Scheme of the bladder wall with the epithelial mucosa, lamina propria, and muscle layers. Different tumour stages and grades of invasion (CIS, Ta-T4) are shown. With permission from Nature Reviews Cancer, copyright (2015) [39].

1.1.2. Risk Factors

The most important risk factors for BC are an inherited genetic predisposition and external exposures to cacinogenic agents. It was shown that the risk for BC was increased two-fold in first degree relatives of patients with a history of BC [13, 20]. However, inherited factors might not necessarily lead to BC but affect the patients' susceptibility to carcinogenic agents [13]. The most important risk factor for BC is tobacco smoking which is estimated to account for 35% and 50% of the cases in women and men, respectively [13, 20]. Tobacco smoke contains high amounts of aromatic amines and polycyclic aromatic hydrocarbons which are both known causers for BC [13]. Compared to non-smokers, cigarette smokers have a 2-4-fold increased risk for BC whereby the risk increases with increasing intensity and/or duration of smoking [20]. However, the risk for BC development is reduced after cessation of smoking (>30% after 1–4 years and >60% after 25 years) but it never returs to the level of non-smokers [20].

Besides, the occupational exposure to carcinogenes is an important risk factor accounting for 5-20% of all BC cases [13, 20]. The exposure to aromatic amines used in chemical, rubber, and dye industries as well as polycyclic aromatic hydrocarbons used in aluminum, coal, and roofing industries have all been associated with the development of BC [20]. Furthermore, an increased risk for BC has been reported in painters, varnishers, and hairdressers [20].

Other risk factors are chronic inflammations of the bladder, schistosomiasis, ionizing radiation, and long-term exposure to pharmaceutical agents such as Cyclophosphamide or Pioglitazone [13, 20].

1.1.3. Diagnosis and Prognosis

The gold standard for diagnosis of BC is cystoscopy which is currently used for detection and resection of BCs [17]. Blue light cystoscopy, in contrast to white light cytoscopy, is more sensitive in detecting inconspicious tumours, including high-risk tumours, and is therefore recommended during initial transurethral resection of bladder tumours, in cases with negative white light cystoscopy but positive urine cytology, and during the initial follow up of patients with CIS or multifocal tumours [17]. Alternatively, narrow band imaging can be used for detection of BCs which, in contrast to blue light cystoscopy, does not require the instillation of photosensitising agents via a urethral catheter [17]. Alike blue light cystoscopy, narrow band imaging improves the detection of recurrent cancers over white light cystoscopy [17].

At the time of diagnosis, approximately 75% of the patients present with NMIBC whereas 25% present with MIBC [20]. For patients with advanced BC the options for a durable disease control are limited and the median survival for patients with >T2 tumours is only 46-77 months [58]. Also, patients with disease recurrence or metastatic disease show a very poor median survival of approximately 12 months [58].

Among the patients with NMIBC, 70% present with Ta, 20% with T1, and 10% with CIS tumours [20]. NMIBCs comprise a heterogenous group of cancers with completely different clinical outcomes: patients with low-grade tumours have a 5-years recurrence rate of 31% and a 5-years progression rate of 0.8% whereas patients with high-grade tumours have a 5-years recurrence rate of 78% and a 5-years progression rate of 45% as well as increased mortality rates [20]. This inter-tumour heterogeneity complicates the evaluation of treatment modalities and makes unified treatment recommendations difficult. Therefore, risk stratifications depending on the patients' tumour grade, and risk for recurrence and progression would be neccessary [20].

1.1.4. Treatment

NMIBC

The first line treatment for NMIBC is transurethral resection of bladder tumours (TURB) but due to high rates of recurrence and progression adjuvant treatments are used [3, 17]. Single instillation (SI) of chemotherapeutics such as mitomycin C, epirubicin or doxorubicin has been shown to act by the destruction of circulating tumour cells resulting from TURB and by an ablative effect on residual tumour cells and small overlooked tumours at the resection site [3]. It was shown that SI given within 24h after TURB significantly reduced the recurrence rate by 11.7-13.0% compared to TURB alone [3]. In low-risk patients, one SI reduces the risk of recurrence and is considered as standard treatment. However, patients with a high risk of recurrence and progression might not benefit from one SI: it was shown that further SI treatments could improve the relapse free survival of patients with an intermediate or high risk by 44% compared to TURB alone [3].

Intravesical Bacillus Calmette-Guerin (BCG) therapy, which induces an inflammatory reaction in the bladder, was shown to significantly improve the recurrence rates compared to intravesical chemotherapy. However, the exact mechanism by which BCG exerts its anti-tumour effects is still unknown [3, 60]. It was shown that BCG after TURB was superior in preventing the recurrence of NMIBC compared to TURB alone or TURB combined with chemotherapy [3]. In detail, tumour progression was observed in 9.8% of the patients treated with BCG compared to 13.8% in the control groups (TURB alone, TURB combined with intravesical chemotherapy or TURB combined with other immunotherapy) [3]. On the other hand it has to be mentioned that intravesical BCG treatment is associated with more side effects compared to intravesical chemotherapy. However, serious side effects are encountered in <5% of the patients [3].

In contrast to patients with Ta or T1 tumours, patients with CIS can not be cured by TURB alone and therefore these patients require an additional treatment such as radical cystectomy or BCG. Additional BCG therapy was shown to increase the complete response rate as well as the percentage of disease free patients and reduced the risk of tumour progression [3].

Patients with NMIBC which progress after initial chemotherapy can benefit from BCG therapy [3]. However, patients with progression after initial BCG therapy are unlikely to respond to further BCG therapy but might benefit from immunotherapy, chemotherapy or combination therapies. Nevertheless, radical cystectomy is still the preferred option for patients with BCG failure [3].

MIBC

The current gold standard for patients with high-risk recurrent NMIBC or metastatic MIBC is radical cystectomy with platinum-based neo-adjuvant chemotherapy being recommended [17]. Randomised clinical trials showed that the combination of methotrexate, vinblastine, adriamycin, and cisplatin had activity in patients with advanced BC [58]. Furthermore, neo-adjuvat administration of cisplatin-based chemotherapy could prolong the median survival of patients with >T2 BC from 46 to 77 months compared to cystectomy alone [58]. Another study showed that the combination of cisplatin-based chemotherapy and radiotherapy after TURBT achieved a complete response rate and could preserve the native bladder in more than 70% of the patients. In addition, the long-term survival rates in this study were comparable with these of standard cystectomy treatments [17]. Although all these approaches are considered as the current gold standard for metastatic BC, treatment failure frequently occurs due to acquired chemoresistance [38].

Another approach for the treatment of high-risk BC is the modulation of the immune system using immune checkpoint blockade. Tumours have evolved multiple mechanisms to evade

the immune system for example by inhibiting T-cell activation and thus tumour cell recognition. However, the inhibitory interaction between these so called checkpoint proteins and their ligands (tumour cell-immune cell interaction) can be used to inhibit the proliferation and function of cancer cells. Immune checkpoint therapy makes use of antibodies that target and block theses immuno-inhibitory interactions between cancer and immune cells thereby activating the immune system and inducing an anti-tumour immune response [38].

In 2010, a clinical trial tested the anti-cytotoxic T-lymphocyte associated Protein 4 (CTLA4) antibody ipilimumab, which is approved for the treatment of unresectable or metastatic melanoma, in 12 patients with localised BC prior to cystectomy [60]. In this trial, a marked increase in the level of lymphocytes was associated with an increased survival. A Phase II clinical trial evaluating ipilimumab in patients with metastatic BC is currently being tested [60].

Furthermore, anti-programmed cell death ligand 1 (PD-L1) therapies are being investigated for a number of cancers and have demonstrated recent successes in BC [60]. In a phase I clinical trial, the anti-PD-L1 antibody atezolizumab was evaluated in 67 patients with metastatic BC showing an objective response rate of 43% in patients with high PD-L1 expression compared to 11% for patients with low PD-L1 expression [60]. In another phase I trial, atezolizumab showed an 25% overall response rate in patients with PD-L1 positive metastatic BC. Moreover, more than half of these patients experienced tumour shrinkage after three months and survived for at least one year after their treatment. In addition, 20% of these patients had a complete response with no signs of cancer after therapy [38]. Based on these promising results, atezolizumab is now being tested in a phase III study in patients with relapse and another study is currenly comparing the effects of atezolizumab in early stage MIBC patients with high PD-L1 expression and BC patients with risk for recurrence [38].

In 2014, the anti-programmed cell death protein 1 (PD-1) antibodies nivolumab and pembrolizumab were approved by the FDA [38] and both substances are currently being tested in multiple preclinical and clinical trials including patients with BC [60].

So far, immune checkpoint therapies appear promising in the treatment of BC. However, there is still much work to be done at the preclinical level to define anti-tumour mechanisms and to explore additional treatment paradigms including novel combination therapies. It is not yet clear if checkpoint inhibition alone is sufficient to induce a durable anti-tumour immunity or if combinations with other treatments such as radiotherapy or cytokine immunotherapy are needed for a durable anti-tumour immunity [60].

1.2. Oncolytic Virotherapy

Oncolytic virotherapy has currently emerged as a new and promising treatment strategy for cancer and preclinical and clinical studies have shown the efficacy and safety of this approach [63]. Oncolytic viruses are designed to specifically infect, replicate, and kill tumour cells without harming normal cells [12]. In addition, oncolytic viruses can evoke an anti-tumour immune response not only against the original tumour but also against distant metastases and a variety of viruses has been used for this approach including Adenoviruses, Vaccina viruses, Reoviruses, Measles viruses, and Herpes simple viruses [63].

The in vivo efficacy of oncolytic viruses was evaluated in different animal models in which the virus was either directly injected into the tumour or given systemically by intravenous or intra-peritoneal injection [12]. Later, viral efficacy was evaluated by tumour growth and survival which were correlated to viral gene expression and particle production [12].

Onyx-015 was the first oncolytic virus which was tested in clinical trials and until now Onyx-015 has been tested in 18 phase I or II trials [63]. In these trials, the specific oncolytic activity of Onyx-

015 in cancer cells with mutated p53 status has been confirmed [63]. Moreover, these clinical trials showed no dose limiting side effects with flue-like symptoms being the most commonly observed side effect [12]. In 2006, the Chinese food and drug administration approved H101, an oncolytic Adenovirus similar to Onyx-015, in combination with chemotherapy for the treatment of nasopharyngeal cancer. However, H101 has not yet been approved in Western countries [63]. In 2015, the oncolytic HSV-1 virus T-VEX (talimogene laherparepvec) was approved by the FDA for the treatment of inoperable melanoma and in 2016 this virus was approved as Imlygic in Europe and Australia [63].

1.2.1. Adenoviruses

Adenoviruses (AdVs) can infect a wide range of species including birds, marsupials, cats, and humans [11]. Clinical symptoms of Adenovirus infection include respiratory disease, gastroenteritis or infections of the eye [52]. Due to their wide tissue tropism, their genomic capacity, and their ability not to integrate into the hosts' genome, Adenoviruses are frequently used as vectors for gene therapy.

Taxonomy

Within the family of Adenoviridae, human Adenoviruses belong to the genus of Mastadenoviridae [31]. Human Adenoviruses are subdivided into seven species (A-G) based on their capacity to agglutinate erythrocytes of humans, rats or monkeys [31, 52]. Depending on serological cross-neutralisation, these species are further subdivided into different types (formerly called serotypes) [31] and until now 87 different types are known of which 51 can infect humans [11]. There exists some correlation between species and their tissue tropism or clinical symptoms: for example, species B1, C, and E mainly cause respiratory diseases, whereas species B, D, and E can induce infections of the eye [52]. Species F in contrast is mainly responsible for infections of the gastrointestinal tract and species B2 infects the kidneys and urinary tract [52]. So far, all gene therapeutic vectors are based on Adenoviruses of species C, type 2 or 5 [11].

Infection and Replication

During Adenovirus infection, the Fibre protein is the first viral component interacting with the cell (Figure 1.2) [52]. Adenoviruses are know to interact with many cellular receptors but the major receptor for most Adenoviruses is the Coxsackie Adenovirus Receptor (CAR) which is a member of the immunoglobulin superfamily being involved in the formation of tight junctions [52]. After initial attachment of the viral Fibre protein with the cellular CAR receptor, the RGD motif in the viral Penton base binds to cellular αvβ3/αvβ5-integrins leading to activation of cellular signalling cascades, cytoskeleton alterations, and virus internalisation via clathrin-coated vesicles and endosomes [52]. The rupture of the endosome releases viral particles into the cytoplasm. These particles are composed of a Hexon shell with a metastable core of virus DNA and DNA associated proteins. In the following, the Hexon shell binds to nuclear pores thereby releasing the core into the nucleus where viral DNA replication and gene expression take place [52]. During Adenovirus infection, the cell gets prepared for optimal conditions for viral replication and gene expression which require the activation of cellular transcription factors, such as key molecules of cell cycle regulation, and S-phase induction [11].

Genomic Organisation and Viral Proteins

Adenoviruses are non enveloped icosahedral DNA viruses with a linear, double stranded genome of approximately 34-36 kb [11, 31]. A schematic depiction of the Adenoviral capsid is shown in Figure 1.2.

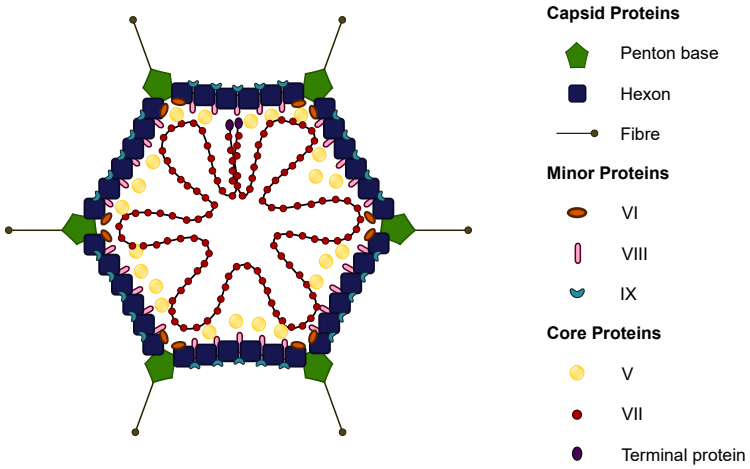

Figure 1.2.: **The Adenovirus Structur.** A schematic depiction of the Adenoviral structure. The Figure was adapted from [52].

The Adenoviral DNA is flanked by two inverted terminal repeats which present the origin of replication [11]. During replication, the Adenoviral DNA is transcribed in a complex transcription pattern in which eight transcription units are transcribed from both DNA strands by RNA polymerase II [11]. Each of these transcription units encodes multiple proteins which are produced by alternative splicing [11].

During replication, Adenoviral genes are transcribed in a complex temporal manner and are therefore divided into three major groups (early, intermediate, and late genes). A schematic of the Adenoviral genome organisation is shown in Figure 1.3. The early genes E1A, E1B, E2, E3, and E4 are transcribed from five promoters and are needed for regulation of viral gene expression and DNA replication [11]. The intermediate genes IX and IVa2 encode minor components of the viral capsid and are expressed at low levels at early times of infection which increase upon time [11]. The late genes L1-L5 encode viral capsid proteins and are transcribed from the major late promoter (MLP) [11].

The E1A Region The E1A gene is transcribed from the E1A promoter at the very left site of the genome (Figure 1.3). Within the Adenovirus genome, this promoter is unique in structure and function and it must work efficiently during early stages of Adenoviral infection. The E1A promoter is composed of the inverted terminal repeats, an enhancer region, and a combination of several binding sites for cellular transcription factors such as E2F1 [5].

The Adenoviral E1A gene is the first transcribed gene and the E1A protein stimulates transcription from other viral promoters and is therefore needed for conductive viral gene expression during replication [11]. Besides, E1A can also transactivate or repress cellular promoters leading to optimal conditions for viral replication within the cell. The E1A gene encodes five different proteins (9S, 10S, 11S, 12S, and 13S) which are produced by alternative splicing. Of these, the E1A12S and E1A13S are the two most important ones [11]. The E1A

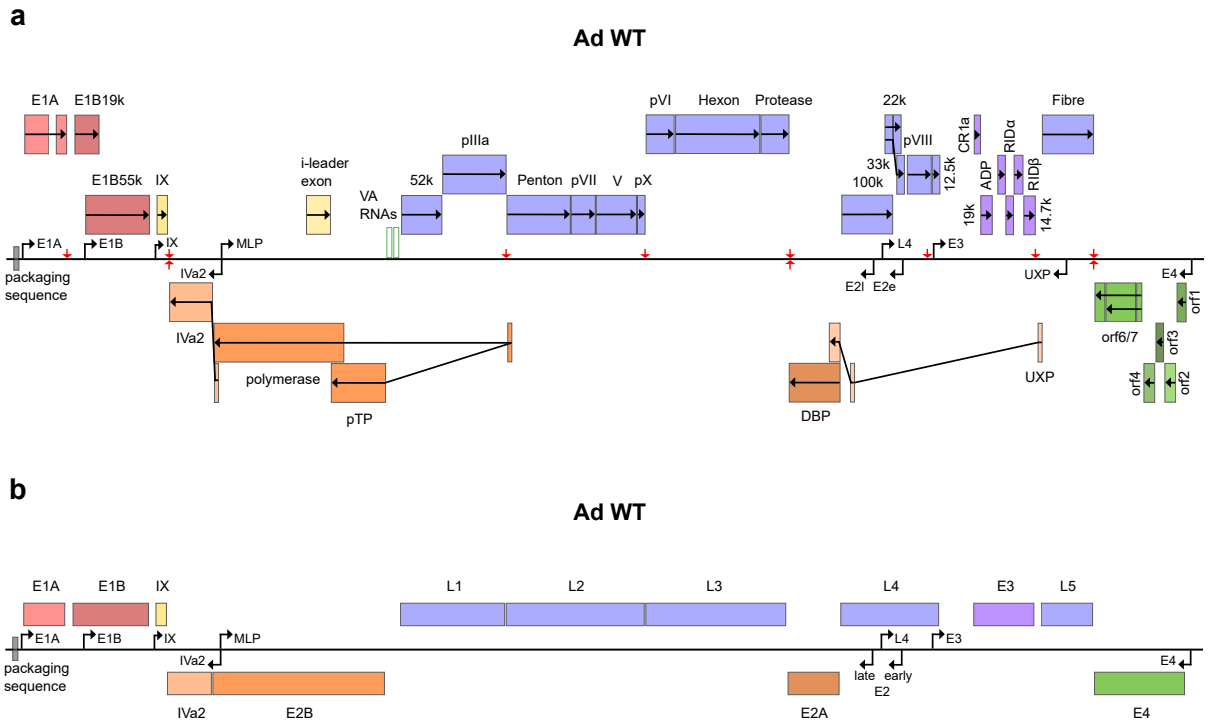

Figure 1.3.: **Genome of the Human Adenovirus WT.** (a) Detailed organisation of the Adenovirus WT genome. Genes transcribed rightwards from the upper strand are shown on top of the line and genes transcribed leftwards from the lower strand are shown beneath the line. Boxes represent viral genes and lines between the boxes indicate alternative splicing variants. Viral promoters and their directions are indicated by small black arrows on the line. Red arrows indicate stop codons. (b) Simplified organisation of the viral genome as it will be used in the following sections. For full details, see text. The Figure in (a) was adapted from [36].

gene encodes three conserved regions (CR) of which the Adenoviral E1A13S possesses all three domains (CR1/2/3) while the E1A12S posses only two of them (CR1/2). E1A can interfere with cellular cell cycle proteins by binding to the Retinoblastoma pocket protein (Rb) via the CR1/2 domain. Through this interaction, transcription factors such as E2F1 are released from the pocket protein leading to cell cycle progression, S-phase induction, and cellular and viral gene expression, and DNA replication (Figure 1.5). Thus, Adenoviral vector mutants with CR2 deletions such as dl-922-947 (delta24) can only replicate in cells with mutated Rb [12]. The CR3 domain of E1A13S in contrast is needed for transactivation of cellular and viral promoters such as the E2 early promoter and is therefore needed for conductive viral gene expression and replication [51]. However, E1A12S also possesses some transactivation activity but to a much lesser extend than E1A13S [5].

The E1B Region The E1B gene is transcribed from the E1B promoter at the left side of the genome. Alike the E1A promoter, this promoter also posseses several closely spaced binding sites for cellular transcription factors which, due to their close proximity, can interact with each other [5]. However, this promoter does not contain any E2F1 binding sites [41].

The E1B gene encodes two proteins which are producd by alternative splicing. The E1B19k protein is a member of the B-cell lymphoma 2 (bcl-2) family, thus inhibiting apoptosis induced by p53 and other cell death proteins. E1B19k is expressed strongly at late times in infection [11].

The other protein encoded by the E1B gene is E1B55k. This protein can form complexes with the viral E4orf6 protein and these complexes are responsible for transportation of late viral mRNAs to the ribosomes [11]. Moreover, E1B55k alone and in complex with E4orf6 can bind to p53 leading to degradation of the latter [11]. Furthermore, E1B55k is involved in Adenoviral replication as the complex with E4orf6 translocates the Y-box binding protein 1 (YB-1) to the nucleus where it stimulates the viral E2 late promoter [33]. Another function of the E1B55k-E4orf6 complex is to stabilise E1A thereby enhancing the activation of E2F1 which in turn leads to activation of viral DNA replication and gene expression [22].

The E2 Region The E2 region is transcribed leftwards from the lower DNA strand and gene expression is controlled by two promoters called E2 early and E2 late (Figure 1.3 E2e and E2l, respectively). The E2 early promoter is active during early and late phases of infection. Alike the E1A promoter, the E2 early promoter contains two E2F1 binding sites [57] and the binding of a transcription factor complex including E2F1, TATA-Box binding protein (TBP), and activating transcription factor (ATF) is required for promoter activation [62]. This transcription complex is further stabilised by E4orf6 which allows E1A to interact with E2F1 leading to viral gene expression [62]. In contrast, the E2 late promoter is activated by the cellular transcription factor YB-1 for which it possesses three binding sites [32].

The E2 gene encodes proteins which are needed for viral DNA synthesis, such as DNA polymerase, primase, and the DNA binding protein (DBP, E2A) [11]. The E2A protein binds to single stranded DNA and is active during viral replication while the E2B protein functions as DNA polymerase and serves as primer for the initiation of DNA synthesis [11].

The E3 Region The Adenoviral E3 region is transcribed rightwards from the E3 promoter which partially overlaps with the upstream control region of the E2 early promoter on the other strand. Therefore, promotor elements and transcription factors of the E2 early promoter could affect E3 transcription [5]. In contrast to the E2 early promoter, the E3 promoter does not contain any E2F1 binding sites [41].

The E3 region is responsible for modulation of the hosts' anti-viral immune response and thus deletions within the E3 region increase inflammatory responses against the infected cell [11]. This region encodes several proteins generated by alternative splicing. The 14.7 protein for example prevents tumour-necrosis factor alpha (TNF-α) induced apoptosis and inhibits cytotoxic T-cell induced apoptosis by downregulation of immunodominant antigens such as E1A [11]. By interfering with major histocompatibility complex I (MHCI) expression on the cell surface, the E3 19k protein also protects the cell against cytotoxic T-cell responses and cytotoxic T-cell induced cell killing [11]. The Adenovirus death protein (ADP) in contrast, causes cell death and is needed for efficient cell lysis at later stages of infection [11].

The E4 Region The E4 region is transcribed leftwards from the very right side of the lower DNA strand (Figure 1.3). In contrast to the E1A and E2 early promoter, the E4 promoter does not contain any E2F1 binding sites [41]. However, E1A induces E4 promoter activity via activation of transcription factors such as p50E4F and ATF [65]. On the other hand, E4 promoter activity is negatively regulated by E2A and by a negative feedback loop of E4orf4 in complex with Protein phosphatase 2A (PP2A) which dephosphorylates transcription factors including E1A, leading to a decreased transactivation of E1A on the E4 promoter [65].

In general, the proteins encoded by the E4 gene regulate viral DNA synthesis, mRNA shuttling, cellular protein synthesis, and cell death [11]. All proteins of this region are produced by alternative splicing. As mentioned before, the E4orf4 protein, in complex with PP2A downregulates expression of E1A regulated genes [65]. Moreover, E4orf4 is responsible for induction of cell death independent of p53 or viral proteins [11]. E4orf6 forms a complex with E1B55k and this complex regulates viral gene expression, viral DNA replication, and apoptosis as mentioned before [11]. E4orf6/7 proteins form complexes with transcription factors such as E2F1 thereby stabilising E2F1 and enhancing E2 gene transcription from the E2 early promoter [11].

Intermediate Genes, Late Genes, and the Major Late Promoter The intermediate genes are transcribed from the two promoters IX and IVa2 on the upper and lower DNA strand, respectively. These promoters are active after DNA replication has started [5]. The late genes are transcribed from the major late promoter (MLP) on the upper DNA strand which is active within one hour post infection (hpi) [41]. The MLP does not possess any E2F1 binding sites and MLP activity is only influenced by E1A [41].

The intermediate and late proteins encode viral capsid proteins such as IX, Hexon (L3), and Fibre (L5) (Figure 1.2 and 1.3) [11].

1.2.2. Principle of Oncolytic Virotherapy

To render oncolytic viruses cancer specific, two major strategies are used. The first class of oncolytic viruses is rendered cancer specific by specific mutations or deletions in genes which normally interfere with cell cycle regulators. For example the Adenoviral E1 proteins which interfere with the cellular Rb or p53 proteins can be mutated or deleted and consequently these viruses can only replicate in actively dividing cancer cells with mutations in the Rb or p53 gene [12]. An example of this type of oncolytic viruses is the oncolytic Adenovirus Onyx-015 which does not express the E1B55k protein and is therefore unable to inactivate p53 in normal cells. However, Onyx-015 can specifically replicate in p53 mutated cancer cells [12, 63]. Another example for this type of oncolytic viruses is the Adenovirus dl922-947 (delta24) which has a deletion in the E1A CR2 domain and is therefore unable to induce cell cycle progression by releasing E2F1 transcription factors from the complex with Rb. Thus, dl922-947 can only replicate in tumour cells with mutated Rb [12].

The second class of oncolytic viruses makes use of tumour specific promoters, such as the prostate specific antigen promoter or the telomerase promoter, to activate viral gene transcription [12]. An example for this type of oncolytic viruses is the Adenovirus CG0070 in which E1A expression is regulated by the cellular E2F1 promoter [50].

So far, clinical trials have shown the safety of oncolytic viruses. However, due to inefficient tumour transduction or immune reactions the in vivo efficacy is very limited [12]. Thus, oncolytic virotherapy needs to be improved for example by combining oncolytic virotherapy with exsisting cancer treatments such as chemotherapeutic agents or target therapies [12].

1.2.3. The Oncolytic Adenovirus XVir-N-31

In this study, the oncolytic Adenovirus XVir-N-31 was used which was first described in 2011 by Holzmüller et al [34]. A scheme of XVir-N-31 and its differences to WT Adenovirus are shown in Figure 1.4. XVir-N-31 has a deletion in the E1A CR3 domain and consequently no E1A13S proteins can be formed. Thus, XVir-N-31 lacks transactivation of E1A13S on viral

early promoters (e.g. E2 early promoter) and therefore the E2 gene expression is totally E2 late dependent. Furthermore, the deletion of E1A13S leads to a reduced transactivation on E4orf6 which, together with E1B55k, is responsible for nuclear translocalisation of YB-1 and consequently E2 late activity. Thus, YB-1 can only bind and activate the E2 late promoter if YB-1 is already in the nucleus which is only the case in tumour cells. Therefore, the E1A13S deletion renders XVir-N-31 YB-1-dependent and cancer specific [34]. Furthermore, XVir-N-31 lacks the E1B19k protein which has an anti-apoptotic function. The E3 region has a deletion of 2681 base pairs (bp) which makes space for a transgene and increases the host's inflammatory immune response. Lastly, the Fibre gene encodes an additional arginyl-glycyl-aspartic acid (RGD) motif for better infection of tumour cells, as these often express low CAR levels [34].

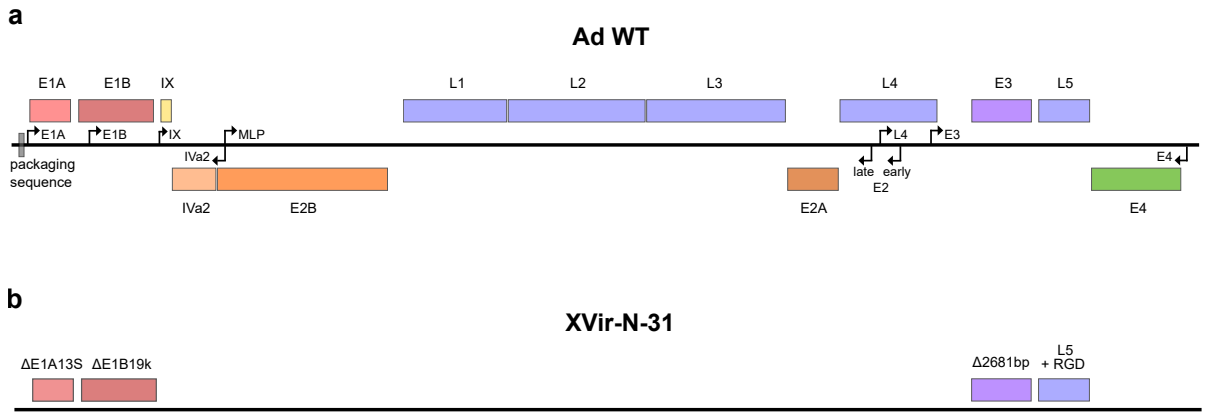

Figure 1.4.: **The Oncolytic Adenovirus XVir-N-31.** (a) Schematic of the Adenoviral WT genome as descried in detail in Chapter 1.2.1. (b) Schematic of XVir-N-31. Note that only regions differing from WT genome are shown. For further details, see text.

1.2.4. Strategies to Improve Oncolytic Virotherapy

Oncolytic virotherapy has shown promising results in preclinical studies but the in vivo efficacy is still limited. Therefore, several strategies are being investigated to enhance oncolytic virotherapy in vivo.

One approach is to integrate a transgene for an enhanced viral anti-tumour activity into the viral E1 or E3 region. These transgenes include proteins with cytotoxic, anti-angiogenic or immunostimulatory activities [12]. Another way to enhance oncolytic virotherapy is to increase the viral tropism and thus the entry into tumour cells for example by an additional RGD motif (see XVir-N-31, Chapter 1.2.3). Besides modifications in the viral genome, additional approaches are investigating the effects of oncolytic virotherapy in combination with anti-tumour agents such as radiotherapy, immunotherapy, chemotherapy or small molecule inhibitors [12].

Improving Oncolytic Virotherapy with Standard Chemotherapeutic Agents

Standard chemotherapeutic agents include mitotic inhibitors, antibiotics, platine salts, alkylating agents, and antimetabolites. These agents link cellular DNA strands leading to cell cycle arrest and cell death. However, these drugs do not only affect tumour cells but also lead to apoptosis in normal cells which causes strong side effects [12]. Studies combining oncolytic virotherapy with standard chemotherapeutic drugs showed that these combination therapies

could indeed enhance viral replication and tumour cell death in some cases. However, the molecular mechanisms underlying these effects were not always thoroughly investigated. Most studies linked the enhanced effects to an increase in apoptosis or an enhanced E1A-induced sensitivity to chemotherapeutic agents [12]. Examples of standard chemotherapeutic agents which were combined with oncolytic virotherapy and the effects on viral replication and tumour cell death are listed in Table 1.1 and a full Table can be found in Chapter A, Table A.1.

In 2002, a study by Berent et al showed that viral replication and tumour cell death were enhanced upon combination with drugs that induced a G2-arrest [6]. This study proposed four different groups of chemotherapeutics which induce a G2-arrest. Agents such as camptothecin, etoposide, daunoblastin or cisplatin strongly increased viral replication (group 1) while replication was only moderately increased upon combination with paclitaxel (group 2). The third group of drugs affected viral replication differentially depending on the doses chosen and included agents such as 5-fluorouracil (5-FU) and hydroxyurea. In contrast, viral replication was inhibited by agents such as actinomycin D independent of the doses chosen (group 4) [6]. However, the molecular mechanisms underlying these effects were not investigated.

Our group has previously shown that the transcription factor YB-1 is important in Adenovirus biology as it activates the viral E2 late promoter (Chapter 1.2.1) [32]. Moreover, it was shown that YB-1 was translocated into the nucleus upon stress signals and irradiation thereby facilitating viral replication [7, 43]. In 2006, Bieler et al showed that a triple combination of irinotecan, trichostatin A, and virotherapy could strongly enhance viral replication and cell lysis [7]. In this combination, the topoisomerase I inhibitor irinotecan led to DNA breaks which caused translocation of YB-1 into the nucleus where it could mediate and activate viral replication via the E2 late promoter. Moreover, irinotecan activated YB-1 via the Akt pathway. Trichostatin A is a histone deacetylase inhibitor which in this study increased the toxicity of irinotecan thereby further activating YB-1. All in all, this triple therapy led to a strongly enhanced viral replication and cell lysis [7].

Another study by Mantwill et al investigated the role of YB-1 in chemoresistant cells [43]. It was shown before that the overexpression of ATP-binding cassette transporters, such as multi drug resistance gene 1 (MDR1) and multi drug resistance associated protein 1 (MRP1), which actively expel chemotherapy drugs from the cell was correlated with therapy resistance and that MDR1 and MRP1 were activated by YB-1 [43]. However, in these chemoresistant cells viral infection by WT and the oncolytic Adenovirus XVir03 led to translocalisation of YB-1 to the viral E2 late promoter were it stimulated viral replication. As YB-1 was recruited to the viral E2 late promoter it could no longer activate MDR1 and MRP1 genes thus leading to a downregulation of MDR1 and MRP1 expression. This downregulation resulted in resensitisation of the cells to chemotherapeutic agents such as daunoblastin and doxetaxel. Furthermore, this combination enhanced viral replication and cell death [43].

Table 1.1.: Combination of Oncolytic Viruses with Standard Chemotherapeutic Drugs; extract from [12], Table 1, with permission from Elsevier. The full Table can be found in Table A.1

Virus	Drug	Tumour origin	Viral replication	Synergy/ additivity	Mechanism other than oncolysis
Mitotic inhibitors					
OBP-401	Docetaxel, Vinorelbin	Different origin, lung	Unmodified	Synergy	n.i.
dl922-947	Paclitaxel	Ovary	Unmodified	n.i.	Abnormal mitosis leading to apoptosis
Antibiotics					
Onyx-015	Doxorubicin	Thyroid	n.i.	Synergy	E1A-induced chemosensitisation?
Anti-metabolites					
Onyx-015	5-FU + Leucovorin	Colon	Increased	n.a.	n.a.
OBP-301 (Telomelysin)	Gemcitabine	Lung	Unmodified	n.i.	Sensitisation to gemcitabine
Platine salts					
Onyx-015	Cisplatin	Liver	n.i.	n.i.	n.a.
OBP-401 (Telomelysin)	Cisplatin	Ovary	n.i.	Additivity	n.i.
Topoisomerase inhibitors					
ΔE1ACR2 ΔE1B19K	Irinotecan	Pancreas	Unmodified	Additivity	Apoptosis
AddlE1B55	Etoposide	Esophagus	Unmodified	Additivity	n.i.
Onyx-015	Mitoxantrone	Prostate	Unmodified	Synergy	CRAd-induced chemosensitisation

CRAd, Conditionally-replicative Adenovirus; n.a., not applicable; n.i., not investigated

Improving Oncolytic Virotherapy with Target Therapies

Another way to enhance oncolytic virotherapy is to combine oncolytic virotherapy with small molecule inhibitors (target therapy) which inhibit several pathways that are highly active in cancer cells for example by inhibiting kinase or receptor activities thereby leading to growth inhibition and cell death [12]. Examples for target therapeutic agents are mTOR inhibitors (RAD001, rapamycin) or inhibitors of histone deacetylases (valproic acid, trichostatin). Alike standard chemotherapeutic agents, small molecule inhibitors could also increase viral replication or tumour cell death in some studies but unfortunately the molecular mechanisms were only poorly investigated. Most studies linked the increased tumour cell death in the combination treatment to enhanced autophagy or increased infection rates [12] but most explanations were only speculative. An extract of small molecule inhibitors which were combined with oncolytic virotherapy and the effects on viral replication and tumour cell death is shown in Table 1.2 and the full Table can be found in Chapter A, Table A.2.

In some studies, the combination of oncolytic virotherapy and mTOR inhibitors showed an increased viral replication and enhanced tumour cell lysis (Table 1.2). In 2013, Cheng et al combined the mTOR inhibitor rapamycin with oncolytic virotherapy which led to an increase in viral E1A expression, enhanced viral replication, and cytotoxicity due to an rapamycin induced increase in autophagy [16]. Another study by Homicsko et al combined oncolytic virotherapy with the mTOR inhibitor RAD001 (everolimus) [35]. In this study, the combination led to an increased oncolytic activity, tumour growth inhibition, immune suppression, and an inhibited angiogenesis which was linked to a better spread of the virus within the tumour and a prolonged survival in vivo [35].

Other studies combined oncolytic virotherapy with several kinase inhibitors. In 2011, Libertini et al combined the oncolytic virus delta24 with the aurora B kinase inhibitor AZD1152. This combination resulted in enhanced viral replication, cytotoxicity, and inhibition of tumour xenograft growth due to increased caspase-3 activity and enhanced apoptosis [42]. Another study combined the oncolytic Adenovirus Onyx-015 with the MEK inhibitor CI1040 showing a cell cycle arrest in G1-phase, an upregulated CAR expression, and an enhanced cytotoxicity in the combination therapy [4]. Moreover, this study showed that virus induced cell death and virus production were more potent in G1-arrested cells [4] which is in stark contrast to the common conception that Adenoviruses require S-phase induction for viral replication. However, the mechanism underlying this observation was not investigated. In 2011, Connell et al combined oncolytic virotherapy with the Chk1 inhibitor UCN-01 [21]. In this study, they observed enhanced DNA damage, viral overreplication, and increased cytotoxicity in the combination therapy suggesting that the unscheduled DNA synthesis and impaired repair mechanisms upon Chk1 inhibition were crucial for the enhanced oncolytic viral activity [21].

Table 1.2.: Combination of Oncolytic Viruses with Target Therapy; extract from [12], Table 2, with permission from Elsevier. The full Table can be found in Table A.2

Virus	Drug	Tumour origin	Viral replication	Synergy/ additivity	Mechanism other than oncolysis
mTOR inhibitors					
Δ24-FibRGD	RAD001	Glia	Unmodified	Synergy	Autophagy
OBP-405	Rapamycin	Glia	Unmodified	Synergy	Autophagy
Adcyc3-E1A (ΔE1B)	Rapamycin	Breast, lung	Increased	Synergy	Autophagy
dl922-947	Rapamycin	Glia	Reduced	n.a.	Autophagy inhibition
Inhibitors of other kinases					
dl922-947	Bevacizumab	Thyroid	Increased	Additivity	Angiogenesis inhibition, drop of interstitial pressure
dl922-947	AZD1152	Thyroid	Increased	Additivity	Polyploidy, caspase-3 activation
Onyx-015	CI-1040	Colon	Reduced	n.i.	Cell cycle arrest
Inhibitors of histone deacetylases					
Telomelysin	Valproic acid, FK228	Lung	Increased	Synergy	Increased cell entry
Onyx-015	Trichostatin	Esophagus	Increased	Synergy	Increased cell entry
CN702	Valproic acid	Prostate, colon	Decreased	Antagonism	Cell cycle arrest
dl922-947	Valproic acid	Colon	Unmodified	n.i.	Induction of polyploidy

CRAd, Conditionally-replicative Adenovirus; n.a., not applicable; n.i., not investigated

1.2.5. Oncolytic Virotherapy in Bladder Cancer

As described before, many patients with NMIBC progress after initial therapy and therefore require additional treatments. Moreover, patients with MIBC, disease recurrence or metastatic disease frequently encounter treatment failures due to acquired chemoresistance [38]. The development of new therapies for BC is therefore urgently needed. The urinary bladder is a suitable organ for oncolytic virotherapy: first, the delivery of agents into the bladder through the urethra is easy and, by means of intravesical BCG therapy, already established [63]. Furthermore, intravesical instillation allows the direct delivery of the virus into the tumour without any interference with and extinction by the immune system as it is observed upon systemical application. Moreover, the papillary structure of the urothelium increases the surface area for topical

application and virus infection [63]. In addition, BCG therapy has shown the sensitivity of BCs to immunotherapeutic approaches suggesting the potential usefulness of other immunomodulating therapies [63]. So far, the potential of oncolytic virotherapy in BC was evaluated in four clinical trials which are listed in Table 1.3 [63].

The oncolytic Adenovirus CG0070 was developed by Ramesh et al. in 2006 [50]. CG0070 encodes the E1A gene under control of the E2F1 promoter which is transcriptionally active in many tumours. Moreover, CG0070 encodes the human Granulocyte-macrophage colony-stimulating factor (GM-CSF) for enhanced anti-tumour activity [50]. In 2012, Burke et al. carried out a phase I trial testing CG0070 in patients with NMIBC who had not responded to BCG therapy [14]. The virus was administered in single or multiple doses (every 28 days for three times or weekly for six times) in combination with dodecyl maltoside to enhance virus transduction [14, 63]. In the single and multi dose cohort the overall response rates were 48.6% and 63.6%, respectively [14, 63]. During this study, no clinical significant serious side effects were reported and grade 1–2 bladder toxicities such as dysuria or bladder pain were the most common side effects [14, 63]. Based on this study, a phase II/III clinial trial is currently testing the effects of combined CG0070 and mitomycin C, interferone, valrubicin or gemcitabine therapy in patients with NMIBC after BCG failure [63]. Another phase II trial is currently testing the effects of weekly intravesical CG0070 therapy in patients with NMIBC who had failed BCG therapy and refused cystectomy [63].

The effects of the replication competent Vaccina virus Dryvax was tested in 2001 in patients with MIBC [63]. In this study, four patients were treated with three intravesical injections of Dryvax before cystectomy. No serios side effects were reported in this study suggesting that even WT Vaccina virus can be safely administered to patients with BC [63]. Moreover, this study showed inflammatory infiltrations and dendritic cell migration to the virus infected site in post-resection evaluations [63] indicating an enhanced immune reaction against the tumour.

Table 1.3.: Current Clinical Trials in Bladder Cancer [63]

Virus	Species	Phase	Tumour type	Delivery
CG0070	Adenovirus	I	NMIBC after BCG failure	IVE with dodecyl maltoside
CG0070	Adenovirus	II/III	NMIBC after BCG failure	IVE with dodecyl maltoside
CG0070	Adenovirus	II	NMIBC after BCG failure with cystectomy refused	IVE with dodecyl maltoside
Dryvax	Vaccinia virus	I	MIBC before cystectomy	IVE

IVE, intra vesical

1.3. Cell Cycle Regulation by Checkpoint Kinases and Cyclin-Dependent Kinases

The cell cycle is tightly regulated by a complex signalling network including transcription factors, pocket proteins, cyclins, cyclin-dependent kinases (CDKs) and their negative regulators. The constitutive expression of CDKs and the temporal expression of several cyclins enables the regulation of specific cell cycle phases by distinct cyclin-CDK complexes [47].

The cell cycle is divided into several phases named gap 1 (G1), synthesis (S), gap 2 (G2), and mitosis (M) [26, 47]. Cells in G0/G1-phase synthesise cyclin D1 in response to mitotic stimuli

which then forms activating complexes with CDK4 and CDK6 (Figure 1.5) [26]. Activated CDK4/6-cyclin D1 complexes phosphorylate pocket proteins such as Rb, p107, and p130 leading to their functional inactivation [47]. In quiescent cells, these pocket proteins bind to transcription factors of the E2F family thereby repressing E2Fs' transcriptional activity and S-phase entry [26, 47]. However, the phosphorylation of pocket proteins dissociates them from the complex with E2Fs leading to E2F-dependent transcriptional activation and cell cycle progression. Genes activated by E2Fs include cyclin A and cyclin E2 which associate with CDK2 and further phosphorylate Rb as well as other mediators of the G1/S transition. This induces a positive feedback loop making the cell pass the so called restriction point thereby further progressing to S/G2-phase [26]. Lastly, cyclin A and cyclin B activate CDK1 which facilitates the onset and progression of mitosis (not shown) [26].

As mentioned before, Adenoviruses rely on the cellular transcription machinery and require S-phase induction for optimal viral replication. Therefore, Adenoviruses have evolved mechanisms to interfere with the cellular cell cycle and to promoter S-phase induction: as shown in Figure 1.5, the Adenoviral E1A protein can interfere with the Rb/E2F pathway by binding to the cellular Rb protein whereby E2F1 transcription factors are released from the complex. Free E2F1 can then activate viral E2 gene expression and viral replication [11].

During cell cycle, the activity of CDKs and cyclins is negatively regulated by two families of cyclin kinase inhibitors: proteins of the INK4 family include p15, p16, p18, and p19 while proteins of the CIP/KIP family include p21, p27, and p57 [26]. Proteins of the INK4 family inhibit CDK4/6 either by reducing their binding with cyclin D1 or by a direct occupation of the catalytic domain [47].

To ensure proper DNA replication and mitosis, a complex signalling network was evolved by the cell to monitore genome integrity during replication and to initiate cell cycle arrest, repair or apoptosis if errors are detected [2]. Upon DNA damage, a multiprotein complex is recruited to the site of damage which causes activation of ataxia telangiectesia mutated (ATM) and ATM and Rad3 related (ATR) [2]. ATM is typically activated upon double strand breaks while ATR is activated upon single strand breaks [2]. Activated ATM and ATR further phosphorylate downstream substrates such as checkpoint kinase 1 and 2, respectively (Chk1 and Chk2) (Figure 1.5). Activated Chk1 phosphorylates the protein phosphatase Cdc25A leading to ubiquitination and degradation of the latter [2]. Thereby, activated Chk1 leads to cell cycle arrest in G0/G1-phase. Moreover, Chk1 phosphorylates Cdc25C thereby preventing phosphorylation and activation of CDK1 which induces a G2-arrest [2]. Chk2 is typically activated by ATR upon single strand breaks which leads to similar effects on Cdc25A and Cdc25C as Chk1 [2].

Another important player in cell cycle regulation is p53 which upon DNA damage mediates cell cycle arrest in G1-phase thereby allowing the cell time for repair and ensuring genome integrity (not shown) [47]. ATM and ATR function as DNA sensors and phosphorylate p53 upon DNA damage. Upon phosphorylation, p53 is released from the complex with mouse double minute 2 homologue (MDM2), thereby preventing p53 from degradation [47]. In the following, accumulated p53 increases the transcription of p21 leading to inhibition of CDK2 and cell cycle arrest in G1-phase [47].

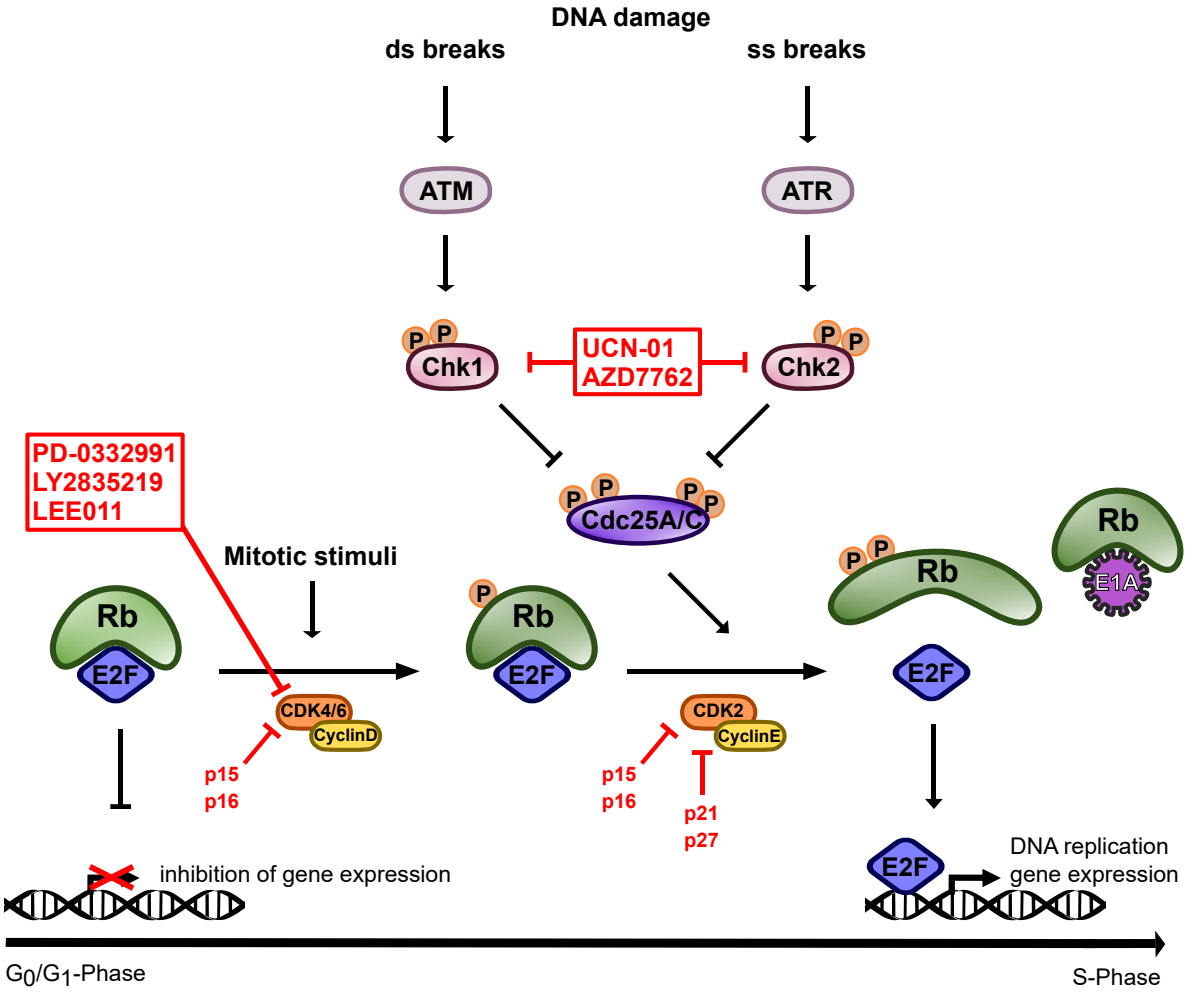

Figure 1.5.: **Cell Cycle Regulation by CDKs and Chks.** Regulation of the cell cycle by pocket proteins (green), E2Fs (blue), CDKs (orange), and cyclins (yellow). CDK4/6 inhibitors (PD-0332991, LY2835219, and LEE011) are shown on the left side. The DNA damage pathway is shown on top with ATM and ATR (grey) being activated upon double strand (ds) or single strand (ss) breaks, respectively. ATM and ATR regulate Chks (rose) and Cdc25 proteins (violet) and Chks are inhibited by UCN-01 or AZD7762. As indicated on the right side, Adenoviruses (violet) can also interfere with this pathway. For full details, see text.

1.4. Small Molecule Inhibitors

The pathways outlined above have important implications in cancer development as many cancers show genetic alterations in cell cycle biology [26]. These genetic alterations include changes in the Rb and cyclin D-CDK4/6 pathway as well as mutations in the DNA repair pathway resulting in impaired cell cycle control and uncontrolled proliferation [2, 26]. Therefore, these cell cycle proteins are an attractive target for targeted drug therapy [26].

1.4.1. Checkpoint Kinase Inhibitors

In normal cells, DNA replication is tightly controlled by several checkpoint pathways including Chk1-dependent and independent pathways that are activated upon DNA damage [2]. Tumour cells in contrast, rely mostly on Chk1 activity upon DNA damage making this pathways an

attractive target for tumour therapy, especially in combination with DNA damage inducing agents such as gemcitabine, cisplatin or 5-fluorouracil [2]. The idea behind this combination is to abrogate remainig cell cycle checkpoints in tumour cells leading to impaired DNA repair and enhanced tumour cell death upon treatment with DNA damage inducing agents [2].

Early works showed that natural substances such as caffein or the staurosporine analogue UCN-01 can interfere with cellular checkpoint pathways by inhibiting ATM and ATR or Chk1, respectively (Figure 1.5) [2]. In the following, it was recognised that UCN-01 could be a useful agent to enhance cytotoxicity in tumour cells in response to DNA damage [2]. Clinical trials testing UCN-01 in combination with several DNA damage inducing agents are still ongoing [2]. However, UCN-01 is not only a Chk1 inhibitor but it also potently inhibits other kinases including Chk2 and CDKs and thus, it is possible that the effects seen upon UCN-01 treatment are also due to inhibition of other pathways [2].

In the following, new and more specific therapeutic agents have been developed and three Chk1/Chk2 inhibitors (XL-844, AZD7762, and PF00477736) have entered phase I clinical trials [2]. All three inhibitors are potent inhibitors of Chk1 and Chk2 (Figure 1.5) which have been shown to abrogate DNA damage induced cell cycle arrest and to enhance the effects of DNA damage inducing agents in vitro and in vivo [2]. However, the efficacy was dependent on the cell line and DNA damaging inducing agent used but a good response was observed for combination with gemcitabine. All three Chk1 inhibitors are currently being tested in clinical phase I trails in combination with gemcitabine or irinotecan [2].

1.4.2. Cyclin-Dependent Kinase Inhibitors

The Rb-CDK4/6 pathway is commonly mutated in a variety of cancers leading to uncontrolled cell cycle progression and cell division. Deregulations in this pathway include loss of function mutations of the Rb, p14, p15 or p16 gene as well as amplifications or activating mutations in the genes encoding for cyclin D1, E2Fs, CDK4 or CDK6 [47]. The inhibition of the CDK4/6 axis leads to dephosphorylation of Rb, repression of E2Fs, and cell cylce arrest in G0/G1-phase. Therefore, the development of CDK4/6 inhibitors as target therapy for cancers might be both efficacious and less toxic compared to standard chemotherapeutic drugs [26, 47].

However, first clinical experience with CDK4/6 inhibitors showed only poor efficacy accompanied by high toxicities and serious adverse effects in clinical studies [26]. These first generation CDK4/6 inhibitors such as flavopiridol, R-roscovitine, and UCN-01 were less specific for CDK4/6 and showed broad activities against several other targets such as other CDKs, Akt, Chk1, and protein kinase C and were therefore considered as pan-CDK inhibitors [26]. This broad activity against several targets might account for their poor efficacy and dose limiting toxicities in clinical studies [26].

In the following, a second generation of ATP-competitive small molecule CDK4/6 inhibitors has been developed [47]. These second generation inhibitors are more specific for CDK4/6 leading to better efficacy and less toxicities in clinical studies [26]. Specific CDK4/6 inhibitors include palbociclib (PD-0332991, Pfizer), abemaciclib (LY-2835219, Eli Lilly), and ribociclib (LEE011, Novartis) (Figure 1.5) which were all tested in preclinical studies in vitro and in vivo including animal models for several cancers such as leukemia, breast cancer, melanoma, glioma, pancreatic cancer, hepatocellular carcinoma, lung adenocarcinoma, sarcoma, ovarian cancer, renal cancer, prostate cancer, and MIBC [47].

Preclinical studies with palbociclib showed G1-arrest, dephosphorylation of Rb, a decrease in E2F-dependent gene expression as well as potent inhibition of tumour growth [26]. However, several reports showed that palbociclib was completely inactive in Rb negative cells and tumour

xenografts making Rb expression a prerequisit for sensitivity to these inhibitors [26, 47]. Phase I clinical trials with palbociclib revealed an excellent bioavailability of the drug with a generally low toxicity profile and phase I/II trials with patients with advanced estrogen receptor positive breast cancer demonstrated a significant clinical activity [26]. In 2015, palbociclib was approved by the FDA as a first-line treatment for patients with advanced estrogen receptor positive, human epidermal growth factor receptor 2 (HER2) negative breast cancer in combination with letrozole [26]. Furthermore, ribociclib was designated by the FDA as break through therapy showing similar efficacy and toxicity profiles as palbociclib [47].

Cyclin-Dependent Kinase Inhibitors in Bladder Cancer

Deregulations in the cell cycle is a common feature of MIBC and has therefore therapeutic potential in this malignancy. More than 50% of MIBC show chromosome 9 deletions which affect the tumour suppressor genes encoding for p14 and p16. Inactivating mutations of the Rb gene occur in 11-20% of MIBC indicating that 80% of the patients might benefit from CDK4/6 inhibition [47].

Our group has recently investigated the effects of CDK4/6 inhibition in MIBC [55]. In this study, palbociclib arrested Rb positive cells in G0/G1-phase and efficiently reduced total and phosphorylated Rb levels in a dose dependent manner. The decrease in Rb protein expression was correlated with a reduction in Rb gene expression levels and a reduction in transcription of E2F target genes such as cyclin A2 and cyclin E2 [55]. Moreover, palbociclib reduced tumour cell proliferation in Rb positive cells which was confirmed in a 3D tumour xenograft model using the chicken chorioallantoic membrane [55].

1.5. Aim of the Study

Oncolytic virotherapy has shown to be a promising treatment modality for a variety of cancers. However, the in vivo efficacy is still limited. It was shown before that combination therapies using small molecule inhbitors (target therapies) could improve the effects of oncolytic virotherapy thereby enhancing virus induced cell death, viral replication, and viral particle formation. Patients with BC frequently encounter disease progression, disease recurrence, and treatment failure due to acquired chemoresistance and therefore the development of new therapies for BC is urgently needed. In this work we aimed to

1) investigate whether Chk1 inhibitors could improve Adenovirus induced cell death in BC cell lines.

2) analyse molecular mechanisms underlying the combination therapy with Chk1 inhibitors.

3) investigate whether CDK4/6 inhibitors could improve Adenovirus induced cell death, viral replication, and viral particle formation in BC cell lines.

4) analyse molecular mechanisms underlying the combination therapy with CDK4/6 inhibitors.

5) investigate cellular and viral factors that might be involved in the improved Adenoviral replication.

2. Materials and Methods

2.1. Materials

2.1.1. Multiple Use Equipment

Table 2.1.: Multiple Use Equipment

Equipment	Source
Analytical balance AT250	Mettler Toledo
Analytical balance Sartorius 2254	Sartorius
Autoclave Sytec DX-65	Systec GmbH
Automatic film processor Curix CP1000	Agfa Healthcare
Bag sealer Folio FS3602	Severin Elektrogeräte GmBH
Biological safety cabinet Herasafe KS12	Thermo Scientific
BVC professional laboratory fluid aspirator	Vacuubrand Gmbh
Centrifuge 5810R	Eppendorf GmbH
Centrifuge ROTINA 35R	Hettich
Chemidoc XRS Imaging System	BioRad
CO_2 incubator HERA Cell240	Thermo Scientific
CO_2 incubator HERA Cell240i	Thermo Scientific
Cold light source Leica L2	Leica Microsystems GmbH
Cryogenic freezing container, 1 Deg C	Nalgene
Electrophoresis power supply EPS 601	Amersham Pharmacia Biotech.
Glassware	Schott AG
Heating and drying oven Heraeus FunctionLine B6	Thermo Scientific
Heating and drying oven Heraeus FunctionLine UT20	Thermo Scientific
Heating block thermostat BT100	Kleinfeld Labortechnik
Ice machine Manitowoc	Manitowoc Ice
Intellimixer RM-2L	Elmi Ltd. Laboratory Equipment
Magnetic Stirrer	Heidolph Instruments GmbH
Microcentrifuge 5430R	Eppendorf GmbH
Microcentrifuge QikSpin QS7000 personal	Edwards Instrument Co.
Micropipettes Pipetman	Gilson Inc.
Microplate reader Vmax Kinetic	Molecular Devices

Continued from Table 2.1

Equipment	**Source**
Microscope AxioVert. 135	Carl Zeiss
Microscope AxioVert. A1	Carl Zeiss
Microscope camera AxioCam ERc 5s	Carl Zeiss
Mini protean system	BioRad
Mini protean tetra cell gel system	BioRad
Mini trans-blot cell transfer system	BioRad
Minishaker IKA MS2	IKA Works Inc.
Multilabel plate reader VICTOR X3	Perkin Elmer
Neubauer chamber	LO Laboroptik
Orbital shaker K15	Edmund Buehler GmbH
Perfect blue gelsystem Mini M	PEQLAB Biotechnologie GmbH
pH Meter 691	Metrohm
Power supply PowerPac HC	BioRad
Spectrophotometer Nanodrop 2000c	Thermo Scientific
Stereo microscope Stemi DV4	Carl Zeiss
Thermal cycler C1000 CFX96	BioRad
Thermal cycler iCycler iQ Real-time PCR detection system	BioRad
Thermal cycler MJ Research PTC-200	BioRad
Vortex-Genie 2	Scientific Industries
Water bath W350	Memmert
Water purification system, Purelab	ELGA Lab water

2.1.2. Disposable Equipment

Table 2.2.: Disposable Equipment

Equipment	Source
Amersham hybond-P PVDF-Membrane	GE-Healthcare
Cell culture plates (96-well, 24-well, 12-well, 6-well, 10cm)	Corning Incorporated
Cell culture plates (24-well)	Techno Plastic Products AG
Cell lifter	Sigma Sigma-Aldrich Chemie GmbH
Chromatography paper Whatman	GE-Healthcare
Conical tubes Falcon (15ml, 50ml)	Greiner GmbH
Cryogenic vials Nunc (1.8ml)	Thermo Scientific
Hard-shell PCR plates (96-well)	BioRad
Lens cleaning paper	The Tiffen company
Needles (27 Gauge)	BD Biosciences
PCR reaction tubes (0.5ml)	Biozym Scientific
PCR sealers microseal 'B' film	BioRad
Pipette tips with/ without filter	Sarstedt
Reaction tubes (0.5ml, 1.5ml, 2ml)	Sarstedt
Serological pipettes	Greiner Bio-One International AG
Sterile filter Nalgene (0.25μm, 0.4μm)	Thermo Scientific
Syringes Omnifix (1ml)	B.Braun Melsungen AG
White polystyrene plates (96-well)	Corning Incorporated
X-ray film CEA RP New	Agfa Healthcare

2.1.3. Kits

Table 2.3.: Kits

Kit	Cat. no	Source
CellTiter-blue Cell Viability Assay	G8080	Promega
High-Capacity cDNA Reverse Transcription Kit	4368813	Thermo Scientific
HiSpeed Plasmid Midi Kit	12643	Qiagen
Liquid DAB+ Substrate Chromogen System	K3468	Dako
mirVANA miRNA Isolation Kit	AM1560	Thermo Scientific
Monarch Gel Extraction Kit	T1020S/L	New England Biolabs
Pierce BCA Protein Assay	23225	Thermo Scientific
QIAprep Spin Miniprep Kit	27104	Qiagen
REAL Detection System	K5001	Dako

2.1.4. Chemicals, Reagents, and Enzymes

Table 2.4.: Chemicals, Reagents, and Enzymes

Material	Source
2-Mercaptoethanol	Sigma-Aldrich Chemie GmbH
80% Ethanol	Brueggemann Alcohol Heilbronn GmbH
96% Ethanol	Otto Fischar GmbH
Agarose Ultrapure	Thermo Scientific
Ammonium persulfate (APS)	Sigma-Aldrich Chemie GmbH
Ampicillin	Sigma-Aldrich Chemie GmbH
Boric acid	Sigma-Aldrich Chemie GmbH
Bovine serum albumin (BSA)	Sigma-Aldrich Chemie GmbH
Bromophenol blue	Serva Electrophoresis GmbH
Calcium chloride (CaCl)	Merck Chemicals GmbH
Chloroform	Sigma-Aldrich Chemie GmbH
Color Prestained Protein Standard, Broad Range	New England Biolabs
Complete mini protease inhibitor	Roche
Developing and fixation solutions Vision X GV60	Roentgen bender GmbH & Co. KG
Dimethyl sulfoxide (DMSO)	Sigma-Aldrich Chemie GmbH
Dithiothreitol (DTT)	Cell-Signaling
DNA ladder 2-Log (0.1 to 10kb)	New England Biolabs GmbH
DNA loading buffer (6x)	Thermo Scientific
Dulbecco's Modified Eagle's Medium (DMEM)	Biochrom
E. coli, DH5α	Kindly provided by Prof. Dr. P. S. Holm, Klinikum rechts der Isar der TUM, Germany
Ethanol absolute	Merck Chemicals GmbH
Ethidiumbromide (10mg/ml)	Sigma-Aldrich Chemie GmbH
Ethylenediaminetetraacetic acid (EDTA, 0.5M)	AppliChem
Fetal bovine serum (FBS)	Biochrom
Fugene HD	Promega Corporation
Geneticin	Life Technologies
Glucose	Sigma-Aldrich Chemie GmbH

Continued from Table 2.4

Material	**Source**
Glycine	Sigma-Aldrich Chemie GmbH
GoTaq qPCR master mix	Promega
GoTaq Green PCR master mix	Promega
Hepes	Sigma-Aldrich Chemie GmbH
Hexadimethrine bromide (Polybrene)	Sigma-Aldrich Chemie GmbH
Hydrogen chloride (HCl)	Merck Chemicals GmbH
Hydrogen peroxide (H_2O_2)	Merck Chemicals GmbH
Isocitrate monohydrate	Sigma-Aldrich Chemie GmbH
Isopropanol	Sigma-Aldrich Chemie GmbH
Lipofectamine RNAimax	Invitrogen
Luminol	Sigma-Aldrich Chemie GmbH
Magnesium chloride (MgCl)	Sigma-Aldrich Chemie GmbH
Methanol	Sigma-Aldrich Chemie GmbH
Non-essential amino acids (NEAA, 100x)	Biochrom
Opti-MEM	Invitrogen
p-Coumaric acid	Sigma-Aldrich Chemie GmbH
Penicillin Streptomycin (PS, 100x)	Sigma-Aldrich Chemie GmbH
Phenol Chloroform Isoamyl Alcohol	Sigma-Aldrich Chemie GmbH
Phosphate buffered saline (PBS, 1x, 10x)	Biochrom
Phosphatase inhibitor Mix II	Serva Electrophoresis GmbH
Phusion High-Fidelity PCR Master Mix	Thermo Scientific
Potassium chloride (KCl)	Merck Chemicals GmbH
Precision plus protein standard	BioRad
Proteinase K	Qiagen
Puromycin	Sigma-Aldrich Chemie GmbH
Restriction enzymes and buffers	New England Biolabs
Roswell Park Memorial Institute medium (RPMI)	Biochrom
Rotiphorese gel 30	Carl Roth
Select agar	Sigma-Aldrich Chemie GmbH
Skimmed milk powder	Nestle
Sodium acetate	Merck Chemicals GmbH

Continued from Table 2.4

Material	**Source**
Sodium azide	Sigma-Aldrich Chemie GmbH
Sodium chloride (NaCl)	Merck Chemicals GmbH
Sodium dodecyl sulfate (SDS)	Sigma-Aldrich Chemie GmbH
Sodium orthovanadate	Sigma-Aldrich Chemie GmbH
Sodium phosphate dibasic	Merck Chemicals GmbH
Sulforhodamine B (SRB)	Sigma-Aldrich Chemie GmbH
T4 DNA Ligase	Thermo Scientific
Taq DNA polymerase	Thermo Scientific
Tetramethylethylenediamine (TEMED)	Carl Roth
Trichloroacetic acid (TCA)	Sigma-Aldrich Chemie GmbH
Tris(hydroxymethyl)-aminomethane	Merck Chemicals GmbH
Triton X-100	Sigma-Aldrich Chemie GmbH
Trypan blue (0.5%)	Biochrom
Trypsin/ EDTA	Biochrom
Tween-20	Serva Electrophoresis GmbH
Yeast extract	Sigma-Aldrich Chemie GmbH

2.1.5. Buffers and Solutions

Table 2.5.: Buffers and Solutions

Buffer	Composition
Blocking solution	1% BSA (w/v) in PBS
Chemiluminescence reagent A	0.1M Tris-HCl (pH 8.5) 2.5mM Luminol 0.4mM p-Coumaric acid
Chemiluminescence reagent B	0.1M Tris-HCl (pH 8.5) 0.18% H_2O_2
DNA Lysisbuffer	10mM Tris-HCl (pH 8) 100mM NaCl 25mM EDTA (pH 8) 0.5% SDS
HBS Buffer (2x)	0.27M NaCl 10mM KCl 1.4mM Sodium phosphate dibasic 42mM Hepes 11mM Glucose pH 7.05
Immunoblotting antibody dilution buffer	5% BSA in TBST 0.02% Sodium azide
Immunoblotting blocking solution	5% non-fat milk powder in TBST
LB agar	LB medium 1.5% Select agar 0.1% Antibiotic
LB medium	0.01% Tryptone 0.005% Yeast extract 0.01% NaCl
Protein loading buffer (4x)	0.25M Tris-HCl (pH 6.8) 8% SDS 0.04% Bromophenol blue 40% Glycerine 100μl 1M DTT to 500μl prior to use
SDS page running buffer (10x)	25nM Tris 192mM Glycine 0.1% SDS (w/v)

Continued from Table 2.5

Buffer	**Composition**
SDS protein lysis buffer (1%)	10mM Tris-HCl (pH 7.2) 1% SDS 1mM Na-orthovanadate one Mini-Protease Inhibitor tablet 10μl/ml phosphatase inhibitor prior to use
Separating gel buffer	1.5M Tris pH 8.8
SRB staining solution (0.5%)	0.5% SRB (w/v) in 1% acetic acid
Stacking gel buffer	0.5M Tris pH 6.8
TBE (10x)	1M Tris 1M Boric acid 0.02M EDTA
TBS (10x)	0.5M Tris pH 7.6
TBST	0.1% Tween-20 in TBS (1x)
TCA (100%)	0.3M TCA in 22.7ml dH_2O
TE (0.1x)	0.1% TE (100x, pH 8)
Transfer buffer (10x)	25nM Tris 192mM Glycine
Transfer buffer (1x)	10% Transfer buffer (10x) 20% Methanol
Tris Base (10mM)	1% Tris Base (1M)

2.1.6. Adenovirus Constructs

Table 2.6.: Adenovirus Constructs

Name	Producer
Ad-GFP	Klaus Mantwill, Klinikum rechts der Isar der TUM, Germany
CMV E1B55k RSV E4	Klaus Mantwill, Klinikum rechts der Isar der TUM, Germany
$\triangle$24	Kindly provided by Dirk Nettelbeck, DKFZ, Heidelberg, Germany
$\triangle$24 CMV	Kindly provided by Dirk Nettelbeck, DKFZ, Heidelberg, Germany
E2F mutant	Klaus Mantwill, Klinikum rechts der Isar der TUM, Germany
XVir-N-31	Klaus Mantwill, Klinikum rechts der Isar der TUM, Germany
WT Adenovirus	Kindly provided by David Curiel, Burmingham, Alabama, US

2.1.7. Small Molecule Inhibitors

Table 2.7.: Small Molecule Inhibitors

Name	Target	Stock conc.	Dissolvent	Company
AZD7762	Chk1/2	10mM	DMSO	Selleck Chemicals
LEE011 (Ribociclib)	CDK4/6	10mM	DMSO	Novartis
LY2835219 (Abemaciclib)	CDK4/6	10mM	Water	Selleck Chemicals
Nutlin-3a	MDM-2	5mM	DMSO	Sigma-Aldrich Chemie GmbH
PD-0332991 (Palbociclib)	CDK4/6	10mM	Water	Sigma-Aldrich Chemie GmbH
UCN-01	Chk1, CDK4/6	1mM	DMSO	Sigma-Aldrich Chemie GmbH

2.1.8. Primers

Table 2.8.: Primers

Name	Reference sequence	Company	Forward primer	Reverse primer
β-actin	NC_000007.14	Eurofins	TAAGTAGGTGCAC AGTAGGTCTGA	AAAGTGCAAAGAA CACGGCTAAG
E1A12S	AY339865_1	Metabion	CGACGAGGATGAA GTCCTGTGTCTG	CTCAGGATAGCAG GCGCCAT
E1A12S short	AY339865_1	Metabion	GAGGATGAAGTCC TGTGT	CTCAGGATAGCAG GCGCCAT
E1A13S	AY339865_1	Metabion	TGTTTGTCTACAG TCCTGTGTCTG	CTCAGGATAGCAG GCGCCAT
E1A13S short	AY339865_1	Metabion	TTGTCTACAGTCC TGTGT	CTCAGGATAGCAG GCGCCAT
E2 early	AY339865_2	Invitrogen	CCGTCATCTCTAC AGCCCAT	GGGCTTTGTCAGA GTCTTGC
E2F1 (qPCR)	NC_018931.2	Life Technologies	ACGCTATGAGACC TCACTGAA	TCCTGGGTCAACC CCTCAAG
E2F1 (cloning)	NM_005225.2	Life Technologies	GCGAATTCCGTG AGCGTCATGGCC TTGG	GCGGATCCTCCA AGCCCTGTCAGA AATCC
E2F2	NC_018912.2	Life Technologies	CGTCCCTGAGTTC CCAACC	GCGAAGTGTCATA CCGAGTCTT
E2 late	AY339865_2	Invitrogen	CTTCCTAGCGACT TTGTGCC	GTCAGAGTGGTAG GCAAGGT
E4orf6	AY339865_1	Metabion	TCCCTCCCAACAC ACAGAGT	GACAGGAAACCGT GTGGAAT
Fibre	AY339865_2	Eurofins	AAGCTAGCCCTGC AAACATCA	CCCAAGCTACCAG TGGCAGTA
GAPDH	NM_001256799.2	MWG	TGGCATGGACTGT GGTCATGAG	ACTGGCGTCTTCA CCACCATGG
Rb	NM_000321.2	Life Technologies	AGCAACCCTCCTA AACCACT	TGTTTGAGGTATC CATGCTATCA

2.1.9. siRNAs

Table 2.9.: siRNAs

Name	Sequence	Company
Control (siRNA Negative Control Hi GC Duplex 2)	-	Life Technologies
Ctrl siRNA pool	multiple	siTOOLs Biotech
E2F1 siRNA pool	multiple	siTOOLs Biotech
MDM2 #5	AATCATCGGACTCAGGTACAT	Qiagen
MDM2 #9	CAGGCAAATGTGCAATACCAA	Qiagen
MDM2 #12	CTCTGTCTTAAATGAGAAGTA	Qiagen

2.1.10. Plasmids

Table 2.10.: Plasmids

Name	Cat. no.	Company
pCDH1-CMV-MCS-EF1-Neo	CD514B-1	System Biosciences
pMD2.G (Lentiviral envelope)	12259	Addgene
psPAX2 (Lentiviral packaging)	12260	Addgene

2.1.11. Antibodies

Table 2.11.: Antibodies

Product	Cat. no.	Application	Dilution	Producer
β-actin	A2066	WB	1:1000	Sigma-Aldrich Chemie GmbH
Akt	4685	WB	1:1000	Cell Signaling Technology
phospho Akt (Thr 308)	2965	WB	1:1000	Cell Signaling Technology
phospho Akt (Ser 473)	3787	WB	1:1000	Cell Signaling Technology
Cdc25A	sc-56264	WB	1:1000	Santa Cruz Biotechnology
CDK2	2546	WB	1:1000	Cell Signaling Technology
Chk 1	sc-377231	WB	1:1000	Santa Cruz Biotechnology

Continued from Table 2.11

Product	Cat. no.	Application	Dilution	Producer
phospho Chk 1 (Ser 317)	2344	WB	1:500	Cell Signaling Technology
Cyclin D1	2978	WB	1:1000	Cell Signaling Technology
Cyclin E2	4132	WB	1:1000	Cell Signaling Technology
DP-1	ABIN487311	WB	1:1000	Antibodies online
E1A	sc-25	WB	1:1000	Santa Cruz Biotechnology
E1B55k		WB	1:10	Kindly provided by M. Dobbelstein, Göttingen University, Germany
E2A		WB	1:100	Kindly provided by M. Dobbelstein, Göttingen University, Germany
E2F1	sc-251	WB	1:250	Santa Cruz Biotechnology
E2F2	ab138515	WB	1:1000	Abcam
E2F3	MA5-11319	WB	1:100	Thermo FisherScientific
E2F4	MA5-11276	WB	1:100	Thermo Fisher Scientific
E2F5	sc-999	WB	1:100	Santa Cruz Biotechnology
E4orf6		WB	1:10	Kindly provided by M. Dobbelstein, Göttingen University, Germany
Erk 1/2	9102	WB	1:1000	Cell Signaling Technology
phospho Erk 1/2 (Thr 202/ Tyr 204)	4376	WB	1:1000	Cell Signaling Technology
GAPDH	2118	WB	1:1000	Cell Signaling Technology
Goat-anti-hexon	AB1056	IHC	1:500	Chemicon
Hexon	ABIN2686029	WB	1:1000	Antibodies online
HRP conjugated rabbit-anti-goat	P0449	IHC	1:1000	Dako
c-Myc	OP10	WB	2.5μg/ml	Calbiochem
p21 Waf1/Cip1	2947	WB	1:1000	Cell Signaling Technology
p27 Kip1	3686	WB	1:1000	Cell Signaling Technology
p107	ab209546	WB	1:1000	Abcam

Continued from Table 2.11

Product	Cat. no.	Application	Dilution	Producer
p130	ab76234	WB	1:1000	Abcam
Peroxidase-conjugated anti-mouse IgG	715-036-150	WB	1:10.000	Dianova
Peroxidase-conjugated anti-rabbit IgG	711-036-152	WB	1:10.000	Dianova
Rb	554136	WB	2μg/ml	BD Biosciences
phospho Rb (Ser 780)	8180	WB	1:1000	Cell Signaling Technology

2.1.12. Cell Culture

Cell Lines

Table 2.12.: Cell Lines

Cell line	Source
253J	Kindly provided by W. Schulz, Heinrich-Heine-University, Düsseldorf, Germany
639V	Kindly provided by W. Schulz, Heinrich-Heine-University, Düsseldorf, Germany
647V	Leibniz Institute DSMZ- German collection of microorganisms and cell cultures, Braunschweig, Germany
Hek293	American type culture collection, Manassas, VA, USA
Hek293T	American type culture collection, Manassas, VA, USA
RT112	Leibniz Institute DSMZ- German collection of microorganisms and cell cultures, Braunschweig, Germany
T24	American type culture collection, Manassas, VA, USA
T24 Myc	Kindly provided by PanQi, Klinikum rechts der Isar der TUM, Germany
T24 shRb1	Kindly provided by PanQi, Klinikum rechts der Isar der TUM, Germany
UMUC3	American type culture collection, Manassas, VA, USA

Cell Culture Media

Table 2.13.: Cell Culture Media

Medium	Composition
Culture medium for cells cultured at 5% CO_2	RPMI 5% FBS 1% NEAA 1% PS
Culture medium for cells cultured at 10% CO_2	DMEM 5% FBS 1% PS
Freezing medium	50% RPMI or DMEM 40% FBS 10% DMSO
Infection medium for cells cultured at 5% CO_2	RPMI 1% NEAA 1% PS
Infection medium for cells cultured at 10% CO_2	DMEM 1% PS

2.1.13. Programmes and Software

Table 2.14.: Programmes and Software

Programme	Website
Adobe Illustrator	www.adobe.com/de/products/illustrator.html
Compusyn	www.combosyn.com/
Inkscape	www.inkscape.org/de/release/0.92.2/
LaTeX	www.miktex.org/download
Libre Office	www.libreoffice.org
Microsoft Office	www.microsoft.com/de-de/download/default.aspx
Photoshop	www.adobe.com/de/products/photoshop.html
SerialCloner	www.serialbasics.free.fr/Serial_Cloner-Download.html

2.2. Methods

2.2.1. Cell Culture

Human cell lines were cultured under sub-confluent conditions in RPMI or DMEM medium (Table 2.13) at 37°C and 5% or 10% CO_2, respectively. 647V, RT112, and T24 cell lines were cultured in RPMI medium and 253J, 639V, UMUC3, and Hek293 cell lines were cultured in

DMEM medium. Cells were grown in 10cm plates under sterile conditions and observed daily under the microscope. In order to keep the cells in S-phase, cells were splitted when reaching 70-80% confluency: culture medium was aspirated and cells were washed with PBS containing 1% EDTA (0.5M, pH 8.0). PBS-EDTA was aspirated and cells were briefly incubated with trypsin until they detached from the plate. Fresh medium was added to stop the trypsin reaction and cells were collected in a 15ml Falcon tube. Cells were centrifuged for 5min at 300rcf and the supernatant was aspirated. The pellet was resuspended in fresh medium and a fraction of cells was transferred onto a new plate for further passaging.

Cells were counted using a Neubauer chamber: a small amount of the cell suspension was mixed with trypan blue in a 1:1 ratio and living cells were counted. The number of cells per ml was calculated as follows:

$$Number\ of\ cells/ml = Average\ of\ cells/quadrant * 2 * 10^4$$

Depending on the cell line and experimental conditions, 0.2-1x10^6, 0.5-3x10^5, 0.125-1x10^5 or 500-700 cells were seeded in 10cm, 6-well, 12-well or 96-well formats, respectively.

Cryoconservation of Cell Lines

For cryoconservation, cells were harvested as described before. After centrifugation, the pellet was resuspended in 1ml freezing medium and transferred into cryovials. Cells were frozen in a freezing container containing isopropanol for 1-2 days at -80°C. Afterwards, cells were transferred to liquid nitrogen. When thawing cells, cryovials were thawn in a waterbath at 37°C, immediately mixed with fresh medium, centrifuged, and cultured as described before.

2.2.2. Small Molecule Inhibitor Treatment

Inhibitors were dissolved as described in Table 2.7 and working concentrations were prepared freshly for immediate use. Depending on the solvent used, control cells were treated with DMSO or H_2O using the same concentration as in the highest treatment group.

2.2.3. Cell Viability Assay

Cell viability upon small molecule inhibitor treatment was analysed using CellTiter-Blue assay. Therefore, 500-700 cells were seeded in 96-well plates and treated in triplicates with increasing concentrations of the inhibitors on the following day. After 72h, cell viability was measured: 10μl of CellTiter-Blue reagent were added to each well and absorbance was measured every hour for up to six hours using a multilabel plate reader at 590nm.

2.2.4. Potency Assay and Combination Treatment

The effect of virus induced cell killing alone and in combination with small molecule inhibitors was analysed in 12-well plates. Therefore, 0.25-0.5x10^5 cells were seeded and infected with increasing concentrations (multiplicity of infection, MOI) of the indicated viruses one or two days later. For combination treatment with CDK4/6 inhibitors, cells were treated with the inhibitor 24h before infection and 1 hour post infection (hpi). The Chk1 inhibitors UCN-01 and AZD7762 were added at 1hpi. Cells were infected in triplicates with the indicated viruses in 200μl medium

without FBS. At 1hpi, complete medium with or without small molecule inhibitors was added to the cells. Four days post infection (dpi), cells were washed with PBS, fixed with 10% trichloroacetic acid (TCA) for 1h at 4°C, and stained with sulforhodamine B (SRB) for 20-30min at room temperature (RT), followed by washing with 1% acetic acid to remove excess of SRB. Dried SRB was dissolved in 10mM tris base and quantification was performed by photometric measurement using a multilabel plate reader at 590nm.

2.2.5. Chou-Talalay Method

Synergistic or antagonistic effects on cell viability were assesed using the Chou-Talalay method which determines the efficacy of drug combinations by calculating the combination index (CI) [18, 19]. According to this method, the effect of a single drug is given by the median effect equation

$$\frac{Fa}{Fu} = (\frac{D}{Dm})m$$

in which D is the dose of a drug, Fa is the fraction affected by this dose, and Fu is the fraction unaffected by the dose. Furthermore, Dm resembles the median effect dose with m determining the shape of the dose-effect relationship (m=1 hyperbolic, m>1 sigmoidal, and m<1 flat curves).

From the median effect of the drugs tested alone and in combination with each other, the CI value is calculated as

$$CI = \frac{D_1}{Dx_1} + \frac{D_2}{Dx_2}$$

where Dx in the denominator stands for the doses D1 and D2 when drugs 1 and 2 are used alone to produce an x% effect. In the numerator, the doses D1 and D2 refer to the combination of drug 1 and 2 which also produces an x% effect. CI values were calculated using the CompuSyn software with CI<1 indicating synergism, CI=1 additivity, and CI>1 antagonism [18, 19].

2.2.6. Hexon-Titretest

Infectious viral particle production in bladder cancer cells was measured by a Hexon-Titretest. For this, 0.5-1x10^5 bladder cancer cells were seeded in 6-well plates and pretreated with inhibitors for 24h. Cells were infected with MOI 50 of the indicated viruses in 400μl medium without FBS. At 1hpi, complete medium with or without small molecule inhibitors was added to the cells. At 3dpi, infected cells and supernatant were harvested using cell scrapers and transferred into a 15ml Falcon tube. Virus was released from intact cells by multiple cycles of freeze-thaw followed by centrifugation at 1600rcf for 10min at RT. The supernatant was transferred into fresh tubes and tested for viral particle production using Hek293 cells. For this, 2x10^5 Hek293 cells were seeded in 0.5ml in a 24-well format. Supernatants from bladder cancer cell lines were serially diluted in medium (10^0-10^{-4}) and Hek293 cells were immediately infected in dublicates with 50μl of each dilution. At 2dpi, Hek293 cells not showing any obvious cytopathic effect (CPE), were fixed and stained for viral Hexon protein: the medium was aspirated, cells were dried at RT for approximately 10min, and fixed with 0.5ml 100% ice-cold methanol for 10min at -20°C. Afterwards, cells were washed twice with 0.5ml 1% BSA-PBS and incubated with 250μl of the primary antibody (AB) goat-anti-hexon, diluted 1:500 in 1% BSA-PBS, for 1h at 37°C. The

primary AB was aspirated and cells were washed twice with 0.5ml 1% BSA-PBS. Secondary rabbit-anti-goat AB was diluted 1:1000 in 1% BSA-PBS and cells were incubated with 250μl for 1h at 37°C. To remove the secondary AB, cells were washed twice with 0.5ml 1% BSA-PBS and stained with 250μl DAB staining solution. Infected cells displayed as dark-brown cells wich were counted under the microscope using 20x magnification and the titre (in infectious units per ml, IFU/ml) was calculated as follows:

$$Titre\ (IFU/ml) = \frac{Average\ number\ of\ positive\ cells/field * fields/well}{Volume\ of\ diluted\ virus\ used\ per\ well\ (ml) * dilution\ factor}$$

2.2.7. Viral Replication

Viral replication in bladder cancer cells was analysed by a Fibre-quantitative PCR (qPCR). Using the $\Delta\Delta$CT method (Chapter 2.2.9), the replication of a virus can be calculated from viral DNA copies per cell (normalisation to GAPDH) in relation to the entry level of the virus to the cells (4hpi value).

Seeding, Pretreatment, and Infection of Cells

Bladder cancer cells were seeded in 6-well plates (0.5-1x10^5 per well) and pretreated with inhibitors for 24h. The next day, cells were infected with MOI 50 of the indicated viruses in 400μl medium without FBS. At 1hpi, complete medium with or without small molecule inhibitors was added to the cells. For DNA extraction, cells were harvested at 4-72hpi: the medium was aspirated and cells were washed with PBS. Adherent cells were lysed using 200μl DNA lysisbuffer and cell scrapers and lysates were digested with 3μl Proteinase K for at least 8h at 56°C.

DNA Isolation

DNA was isolated using phenol chloroform extraction method. For this, lysates were mixed with 200μl phenol chloroform isoamyl alcohol and mixed thoroughly by vortexing. The mixture was incubated on ice for 5min and centrifuged for 3min at 16,000rcf, 4°C. The upper phase containing the DNA was carefully removed, transferred into a new tube, and mixed with 200μl chloroform to remove phenol rests. Samples were mixed by vortexing and incubated on ice for 5min. Afterwards, samples were centrifuged for 3min at 16,000rcf, 4°C. The upper phase was removed, transferred into a new tube and mixed with 800μl 100% EtOH, 50μl 3M Na-acetat, and one drop of glycogen to facilitate DNA precipitation. Tubes were thoroughly inverted and centrifuged for 30min at 16,000rcf, 4°C. The supernatant was discarded and DNA pellets were washed with 75% EtOH for 10min at RT followed by centrifugation for 5min at 16,000rcf, RT. The EtOH was discarded and pellets were dried in an incubator at 37°C until they became colourless. The pellet was resuspended in 50μl 0.1x TE buffer and samples were incubated in a thermomixer at 40°C, 400rpm to completely dissolve the DNA. Afterwards, DNA concentrations were measured with a Nano drop and samples were diluted to 10ng/μl for further use in qPCR (Chapter 2.2.9).

2.2.8. Gene Expression Analysis

The expression level of cellular and viral genes upon inhibitor treatment and/or virus infection was analysed by reverse transcription-qPCR (RT-qPCR). RNA was extracted from the cells and

reversely transcribed to cDNA. Changes in gene expression levels were analysed by qPCR, normalising to a housekeeping gene (GAPDH) and untreated control samples ($\Delta\Delta$CT method, Chapter 2.2.9).

Seeding, Pretreatment, and Infection of Cells

Bladder cancer cells were seeded in 6-well plates (0.5-1x10^5 per well) and either treated with the inhibitors for 24-48h or, for determination of viral gene expression, pretreated with inhibitors for 24h. Cells were infected with MOI 50 of the indicated viruses in 400μl medium without FBS. At 1hpi, complete medium with or without small molecule inhibitors was added to the cells. For gene expression analysis, cells were harvested at indicated time points: the medium was aspirated and cells were washed with PBS. Adherent cells were harvested using 200μl mirVANA miRNA Lysisbuffer and cell scrapers.

RNA Extraction

RNA was isolated using phenol chloroform extraction: 200μl acidic phenol chloroform were added to the lysates and mixed thoroughly by vortexing. Afterwards, samples were centrifuged for 15min at 12,000rcf, 4°C. The upper phase containing the RNA was carefully removed and transferred into a new tube. To remove phenol chloroform rests, samples were mixed with 0.5ml isopropanol, incubated on ice for 10min, and centrifuged for 10min at 12,000rcf, 4°C. The supernatant was discarded and RNA pellets were washed with 0.75ml 70% EtOH, followed by centrifugation for 5min at 7,600rcf, 4°C. The supernatant was discarded and the pellet was dried at RT until it became colourless. To dissolve the RNA, the pellet was resuspended in 20μl RNAse-free H_2O and incubated in a thermomixer for 10min at 55°C, 500rpm. RNA concentration was measured by a Nano drop.

Reverse Transcription

For analysis of gene expression levels using qPCR, RNA samples were reversely transcribed to cDNA. For this, a master mix containg reverse transcriptase, deoxynucleoside triphosphates (dNTPs), and random hexamer primers was prepared as shown in Table 2.15. RNA was added and samples were incubated in a multicycler using the programme listed in Table 2.16. Assuming a cDNA concentration of 2μg/20μl, samples were diluted to 10ng/μl for further use in qPCR (Chapter 2.2.9).

Table 2.15.: Master Mix Reverse Transcription

Ingredient	Amount (1x)
RT buffer (10x)	2μl
dNTP mix (25x, 100mM)	0.8μl
RT random primer (10x)	2μl *
MultiScribe Reverse Transcriptase	1μl
RNAse inhibitor	0.8μl
RNA	2μg
H_2O	add 20μl

* For RT of viral genes, gene specifc primer (E2 early rev, E1A fw, E4orf6 fw) at a concentration of 0.1μM instead of random hexamers were used.

Table 2.16.: Reverse Transcription Programme

Step	Temperature	Duration	Process
1	25°C	10 min	Initiation
2	37°C	120 min	Elongation
3	85°C	5 min	Inactivation

2.2.9. qPCR

In order to analyse viral replication or changes in gene expression levels, qPCR was performed using either DNA samples (Chapter 2.2.7) or cDNA samples (Chapter 2.2.8), respectively.

Master mixes for qPCR were prepared as listed in Tables 2.17-2.20. Reactions were carried out in 96-well plates mixing 10μl of the respective master mix and 50ng of either DNA or cDNA (10ng/μl). Plates were sealed with foil, centrifuged briefly, and analysed on a Real-Time PCR detection system using the programmes listed in Table 2.21-2.24. Relative quantification was performed using the comparative $\Delta\Delta$CT method [8, 49]:

$$\Delta CT = CT\ (gene\ of\ interest) - CT\ (house\ keeping\ gene)$$

$$\Delta\Delta CT = \Delta CT\ (treated\ sample) - \Delta CT\ (control\ sample)$$

$$Relative\ normalised\ gene\ expression = 2^{-(\Delta\Delta CT)}$$

For replication analysis, samples were normalised to GAPDH and 4hpi values. For analysis of gene expression, samples were normalised to GAPDH and values of untreated samples.

Table 2.17.: Master Mix qPCR Fibre and Viral Genes

Ingredient	Amount (1x)
GoTaq qPCR master mix	7.5μl
Fibre primer fw (10μM)	0.75μl
Fibre primer rev (10μM)	0.75μl
H_2O	1μl

Table 2.18.: Master Mix qPCR Rb

Ingredient	Amount (1x)
GoTaq qPCR master mix	5μl
Rb primer fw (10μM)	0.25μl
Rb primer rev (10μM)	0.25μl
H_2O	4.5μl

Table 2.19.: Master Mix qPCR E2Fs

Ingredient	Amount (1x)
GoTaq qPCR master mix	5μl
E2F primer fw (10μM)	0.5μl
E2F primer rev (10μM)	0.5μl
H_2O	4μl

Table 2.20.: Master Mix qPCR GAPDH

Ingredient	Amount (1x)
GoTaq qPCR master mix	7.5μl
GAPDH primer fw (10μM)	0.375μl
GAPDH primer rev (10μM)	0.375μl
H_2O	1.75μl

Table 2.21.: qPCR Programme for Fibre

Step	Temperature	Duration	Process
1	94°C	120 sec	Initiation
2	94°C	15 sec	Denaturation
3	60°C	15 sec	Annealing
4	72°C	15 sec	Polymerase activity (go to step 2, 45x)

Table 2.22.: qPCR Programme for Viral Genes

Step	Temperature	Duration	Process
1	94°C	90 sec	Initiation
2	94°C	15 sec	Denaturation
3	58°C	15 sec	Annealing
4	72°C	15 sec	Polymerase activity (go to step 2, 45x)

Table 2.23.: qPCR Programme for Rb

Step	Temperature	Duration	Process
1	94°C	120 sec	Initiation
2	94°C	15 sec	Denaturation
3	60°C	30 sec	Annealing
4	72°C	60 sec	Polymerase activity (go to step 2, 44x)

Table 2.24.: qPCR Programme for E2Fs

Step	Temperature	Duration	Process
1	95°C	120 sec	Initiation
2	95°C	15 sec	Denaturation
3	60°C	30 sec	Annealing
4	72°C	30 sec	Polymerase activity (go to step 2, 40x)

2.2.10. Immunoblotting

The expression level of cellular and viral proteins upon inhibitor treatment and/or virus infection was analysed by immunoblotting. For this, proteins were extracted from the cells, subjected to gel electrophoresis, blotted onto a membrane and incubated with ABs against the desired protein. Using a chemiluminescent reaction, proteins were visualised by autoradiography [46].

Seeding, Pretreatment, and Infection of Cells

Bladder cancer cells were seeded in 10cm plates (0.2-1x10^6 cells). For expression analysis of cellular proteins, cells were treated daily with the inhibitors or corresponding control. For determination of viral or cellular proteins upon virus infection, cells were pretreated with inhibitors for 24h and infected with MOI 50 of the indicated viruses in 2ml medium without FBS. At 1hpi, complete medium with or without small molecule inhibitors was added to the cells.

Preparation of Protein Lysates

At indicated time points, protein lysates were prepared on ice: the medium was aspirated and cells were washed twice with ice-cold PBS. The PBS was aspirated thoroughly and cells were harvested using 400-500μl 1% SDS lysis buffer containing phosphatase and protease inhibitors and cell scrapers. To break down DNA molecules and to remove the viscosity, shear forces were applied to the samples using a 27-gauge needle. Afterwards, samples were centrifuged for 30min at 30,000rcf, 4°C. The supernatant was transferred into new tubes and samples were either used for subsequent immunoblotting or stored at -80°C [46].

BCA Assay

Quantifcation of protein samples was performed by a BCA assay according to the manual. A BSA standard series was prepared and 112.5μl working reagent (mixture of Part A and B in a 50:1 ratio) were pipetted into a 96-well plate. In dublicates, 12.5μl of BSA standard or samples were added to the reagent and the plate was incubated in an incubator for 30min at 37°C. Afterwards, the absorbance was measured at 562nm and the protein concentration was calculated using the BSA standard reference curve. Samples were adjusted to equal protein concentrations by dilution with lysis buffer. For denaturation and immunoblotting, a mixture of 4x protein loading buffer and DTT was prepared and added to the adjusted samples followed by boiling of the samples for 5min at 100°C.

SDS Gel Electrophoresis

Depending on the protein size and the desired separation of the proteins, a 6, 8, 10, 12 or 15% separating gel was used. As an example, the composition of a 15% gel is shown in Table 2.25. The stacking gel was poured into gel casting chambers and covered with isopropanol to ensure proper demarcation and polimerisation. The stacking gel was prepared as described in Table 2.26. The isopropanol was removed, the stacking gel was poured on top of the separating gel, and a comb was inserted. Completely polimerised gels were fixed in the gel electrophoresis system and protein samples as well as a protein standard ladder were loaded onto the gel. Electrophoresis was carried out in 1x SDS page running buffer at 90V until the samples had entered the separating gel and then continued at 150V [46].

Table 2.25.: 15% Polyacrylamide Separating Gel

Ingredient	**Volume (ml)**
H_2O	2.45
Tris (1.5M, pH 8.8)	2.5
Acrylamide (30%)	5
APS (10%)	0.05
TEMED	0.01
Total	10

Table 2.26.: Polyacrylamide Stacking Gel

Ingredient	**Volume (ml)**
H_2O	3.07
Tris (0.5M, pH 6.8)	1.25
Acrylamide (30%)	0.65
APS (10%)	0.025
TEMED	0.005
Total	5

Protein Transfer and Blocking

Proteins were transferred onto a PVDF membrane: the membrane was activated in methanol for 2-5min and blotting paper and sponges were preincubated in blotting buffer. The stacking gel was removed and the separating gel was incubated in blotting buffer to remove excess of the running buffer. The separating gel and the membrane were assembled between two layers of blotting paper and sponges and the transfer was carried out in cold 1x transfer buffer for 1-2h at 100V. Afterwards, the membrane was transferred into a 50ml Falcon tube and blocked for nonspecific binding by incubation in blocking solution for 1h at RT [46].

Immunodetection

Primary ABs against the desired protein were diltuted as described in Table 2.11. After blocking, membranes were washed with TBST and incubated with the ABs overnight at 4°C. The next day, membranes were washed several times with TBST and incubated with the secondary AB, diluted in blocking solution, for 30min at RT. Membranes were washed with TBST and proteins were

detected using the ECL reaction. Chemiluminescent signals were visualised by autoradiography films [46].

2.2.11. siRNA Transfection

Transient gene knockdown was performed by reverse transfection of bladder cancer cells with siRNA. Transfection reagents and amounts for 24- and 6-well plates are listed in Table 2.27. First, a 50nM siRNA predilution stock was prepared and respective amounts were mixed with Opti-MEM (column 2 and 3) resulting in a final siRNA concentration of 1nM. Secondly, RNAiMax transfection reagent was mixed with Opti-MEM (column 4 and 5). Both mixes were thoroughly vortexed and briefly centrifuged. Next, a transfection mix was prepared by combining siRNA and RNAiMax dilutions (step 1 and 2) in a 1:1 ratio. The mix was vortexed, centrifuged, and incubated for 5min at RT. Afterwards, the mix was transferred to the bottom of the cell culture plate. Cells were harvested and counted as described in Chapter 2.2.1 and added to the plates. Finally, cells were gently mixed with the transfection reagent by pipetting.

Table 2.27.: siRNA Transfection

Plate	**OptiMEM** (siRNA dilution)	**siRNA** (50nM)	**OptiMEM** (RNAiMax dilution)	**RNAi Max**	**Transfection mix/well**	**Cell number**	**Total** (ml)
6-well	210μl	40μl *	246μl	4μl	500μl	3x10^5 in 1500μl	2
24-well	40μl	10μl *	49μl	1μl	100μl	6x10^4 in 400μl	0.5

* siRNA final concentration 1nM

2.2.12. Production of E2F1 Overexpressing Cells

In order to overexpress E2F1 in bladder cancer cells, the gene was cloned into a plasmid containing a Cytomegalie virus (CMV) promoter (pCDH1-CMV-MCS-EF1-Neo). For this, cDNA was amplified using gene specific primers and the PCR product was purified and cloned into the vector. Lentivirus was produced in Hek293T cells and bladder cancer cells were infected with the virus and selected by antibiotic selection.

Cloning

cDNA was obtained from untreated RT112 cells as described in Chapter 2.2.8. For amplification of E2F1, gene specific primers listed in Table 2.8 were used. To ensure proper gene amplification, a high-fidelity polymerase was used and a PCR mix was prepared as shown in Table 2.28. As the gene sequence of E2F1 is rich in G and C nucleotides, DMSO was added to the master mix to facilitate denaturation and annealing of the primers.

In order to reduce unspecific binding of the primers and thus unspecific PCR products, a touchdown PCR was performed as shown in Table 2.29.

Table 2.28.: Master Mix E2F1 PCR

Ingredient	Amount
Phusion High-Fidelity PCR Master Mix (2x)	10μl
E2F1 primer fw	1μl
E2F1 primer rev	1μl
DMSO	1μl
cDNA	50ng
H_2O	add 20μl

Table 2.29.: Touchdown PCR Programme

Step	Temperature	Duration	Process
1	98°C	90 sec	Initiation
2	98°C	10 sec	Denaturation
3	68°C	15 sec	Annealing (decrease by 1°C every cycle)
4	72°C	45 sec	Polymerase activity (go to step 2, 10x)
5	98°C	10 sec	Denaturation
6	58°C	15 sec	Annealing
7	72°C	45 sec	Polymerase activity (go to step 5, 40x)
8	72°C	60 sec	Final elongation

The PCR products were loaded onto a 1% agarose gel (1g agarose in 100ml TBE (1x), 0.005% ethidiumbromide) and run at 100V for approximately 1h. Bands at the expected size of 1300bp were cut out from the gel and purified using a Monarch Gel Extraction Kit according to the manual. Extracted DNA was eluted in H_2O and concentration was measured with a Nano drop.

The pCDH1-CMV-MCS-EF1-Neo vector (Table 2.10) was digested with Swa I as shown in Table 2.30 and the reaction was carried out at RT for 1h, followed by 10min at 37°C to dephosphorylate DNA ends. Afterwards, 170μl 0.1X TE buffer were added to the reaction and DNA was extracted using phenol chloroform extraction as described in Chapter 2.2.7. In the end, DNA pellets were dissolved in 20μl 0.1X TE buffer.

Table 2.30.: Vector Digestion

Ingredient	Amount
Buffer 3.1	3μl
Swa I	1μl
Fast AP	1μl
Vector	2μl
dH_2O	add 30μl

The E2F1 PCR product was cloned into the digested vector using T4 ligase and a ligation mix was prepared as shown in Table 2.31. The reaction was carried out for 1h at RT, followed by subsequent transformation of DH5α bacteria: 2μl of the ligation mix were added to 50μl

bacteria and the mix was incubated for 10min on ice, followed by a heat-shock for 40sec at 42°C, and another incubation on ice for 5min. Afterwards, 200μl LB medium were added to the bacteria and they were shaken for 1h at 37°C. Finally, the bacteria suspension was plated on LB ampicillin plates and incubated over night at 37°C.

Table 2.31.: Vector Ligation

Ingredient	Amount
Buffer (10x)	2μl
T4 ligase	2μl
Vector (digested)	6μl
PCR product (insert)	10μl

Colony Screen

The next day, colonies on the plate were picked and analysed by a colony screen for integration of the target gene. For this, a master mix was prepared as shown in Table 2.32. Colonies were picked with a pipette tip and the tip was transferred to the PCR tubes containing the master mix for addition of DNA. For amplification of clones, the tip was then transferred to a tube containing 300μl LB medium and tubes were shaken at 37°C. The PCR was performed according to the programme listed in Table 2.33 and samples were loaded onto an agarose gel as described before.

Table 2.32.: Master Mix Colony Screen

Ingredient	Amount
GoTaq Green PCR master mix (2x)	10μl
E2F1 qPCR primer fw	1μl
E2F1 qPCR primer rev	1μl
DMSO	1μl
dH_2O	add 20μl

Table 2.33.: PCR Programme for Colony Screen

Step	Temperature	Duration	Process
1	95°C	120 sec	Initiation
2	95°C	40 sec	Denaturation
3	60°C	40 sec	Annealing
4	72°C	40 sec	Polymerase activity (go to step 2, 35x)
5	72°C	60 sec	Final elongation

Plasmid Amplification

Positive clones, empty vector plamids which served as controls, as well as plasmids for lentivirus production (Table 2.10) were amplified in 10 or 100ml LB medium containing 0.1% ampicillin over night at 37°C. The next day, bacteria were harvested by centrifugation and a mini or midi prep was performed, respectively, according to the manual.

Lentivirus Production

Lentivirus was produced in Hek293T cells and cells were transfected with lentiviral plasmids using calcium phosphate precipitation. For this, 2-2.5x10^6 Hek293T cells were seeded in a 10cm dish and transfected with the plasmids the following day. The calcium phosphate precipitation mix was prepared as shown in Table 2.34. All ingredients were mixed thoroughly and kept at RT for 20-25min. Afterwards, 1ml was added dropwise on the cells and mixed gently with the medium. Six to eight hours after transfection, the medium was aspirated and 6ml fresh medium were added to the cells. Two days after transfection, the medium containing the assembled lentivirus was collected in a 15ml Falcon tube and centrifuged for 5min at 3000rcf. Cell debris was removed by filtering through a 0.45 μm filter.

Table 2.34.: Calcium Phosphate Precipitate

Ingredient	**Amount**
Transfer vector	20μg
Packaging plasmid	15μg
Envelope plasmid	6μg
dH_2O	add 500μl
HBS (2x)	500μl
CaCl (2.5M)	50μl

Lentivirus Infection and Production of Stable Cell Lines

For infection, 1x10^6 bladder cancer cells were seeded one day before infection in 10cm plates. The next day, cells were infected with 1ml virus and polybrene at a final concentration of 8μg/ml was added to the cells to facilitate infection. One day after infection, cells which had integrated the virus and subsequently the Neomycin resistence gene were selected with Geneticin using 0.5mg/ml. Cells were kept under selection for approximately one week, until uninfected control cells were completely dead.

3. Results

3.1. Effects of Oncolytic Virotherapy on Bladder Cancer Cell Lines

The potential of the oncolytic Adenovirus XVir-N-31 on human bladder cancer cell lines was analysed by a potency assay on six human bladder cancer cell lines. As shown in Figure 3.1, all tested cell lines showed a decrease in cell viability upon increasing MOIs of the virus. 647V, 253J, and UMUC3 cells were highly susceptible for the virus as low MOIs of <15 were sufficient to cause a decrease in cell viability. T24 cells showed a decrease in cell viability at MOIs of >40 and were therefore considered to be intermediately susceptible. 639V and RT112 cells in contrast, were relatively resistant as high MOIs of >100 and >300, respectively were necessary to cause a virus induced cell death. These differences in infectivity might be due to different CAR expression levels on the cell surface with T24, 639V, and RT112 expressing low to almost no CAR (personal communication, AG Holm).

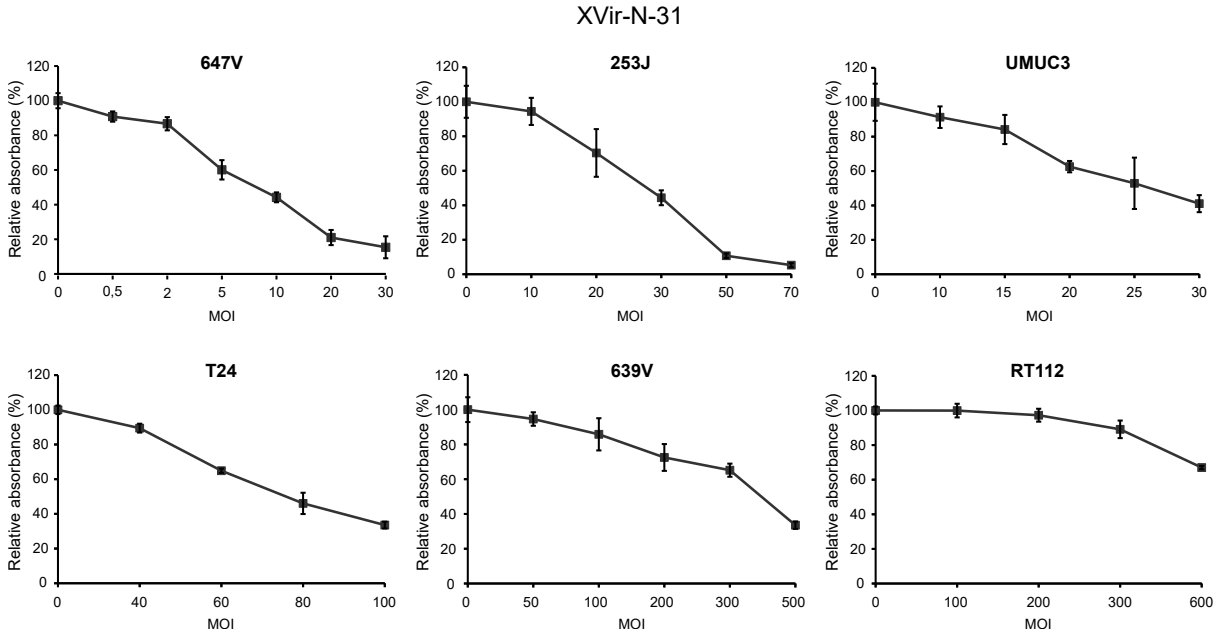

Figure 3.1.: **Oncolytic Virotherapy Is Effective in Human Bladder Cancer Cell Lines.** Bladder cancer cell lines were infected with increasing MOIs of the oncolytic Adenovirus XVir-N-31 and cell viability was analysed at 4dpi. Error bars S.D.

3.2. Combining Oncolytic Virotherapy with Chk1 Inhibition

In 2011, a study by Connell et al showed that Chk1 inhibition by UCN-01 could increase the effects of oncolytic virotherapy in ovarian cancer cells in vitro and in vivo [21]. Therefore, we sought to investigate whether Chk1 inhibition by UCN-01 could also increase the effects of XVir-N-31 in bladder cancer cell lines. As UCN-01 is a non-specific inhibitor with effects on targets other than Chk1 [2, 26], the second generation Chk1 inhibitor AZD7762 was tested in parallel.

3.2.1. Chk1 Inhibitors Efficiently Decrease Cell Viability in Bladder Cancer Cell Lines

First, the two Chk1 inhibitors UCN-01 and AZD7762 were tested in monotherapy for their effects on cell viability in the three bladder cancer cell lines T24, RT112, and UMUC3. As shown in Figure 3.2a, UCN-01 efficiently decreased cell viability at low nano molar concentrations with IC_{50} values of approximately 40-70nM for all cell lines. For further combination experiments with UCN-01, a concentration of 20nM was chosen for UMUC3 and T24 and 40nM were chosen for RT112 as these concentrations had a low effect on cell viability. AZD7762 decreased cell viability more efficiently in T24 cells compared to UMUC3 and RT112 cells with IC_{50} values of approximately 200 and 400nM, respectively (Figure 3.2b). For further combination experiments with AZD7762, a concentration of 80nM with a low effect on cell viability was chosen for T24, UMUC3, and RT112 cells.

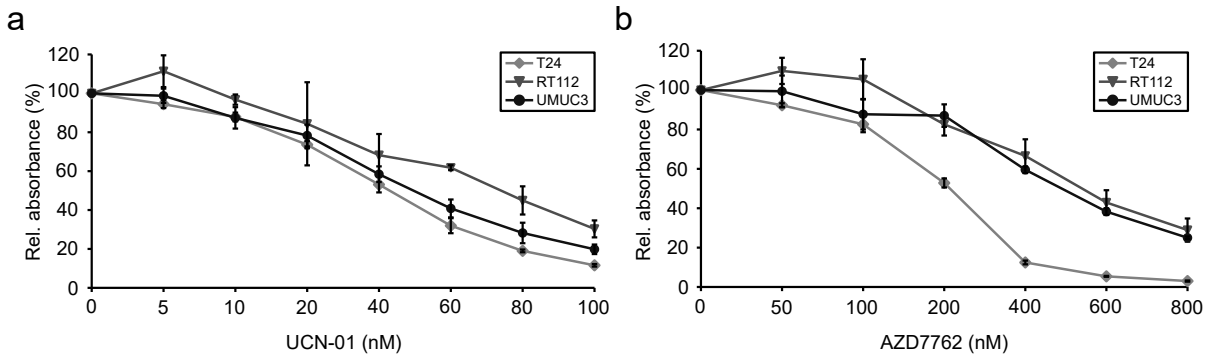

Figure 3.2.: **Chk1 Inhibition Decreases Cell Viability in Rb Positive Cell Lines.** To test the effect of Chk1 inhibition on bladder cancer cells, T24, RT112, and UMUC3 cells were treated with increasing concentrations of UCN-01 (a) or AZD7762 (b) and cell viability was analysed after 72h. Error bars S.D.

3.2.2. UCN-01 Has Effects on Other Pathways Besides Chk1

The biochemical activity of UCN-01 and AZD7762 on Chk1 and pChk1 expression was analysed by immunoblotting. As shown in Figure 3.3a, expression of total Chk1 decreased upon treatment with >20nM UCN-01. Due to the release of a negative feedback loop by Chk1 inhibition, the expression of pChk1 increased upon treatment with 5-20nM UCN-01 indicating activity of the inhibitor on Chk1 at these concentrations. The expression level of the downstream target Cdc25A was only slightly increased upon UCN-01 treatment. As UCN-01 is known to have activities against Chk1 as well as against several CDKs, AKT, and protein kinase C [26], we also investigated the effects of UCN-01 on Rb and E2F1 expression levels because both proteins are involved in Adenovirus biology and play an important role in cell cylce progression. Figure 3.3a shows that UCN-01 downregulated total Rb and pRb levels at concentrations >20nM. This downregulation of pRb levels was already described earlier [1, 26, 61]. Expression levels of E2F1 were not affected by UCN-01.

As shown in Figure 3.3b, the specific Chk1 inhibitor AZD7762 efficiently inhibited Chk1 activity as the expression of Chk1 and Cdc25A increased upon treatment with >10nM and the expression of pChk1 increased upon concentrations of 80nM. In contrast to UCN-01, AZD7762 had no effects on Rb, pRb or E2F1 expression indicating higher specificity of this inhibitor.

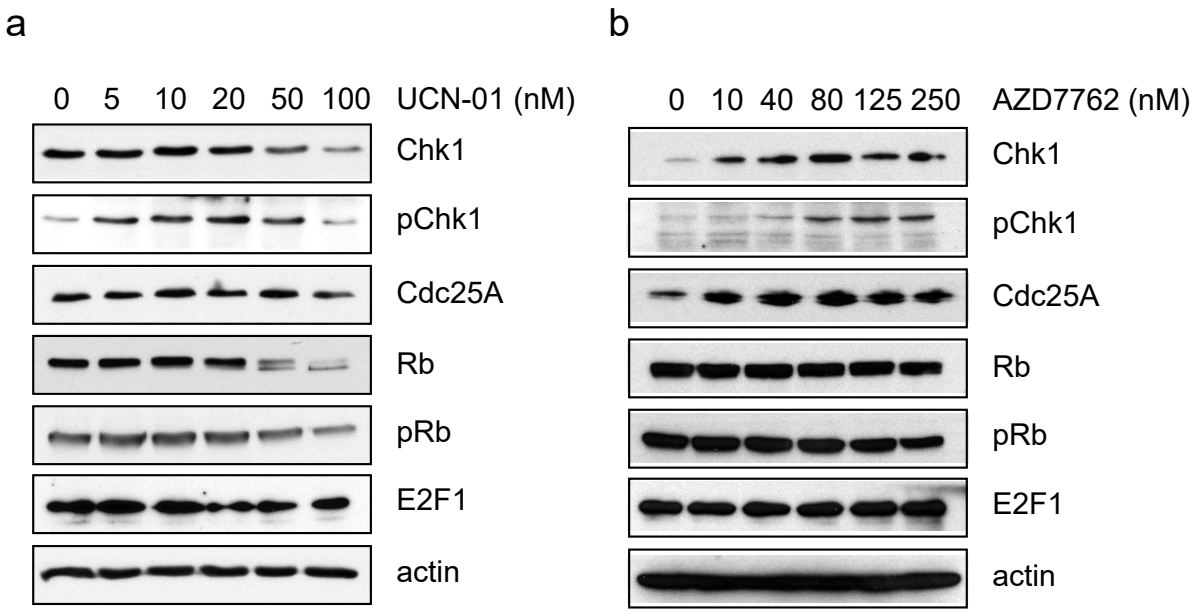

Figure 3.3.: **UCN-01 but not AZD7762 Inhibits Chk1 and Rb.** T24 cells were treated with increasing concentrations of UCN-01 (a) or AZD7762 (b) and protein expression was analysed after 24h.

3.2.3. Chk1 Inhibition by UCN-01 Increases Virus Induced Cell Death in Rb Positive Cell Lines

Secondly, a combination therapy using XVir-N-31 and the Chk1 inhibitor UCN-01 was performed. For this, RT112, T24, UMUC3, and 253J cells were treated with UCN-01 and/or infected with XVir-N-31 using MOIs with a low effect on cell viability. Low concentrations of the inhibitor and the virus were chosen to obtain maxium effects in the combination treatment. As shown in Figure 3.4, the combination with UCN-01 had an additional effect on cell viability of 37% for RT112, 61% for T24, 52% for UMUC3, and 67% for 253J cells, respectively compared to XVir-N-31 alone.

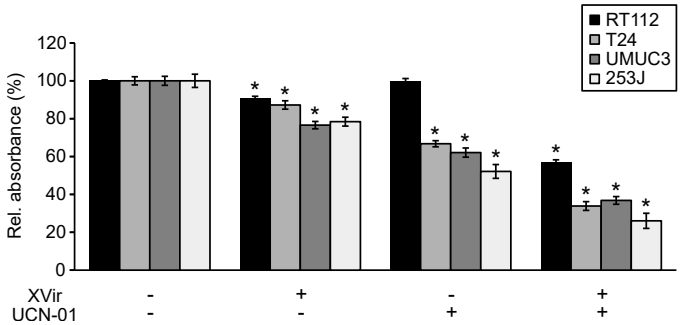

Figure 3.4.: **Chk1 Inhibition by UCN-01 Increases Virus Induced Cell Death in Rb Positive Cell Lines.** RT112 were treated with 40nM UCN-01 and infected with MOI 400 of XVir-N-31. T24 and UMUC3 cells were treated with 20nM UCN-01 and/or infected with MOI 40 and 20, respectively. 253J cells were treated with 10nM UCN-01 and infected with MOI 20 of XVir-N-31. Cell viability was assessed at 4dpi. Values are averages of at least two independent experiments. Error bars S.E., $p<0.05$.

3.2.4. Chk1 Inhibition by UCN-01 Does not Increase Virus Induced Cell Death in Rb Negative Cell Lines

The Rb protein plays an important role in the Chk1 pathway and we therefore sought to investigate whether Chk1 inhibition by UCN-01 could also increase virus induced cell death in the two Rb negative cell lines 647V and 639V. As described before, 647V and 639V cells were treated with UCN-01 and/or infected with XVir-N-31 using MOIs with a low effect on cell viability. As shown in Figure 3.5, Rb negative cells were resistant to UCN-01 treatment also at high concentrations of the inhibitor and the combination could not increase virus induced cell death in these cell lines.

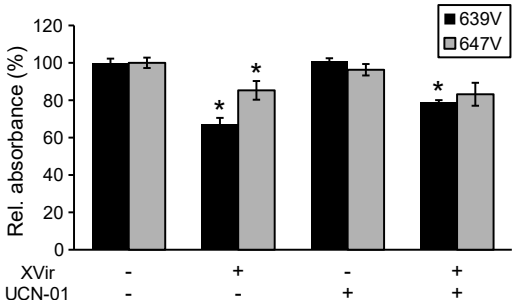

Figure 3.5.: **Chk1 Inhibition by UCN-01 Does not Increase Virus Induced Cell Death in Rb Negative Cell Lines.** 647V and 639V cells were treated with UCN-01 (20nM) and/or infected with XVir-N-31 (MOI 2 and 200, respectively). Cell viability was assessed at 4dpi. Values are averages of at least two independent experiments. Error bars S.E., $p<0.05$.

3.2.5. Specific Chk1 Inhibition Does not Increase Virus Induced Cell Death

UCN-01 is a non-specific Chk1 inhibitor with effects on targets other than Chk1 [2, 26] and we therefore wanted to invstigate whether the increase in virus induced cell death upon combination treatment with UCN-01 were due to Chk1 inhibition or due to other, non-specific effects of UCN-01. To test this, we combined the specific Chk1 inhibitor AZD7762 with XVir-N-31 (Figure 3.6): T24, UMUC3, and RT112 cells were treated with AZD7762 and/or infected with MOIs of XVir-N-31 that had a low effect on cell viability. As shown in Figure 3.6, the combination with the specific Chk1 inhibitor AZD7762 could not increase the oncolytic effects of XVir-N-31. Thus, the effects upon combination with UCN-01 might be due to non-specific effects of the inhibitor on targets other than Chk1.

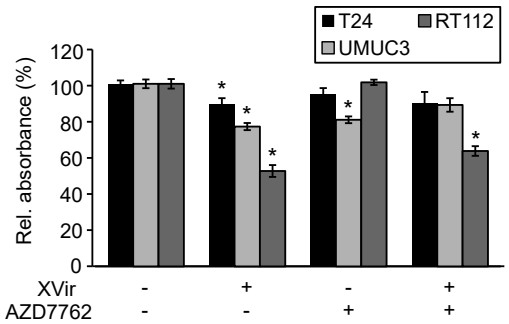

Figure 3.6.: **Chk1 Inhibition by AZD7762 Does not Increase Virus Induced Cell Death in Rb Positive Cell Lines.** T24, UMUC3, and RT112 cells were treated with AZD7762 (80nM) and/or infected with XVir-N-31 (MOI 40, MOI 20, and MOI 400, respectively). Cell viability was assessed at 4dpi. Values are averages of at least two independent experiments. Error bars S.E., $p<0.05$.

3.2.6. Chk1 Inhibitors have Synergistic or Antagonistic Effects on Oncolytic Virotherapy

As treatment with UCN-01 showed an additional effect on cell viability in combination with XVir-N-31, we sought to investigate whether higher or lower concentrations of UCN-01 and/or higher or lower MOIs of XVir-N-31 had the same effect and whether these combinations were synergistc. For this, the four bladder cancer cell lines T24, UMUC3, RT112, and 253J cells were treated with up to four different doses of UCN-01 and up to five different MOIs of the virus. Every dose of the inhibitor was combined with every MOI of the virus and the combination index (CI) was calulated as described in Chapter 2.2.5.

T24 and UMUC3 cells were treated with UCN-01 at 10, 20, 40, and 60nM. T24 cells were infected with XVir-N-31 at MOI 40, 60, 80, 100, and 110 and UMUC3 cells were infected with MOI 10, 15, 20, and 25. As shown in Figure 3.7a and b, combinations for T24 and UMUC3 cells resulted in CI values between 0.23-0.72 and 0.43-0.89, respectively. RT112 cells were treated with UCN-01 at 10, 20, and 40nM and infected with XVir-N-31 at MOI 200, 300, and 400. For these cells, combinations resulted in CI values of 0.02-0.79 (Figure 3.7c). 253J cells were treated with UCN-01 at 5 and 10nM and infected with XVir-N-31 at MOI 10, 15, and 20. The CI values for combinations in this cell line were between 0.33-0.71 (Figure 3.7d). As CI values for all four cell lines were below one, the effect of UCN-01 was considered to be synergistic in combination with XVir-N-31.

As shown before, the specific inhibitor AZD7762 did not cause any additional effects in cell viability in combination with the virus and we therefore sought to combine different concentrations of AZD7762 with different concentrations of XVir-N-31 to see whether higher concentrations might have an additional effect. As described before, bladder cancer cell lines were treated with up to four different doses of AZD7762 and up to five different MOIs of the virus. Every dose of the inhibitor was combined with every MOI of the virus and the CI was calculated. T24 and UMUC3 cells were treated with AZD7762 at 80, 100, 250, and 300nM. T24 cells were infected with XVir-N-31 at MOI 40, 60, 80, 100, and 110 and UMUC3 cells were infected with MOI 10, 15, 20, and 25. As shown in Figure 3.7a and b, combinations with AZD7762 resulted in CI values of 0.72-1.41 for T24 and 1.54-3.91 for UMUC3 cells. RT112 cells were treated with AZD7762 at 80, 250, and 300nM and infected with XVir-N-31 at MOI 200, 300, and 400. For these cells,

combinations resulted in CI values of 0.9-1.62 (Figure 3.7c). Thus, combinations with AZD7762 showed rather additive or antagonistic effects on virus induced cell death, especially in UMUC3 cells.

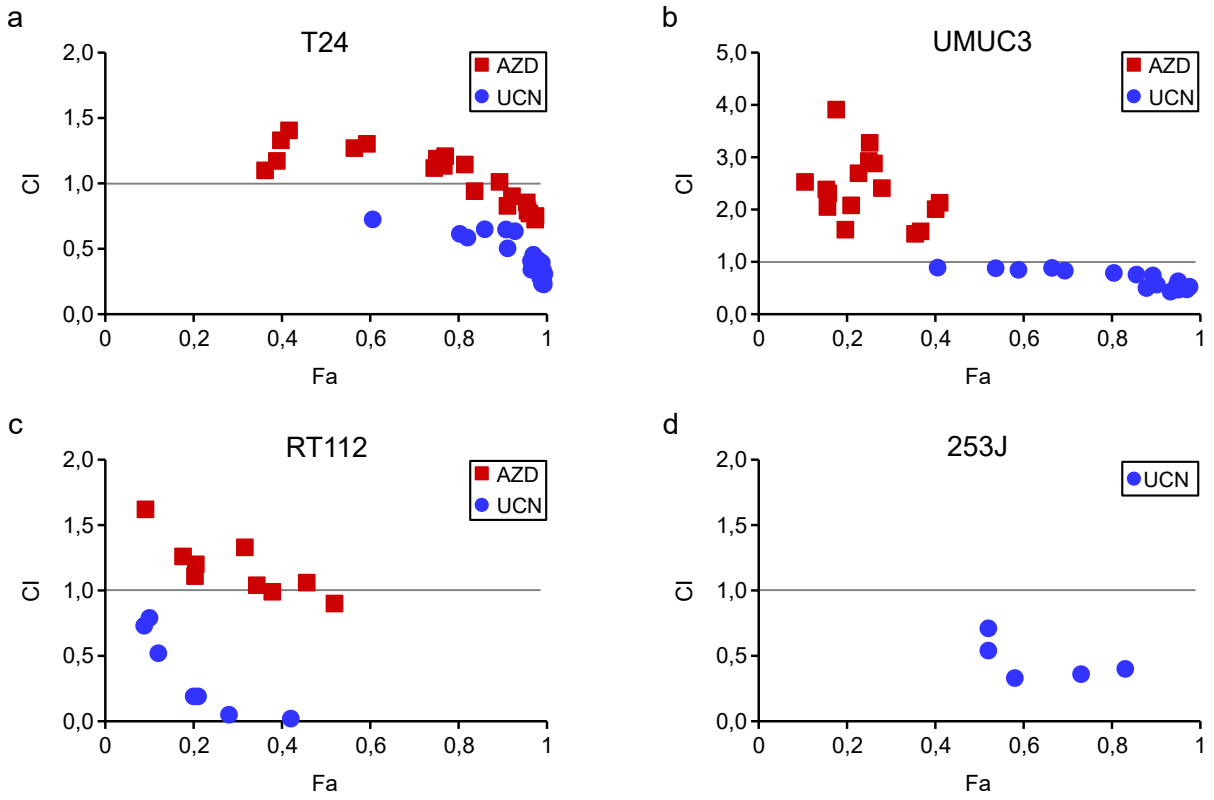

Figure 3.7.: **Synergistic or Antagonistic Effects in Combination with UCN-01 or AZD7762.** Bladder cancer cell lines were treated with different concentrations of UCN-01 (blue circles) or AZD7762 (red squares) and infected with different MOIs of XVir-N-31. X-axes show the Fraction affected (Fa) by the combination and Y-axes show the CI values (note the different scale for UMUC3). Each combination is represented by one dot/square. Values indicate synergism, additivity or antagonism if CI<1, CI=1 or CI>1 [18, 19]. The line indicates a CI value of one.

3.3. Combining Oncolytic Virotherapy with CDK4/6 Inhibition

UCN-01 is a non-specific inhibitor with activities against several pathways including CDK4/6 [2, 26]. As UCN-01 but not AZD7762 treatment strongly affected Rb and pRb protein expression (Figure 3.3) similar to other CDK4/6 inhibitors [1, 2, 55, 61], we next tested whether the enhanced virus induced cell death in combination with UCN-01 was due to effects on the CDK4/6 pathway. For this, the specific CDK4/6 inhbitors PD-0332991 (palbociclib), LY2835219 (abemaciclib), and LEE011 (ribociclib) were tested in combination with oncolytic virotherapy.

3.3.1. CDK4/6 Inhibitors Are Efficient in Bladder Cancer Cells

First, the three CDK4/6 inhibitors were tested in monotherapy for their effects on cell viability in T24 cells. As shown in Figure 3.8a and b, PD-0332991 and LY2835219 efficiently decreased cell viability with IC_{50} values of approximately 500nM. LEE011 in contrast did not completely kill T24 cells as higher doses of >5μM did not further reduce cell viability by >40-50% (Figure 3.8c). For

further combination experiments, concentrations of 500-1000nM were chosen for PD-0332991 and LY2835219. For LEE011, concentrations of 5-10μM were chosen.

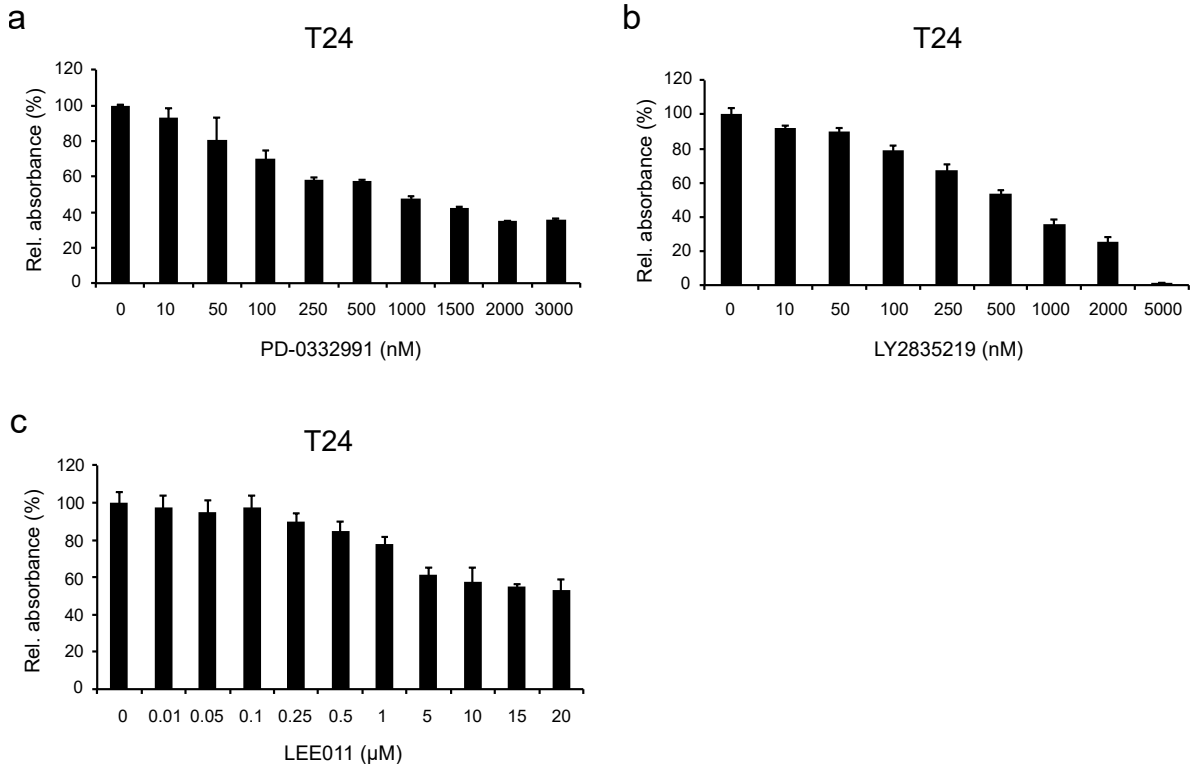

Figure 3.8.: **CDK4/6 Inhibition Efficiently Decreases Cell Viability.** To test the effect of CDK4/6 inhibition on T24 bladder cancer cells, cells were treated with increasing concentrations of PD-0332991 (a), LY2835219 (b) or LEE011 (c) and cell viability was analysed after 72h. Error bars S.D.

In a next step, the biochemical effects on cell cycle proteins upon CDK4/6 inhibition were analysed. For this, T24 cells were treated with PD-0332991 (0.5 or 1μM), LY2835219 (1μM) or LEE011 (10μM) for up to three days and expression of several cell cycle proteins was analysed. As shown in Figure 3.9, CDK4/6 inhibition decreased expression of E2F1 at day one. However, upon treatment with 1μM PD-0332991/LY2835219 or 10μM LEE011, E2F1 protein expression was upregulated again starting from day two. Interestingly, expression was not upregulated again with 0.5μM PD-0332991. E2F2 expression was not changed upon CDK4/6 inhibition while E2F3 was upregulated upon time with all three inhibitors tested. E2F4 and E2F5 were differentially regulated upon CDK4/6 inhibition. Expression of CDK2 was not majorly affected by CDK4/6 inhibition while cyclin D1 was upregulated and cyclin E1 was downregulated upon time. Expression of Rb and pRb decreased at day one but started to come back at day two upon treatment with 1μM PD-0332991/LY2835219 or 10μM LEE011 but not with 0.5μM PD-0332991.

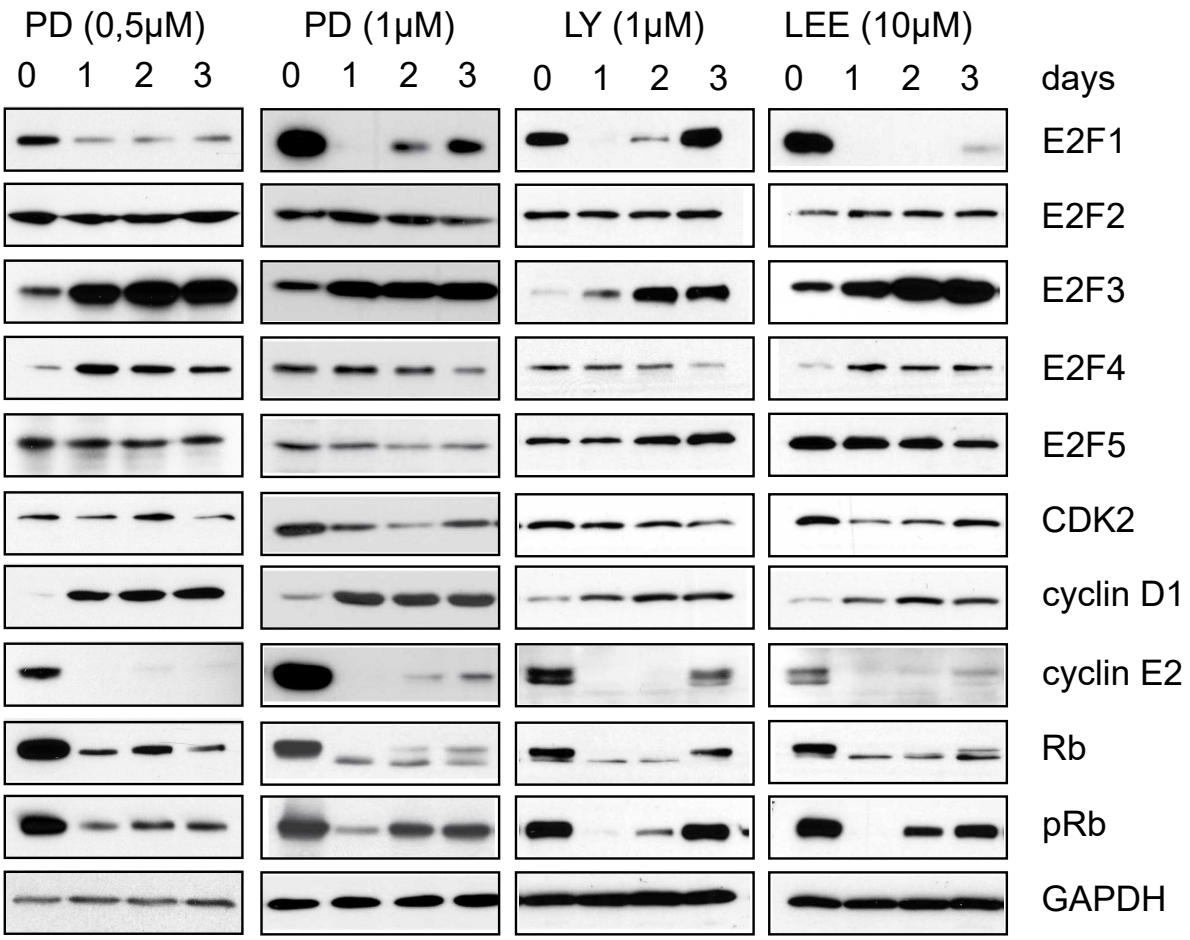

Figure 3.9.: **Expression of Various Cell Cycle Proteins Is Affected by CDK4/6 Inhibition.** T24 cells were treated daily with PD-0332991, LY2835219 or LEE011 for up to thee days and expression of cellular cell cycle proteins was analysed.

3.3.2. CDK4/6 Inhibition Enhances Oncolytic Virotherapy in Rb Positive Cell Lines

CDK4/6 Inhibition Increases Virus Induced Cell Death

In a next step, the specific CDK4/6 inhibitor PD-0332991 was combined with the oncolytic Adenovirus XVir-N-31 and cell viability upon combination treatment was analysed in the three bladder cancer cell lines T24, RT112, and 253J. As shown in Figure 3.10, combination treatment with PD-0332991 efficiently increased virus induced cell death by 45-94% compared to single treatment.

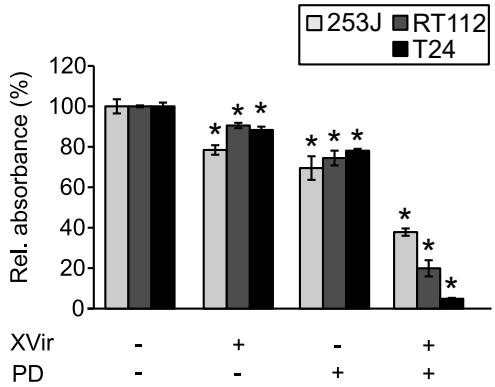

Figure 3.10.: **CDK4/6 Inhibition by PD-0332991 Increases Virus Induced Cell Death in Rb Positive Cell Lines.** T24, RT112, and 253J cells were infected with XVir-N-31 (T24 MOI 50, RT112 MOI 400, 253J MOI 20) and where indicated treated with PD-0332991 (T24 500nM, RT112 2000nM, 253J 100nM). Cell viability was analysed at 4dpi. Values are averages of at least two independent experiments. Error bars S.E., $p<0.05$.

As treatment with PD-0332991 showed an additional effect on cell viability in combination with XVir-N-31, we sought to investigate whether this combination was synergistic. For this, the four bladder cancer cell lines T24, UMUC3, RT112, and 253J cells were treated with up to four different doses of PD-0332991 and up to five different MOIs of the virus. Every dose of the inhibitor was combined with every MOI of the virus and the CI value was calulated.

T24 and UMUC3 cells were treated with PD-0332991 at 100, 250, 5000, and 1000nM. T24 cells were infected with XVir-N-31 at MOI 40, 60, 80, 100, and 110 and UMUC3 cells were infected with MOI 10, 15, 20, 25, and 30. As shown in Figure 3.11a and b, combinations for T24 and UMUC3 cells resulted in CI values between 0.11-0.44 and 0.26-0.42, respectively. RT112 cells were treated with PD-0332991 at 500 and 1000nM and infected with XVir-N-31 at MOI 200, 300, and 400. CI values for RT112 were between 0.002-0.44 (Figure 3.11c). 253J cells were more sensitive to PD-0332991 and were therefore treated with concentrations of 50 and 100nM and infected with XVir-N-31 at MOI 15 and 20. Combinations in this cell line resulted in CI values between 0.99-1.8 (Figure 3.7d). As CI values for T24, UMUC3, and RT112 cells were far below one, the combination was considered to be strongly synergistic in these cell lines. For 253J cells, the combination was considered to be rather additive.

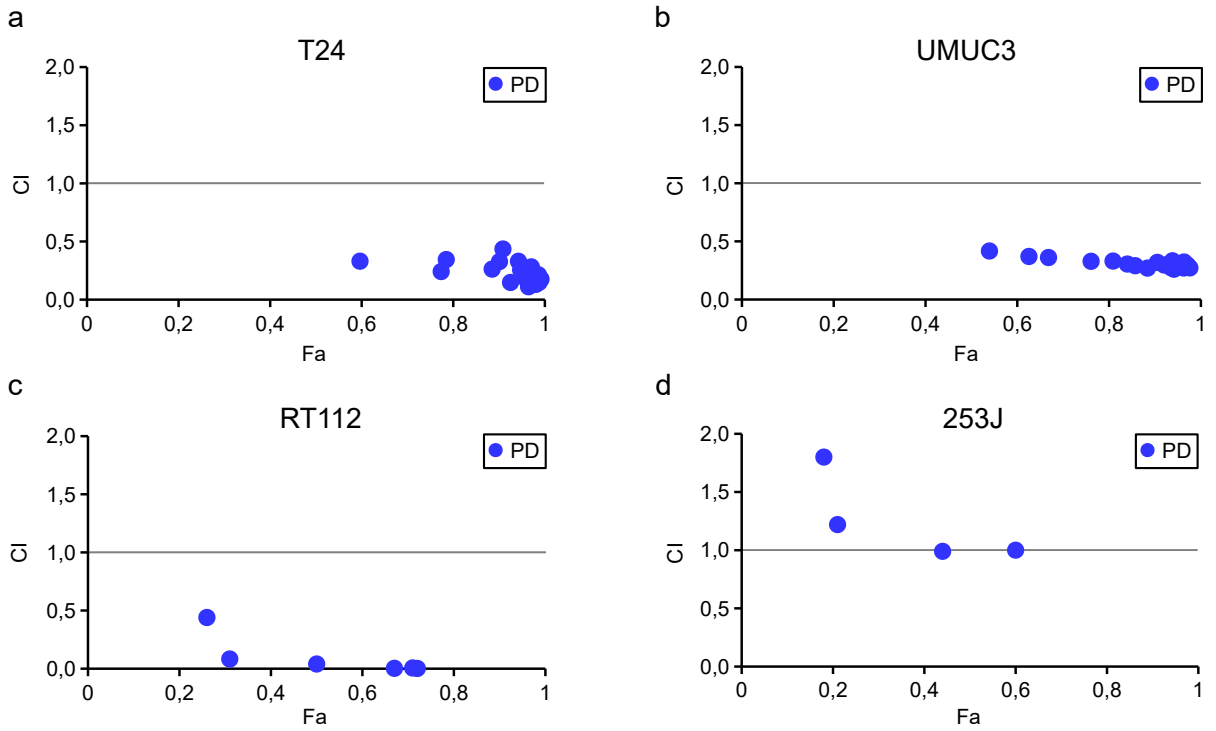

Figure 3.11.: **Synergistic Effects in Combination with PD-0332991 in Rb Positive Cell Lines.** Bladder cancer cell lines were treated with different concentrations of PD-0332001 and infected with different MOIs of XVir-N-31. X-axes show the Fraction affected (Fa) by the combination and Y-axes show the CI values. Each combination is represented by one dot. Values indicate synergism, additivity or antagonism if CI<1, CI=1 or CI>1 [18, 19]. The line indicates a CI value of one.

The specific CDK4/6 inhibitor PD-0332991 showed synergistic effects in combination with oncolytic virotherapy and we therefore sought to investigate whether the other CDK4/6 inhibitors LY2835219 and LEE011 had the same effect. For this, T24 cells were treated with CDK4/6 inhibitors and infected with XVir-N-31 or WT Adenovirus and cell viability was analysed. At this point, WT Adenovirus was included to see whether the effects seen in combination with XVir-N-31 were due to a general mechanism of Adenovirus biology. As shown in Figure 3.12, combination treatment efficiently decreased cell viability by >90% with all three inhibitors and both viruses tested.

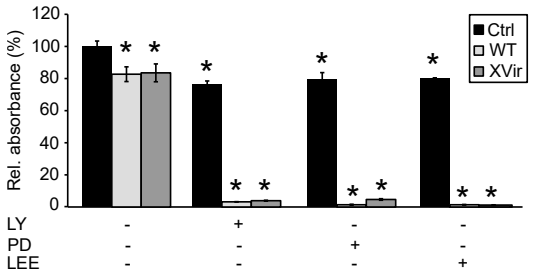

Figure 3.12.: **Specific CDK4/6 Inhibition Increases Virus Induced Cell Death.** T24 cells were treated with CDK4/6 inhibitors (LY2835219 and PD-0332991 500nM, LEE011 5000nM) and infected with XVir-N-31 (MOI 60) or WT Adenovirus (MOI 80). Cell viability was analysed at 4dpi. Values are averages of up to four independent experiments. Error bars S.E., p<0.05.

CDK4/6 Inhibition Increases Viral Replication

To analyse whether the synergistic effects on cell viability were accompanied by an increase in viral replication, T24, RT112, and 253J cells were treated with PD-0332991, infected with XVir-N-31, and viral replication was analysed by Fibre-qPCR. As shown in Figure 3.13, combination with PD-0332991 increased viral replication of XVir-N-31 13-73-fold in T24, 2-8-fold in RT112, and 1.2-2-fold in 253J cells.

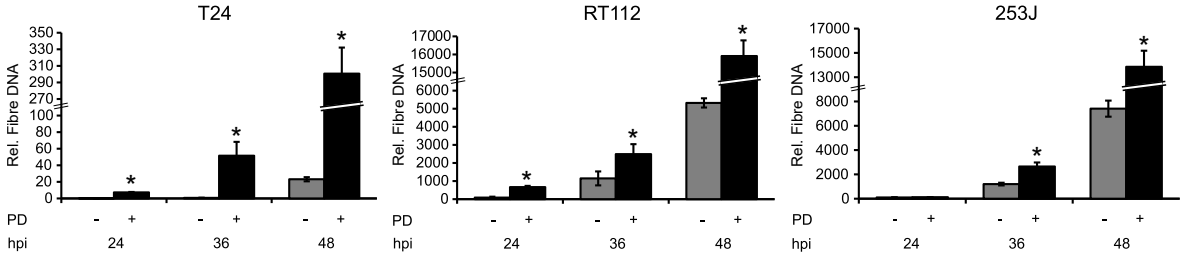

Figure 3.13.: **CDK4/6 Inhibition by PD-0332991 Increases Viral Replication in Rb Positive Cell Lines.** Cells were infected with XVir-N-31 (T24 MOI 50, RT112 MOI 450, 253J MOI 25) and where indicated treated with PD-0332991 (T24 500nM, RT112 2000nM, 253J 100nM). Viral replication was analysed at indicated time points. Error bars S.D., $p<0.05$.

Next, we sought to investigate whether the specific CDK4/6 inhibitors LY2835219 and LEE011 could also increase viral replication of XVir-N-31 and WT Adenovirus in T24 cells. As shown in Figure 3.14, all three CDK4/6 inhibitors strongly increased viral replication for both viruses: LEE011 increased viral replication of XVir-N-31 and WT Adenovirus 6-52- and 3-18-fold, respectively (Figure 3.14, left). LY2835219 increased viral replication of XVir-N-31 and WT 3-9- and 11-18-fold, respectively (Figure 3.14, middle) and PD-0332991 increased viral replication of XVir-N-31 and WT 6-50- and 3-7-fold, respectively (Figure 3.14, right).

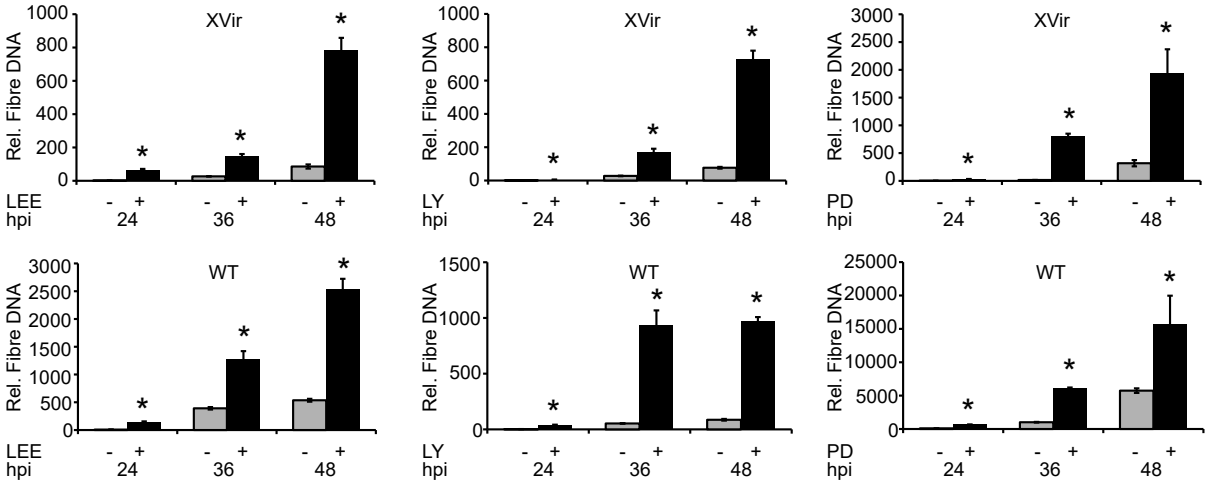

Figure 3.14.: **Specific CDK4/6 Inhibition Increases Viral Replication.** T24 cells were infected with XVir-N-31 or WT Adenovirus (MOI 50) and where indicated treated with CDK4/6 inhibitors (LY2835219 and PD-0332991 500nM, LEE011 5000nM). Viral replication was analysed at indicated time points. Error bars S.D., $p<0.05$.

CDK4/6 Inhibition Increases Viral Particle Formation

The production of infectious viral particles is of great importance for an efficient oncolytic virotherapy and we therefore wanted to investigate whether CDK4/6 inhibition could also increase the production of infectious viral particles. First, T24, RT112, and 253J cells were treated with PD-0332991, infected with XVir-N-31, and the production of viral particles in these bladder cancer cell lines was analysed by a Hexon-Titre Test. As shown in Figure 3.15, CDK4/6 inhibition by PD-0332991 increased viral particle production of XVir-N-31 2-4.5-fold compared to untreated cells.

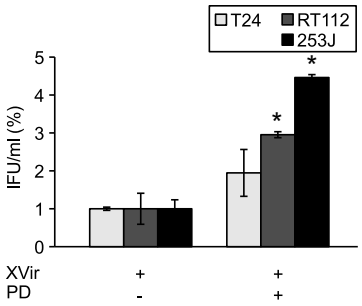

Figure 3.15.: **CDK4/6 Inhibition by PD-0332991 Increases Infectious Viral Particle Production in Rb Positive Cell Lines.** Cells were infected with XVir-N-31 (T24 MOI 50, RT112 MOI 450, 253J MOI 25) and where indicated treated with PD-0332991 (T24 500nM, RT112 2000nM, 253J 100nM). The increase in viral titre upon CDK4/6 inhibition is given in infectious units/ml (IFU/ml). Values are averages of at least two independent experiments and values of untreated samples were set to one. Error bars S.E., $p<0.05$.

In a next step, the production of infectious viral particles of XVir-N-31 and WT Adenovirus upon CDK4/6 inhibition with all three inhibitors was analysed in T24 cells. Figure 3.16 shows that all three inhibitors strongly increased the viral titre for both viruses. The production of infectious viral particles was increased 3-fold by LEE011 and PD-0332991 and 5-fold by LY2835219 for both XVir-N-31 and WT Adenovirus.

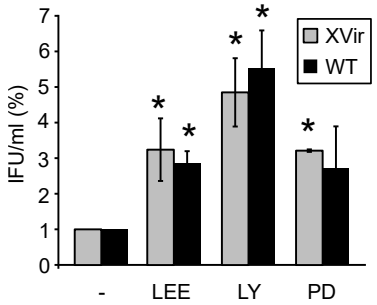

Figure 3.16.: **Specific CDK4/6 Inhibition Increases Infectious Viral Particle Production.** T24 cells were infected with XVir-N-31 or WT Adenovirus (MOI 50) and where indicated treated with CDK4/6 inhibitors (LY2835219 and PD-0332991 500nM, LEE011 5000nM). The increase in viral titre upon CDK4/6 inhibition is given in infectious units/ml (IFU/ml). Values are averages of at least two independent experiments and values of untreated samples were set to one. Error bars S.E., $p<0.05$.

3.3.3. CDK4/6 Inhibition Does not Enhance Oncolytic Virotherapy in Rb Negative Cell Lines

Rb negative cell lines are resistant to CDK4/6 inhibitors as reported previoulsy by others and our group [55]. To analyse the mechanism responsible for the synergistic effects upon combination therapy with CDK4/6 inhibition, we next wanted to analyse the effects on oncolytic virotherapy upon CDK4/6 inhibition in Rb negative cell lines.

Rb Negative Cell Lines Do not Respond to CDK4/6 Inhibition

As shown before, CDK4/6 inhibition lead to a strong decrease in E2F1 protein expression in responding cell lines (Figure 3.9) and therefore E2F1 expression upon CDK4/6 inhibition was analysed as a functional readout in Rb negative cell lines. For this, the two Rb negative cell lines 647V and 639V were treated with the CDK4/6 inhibitor PD-0332991 and functional response of the cells was analysed by immunoblotting. As shown in Figure 3.17, Rb negative cell lines showed a slight downregulation of E2F1 protein expression upon treatment with high doses of PD-0332991 at 24 but not at 48h indicating resistance of these cells to CDK4/6 inhibition.

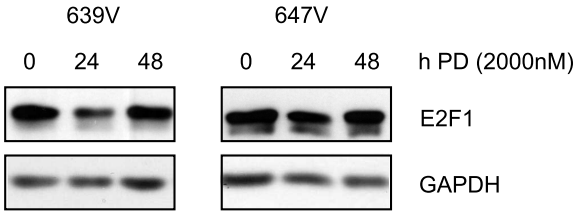

Figure 3.17.: **E2F1 Is not Completely Downregulated upon CDK4/6 Inhibition in Rb Negative Cell Lines.** 647V and 639V cells were treated with PD-0332991 (2000nM) and E2F1 protein expression was analysed at indicated time points. Data were kindly provided by Judith Schäfers.

In a next step we sought to analyse whether T24 Rb knockout cells (T24 shRb1) were also resistant to CDK4/6 inhibition. Similar to intrinsical Rb negative cells, T24 shRb1 did not respond to CDK4/6 inhibition as they did not show any decrease in E2F1 protein expression upon treatment (Figure 3.18). In contrast, T24 control cells showed a strong downregulation of E2F1 and Rb protein expression upon CDK4/6 inhibition by PD-0332991.

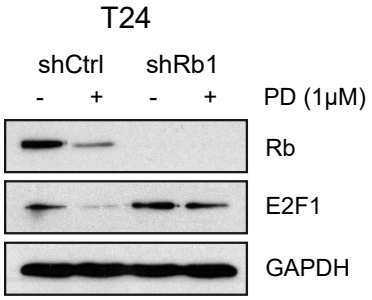

Figure 3.18.: **CDK4/6 Inhibition Requires Rb for Downregulation of E2F1.** T24 shRb1 and control cells were treated with PD-0332991 (1μM) and E2F1 and Rb protein expression was analysed after 24h.

CDK4/6 Inhibition Does not Increase Virus Induced Cell Death in Rb Negative Cell Lines

Next, the effects of CDK4/6 inhibition on oncolytic virotherapy were analysed in Rb negative cells. For this, the two Rb negative cell lines 647V and 639V were treated with PD-0332991, infected with XVir-N-31, and cell viability was analysed. As shown in Figure 3.19, Rb negative cell lines did not show any additional effect in the combination treatment compared to monotherapy.

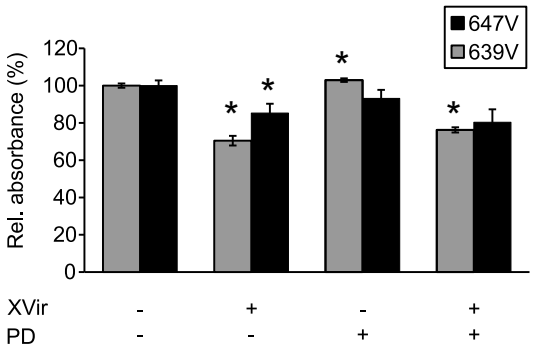

Figure 3.19.: **CDK4/6 Inhibition by PD-0332991 Does not Increase Virus Induced Cell Death in Rb Negative Cell Lines.** 647V and 639V cell lines were infected with XVir-N-31 (639V MOI 200 and 647V MOI 2) and where indicated treated with PD-0332991 (2000nM). Cell viability was analysed at 4dpi. Values are averages of at least two independent experiments. Error bars S.E., $p<0.05$.

In a next step, cell viability upon combination with CDK4/6 inhibition was analysed in T24 shRb1 cells: as shown in Figure 3.20, combination treatment with PD-0332991 increased virus induced cell death by more than 95% in T24 control cells. In T24 shRb1 cells in contrast, combination with PD-0332991 increased virus induced cell death by only 30% compared to monotherapy. Thus, the enhanced effect in combination with CDK4/6 inhibition was diminished in Rb negative cells.

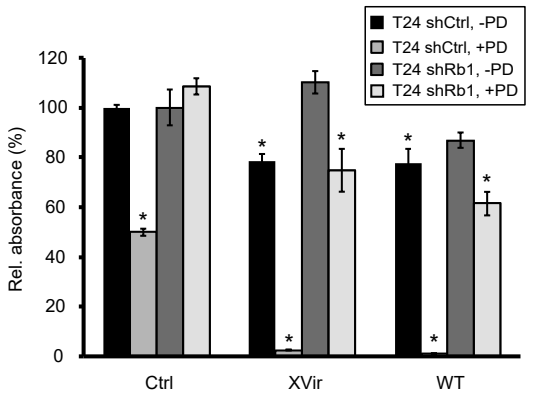

Figure 3.20.: **Reduced Effects on Virus Induced Cell Death upon Combination with CDK4/6 Inhibition in T24 shRb1 Cells.** T24 shRb1 and control cells were treated with PD-0332991 (1μM) and infected with XVir-N-31 (MOI 60) or WT Adenovirus (MOI 120). Cell viability was assessed at 4dpi. Error bars S.D., $p<0.05$.

CDK4/6 Inhibition Does not Increase Viral Replication in Rb Negative Cell Lines

The effects of CDK4/6 inhibition on viral replication in Rb negative cell lines were then analysed by Fibre qPCR. As shown in Figure 3.21, 639V cells did not show an increase but a 30-50% decrease in replication upon CDK4/6 inhibition. Thus, upon CDK4/6 inhibition 639V cells showed the opposite effects on viral replication compared to Rb positive cell lines. In contrast, 647V cells showed a slight increase in viral replication upon combination treatment. However, this increase was not as strong as in Rb positive cell lines.

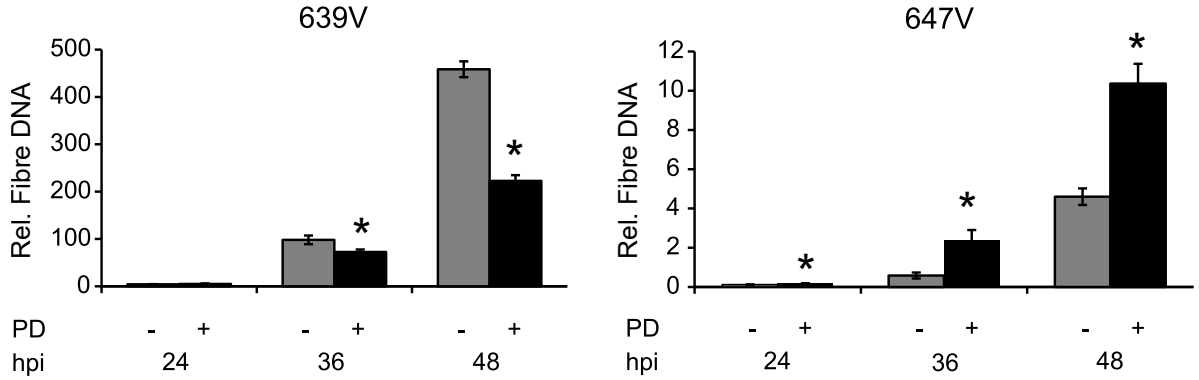

Figure 3.21.: **CDK4/6 Inhibition by PD-0332991 Does not Increase Viral Replication in Rb Negative Cell Lines.** 639V and 647V cells were infected with XVir-N-31 (639V MOI 300 and 647V MOI 4) and where indicated treated with PD-0332991 (2000nM). Viral replication was analysed at indicated time points. Error bars S.D., $p<0.05$.

In a next step, we analysed the effects of CDK4/6 inhibition on viral replication in T24 shRb1 and control cells (Figure 3.22): in T24 control cells, CDK4/6 inhibition increased viral replication of XVir-N-31 and WT Adenovirus 10- and 25-fold, respectively. In contrast, in T24 shRb1 cells CDK4/6 inhibition increased viral replication of XVir-N-31 and WT only 0.5- and 1.4-fold, respectively. According to these results, Rb seems to be an important player and a prerequisite for an enhanced oncolytic virotherapy in combination with CDK4/6 inhibitors.

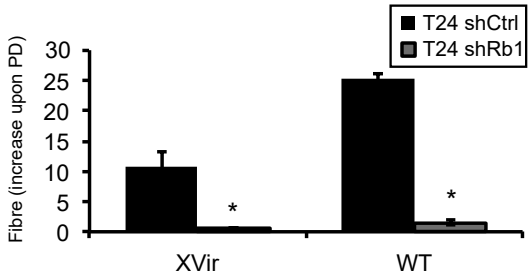

Figure 3.22.: **CDK4/6 Inhibition by PD-0332991 Does not Increase Viral Replication in T24 shRb1 Cells.** T24 shRb1 and T24 control cells were treated with PD-0332991 (1μM) and infected with the indicated viruses (MOI 50). Viral replication was analysed at 24hpi. Values show the increase in replication upon treatment. Error bars S.D., $p<0.05$.

CDK4/6 Inhibition Does not Increase Viral Particle Formation in Rb Negative Cell Lines

In a last step, we wanted to investigate whether infectious viral particle production was changed upon CDK4/6 inhibition in Rb negative cell lines. Figure 3.23 shows that upon PD-0332991

treatment infectious viral particle production was reduced by 38% in 639V cells but was not changed in 647V cells.

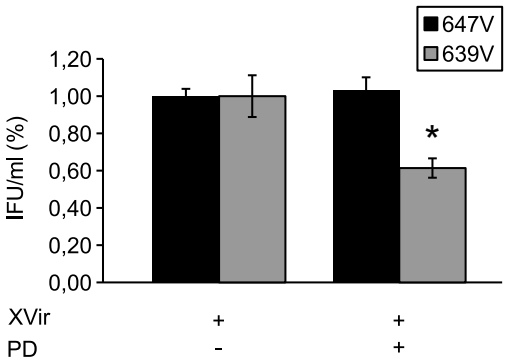

Figure 3.23.: **CDK4/6 Inhibition by PD-0332991 Does not Increase Infectious Viral Particle Production in Rb Negative Cell Lines.** 639V and 647V cells were infected with XVir-N-31 (639V MOI 300 and 647V MOI 4) and where indicated treated with PD-0332991 (2000nM). The increase in viral titre upon CDK4/6 inhibition is given in infectious units/ml (IFU/ml). Values are averages of at least two independent experiments and values of untreated samples were set to one. Error bars S.E., $p<0.05$.

Next, we analysed infectious viral particle formation in T24 shRb1 and control cells (Figure 3.24). Similar to previous results, CDK4/6 inhibition enhanced infectious viral particle formation in T24 control cells 18- and 3-fold for XVir-N-31 and WT Adenovirus, respectively. However, in T24 shRb1 cells viral particle formation was only increased 1.6-fold for both viruses.

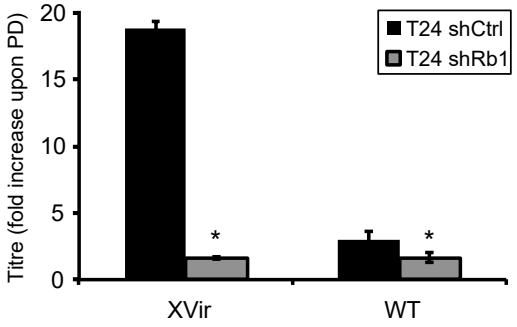

Figure 3.24.: **CDK4/6 Inhibition by PD-0332991 Does not Increase Infectious Viral Particle Formation in T24 shRb1 Cells.** T24 shRb1 and T24 control cells were treated with PD-0332991 (1μM) and infected with the indicated viruses (MOI 50). The increase in viral titre upon CDK4/6 inhibition is given in infectious units/ml (IFU/ml). Values are averages of at least two independent experiments. Error bars S.E., $p<0.05$.

3.4. Effects of Combined CDK4/6 Inhibition and Oncolytic Virotherapy on Cellular Targets

Adenoviruses interfere with cellular signalling pathways at multiple sites and E1A is known to transactivate or repress cellular promoters [5, 11]. We therefore analysed whether gene expression of key molecules of the CDK4/6 pathway were affected by Adenovirus infection and/or CDK4/6 inhibition. For this, E2F1 and Rb gene expression were analysed after virus

infection, CDK4/6 inhibition by PD-0332991 or a combination of both. As shown in Figure 3.25a, CDK4/6 inhibition by PD-0332991 reduced E2F1 gene expression by 42 and 58% at 500 and 2000nM, respectively compared to control. Infection with XVir-N-31 alone caused a reduction in gene expression of 51% compared to control. However, in combination with 500 and 2000nM PD-0332991 XVir-N-31 increased E2F1 gene expression 2.4- and 4-fold, respectively compared to uninfected cells. Infection with WT Adenovirus reduced E2F1 gene expression by 23% compared to control. In combination with 500 and 2000nM PD-0332991, WT Adenovirus increased E2F1 gene expression 2.9- and 3.6-fold, respectively compared to uninfected cells.

As shown in Figure 3.25b, Rb gene expression was reduced by 11% upon treatment with 500nM PD-0332991. No change in expression was observed with 2000nM PD-0332991. XVir-N-31 alone did not change Rb gene expression levels. However, in combination with 500 and 2000nM PD-0332991 XVir-N-31 increased Rb gene expression levels by 23 and 10%, respectively compared to uninfected cells. Infection with WT Adenovirus alone did not affect Rb gene expression but upon combination with 500 or 2000nM PD-0332991 expression was increased by 49%.

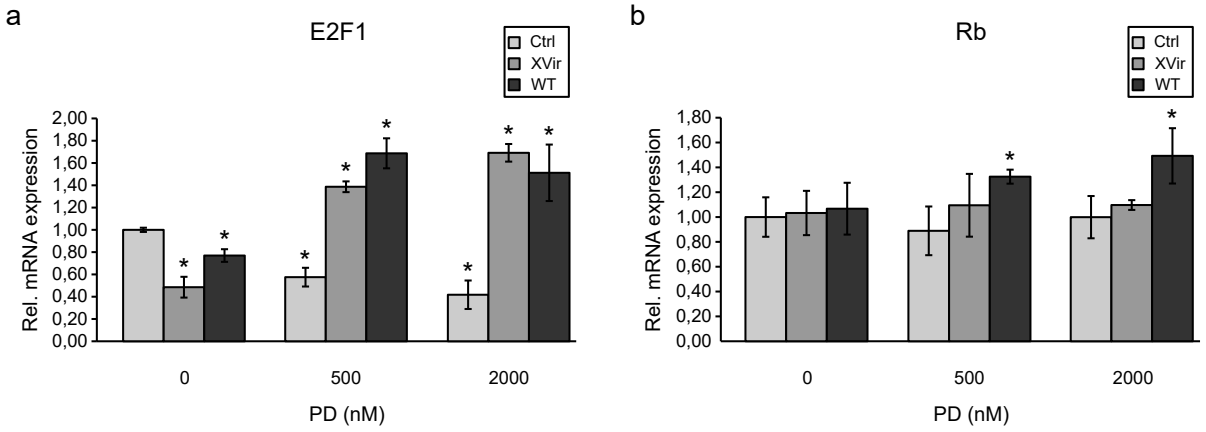

Figure 3.25.: **Adenovirus Infection Induces E2F1 and Rb Gene Expression upon CDK4/6 Inhibition.** T24 cells were treated with PD-0332991 and infected with the indicated viruses (MOI 50). At 24hpi, RNA was extracted and analysed by RT-qPCR. Values were normalised to GAPDH and values of untreated samples. Error bars S.D., $p<0.05$.

As Andeoviruses were able to increase E2F1 and Rb gene expression levels upon combination with CDK4/6 inhibition, we next analysed whether the expression of several cell cycle proteins was also affected by this combination. T24 cells were treated with the CDK4/6 inhibitor PD-0332991 and/or infected with XVir-N-31 or WT Adenovirus and the expression of several cellular proteins was analysed at 12, 24 or 36hpi. As shown in Figure 3.26, at all time points tested E2F1 protein expression was downregulated by monotherapy with CDK4/6 inhibition as already observed before (Figure 3.9, PD 0.5μM). However, combination with Adenovirus infection caused a strong upregulation of E2F1 starting from 12hpi. Thus, Adenoviral infection completely reversed the effects of CDK4/6 inhibition on E2F1 protein expression. Expression of Rb and pRb were downregulated upon monotherapy with CDK4/6 inhibition or virus infection. However, downregulation of Rb and pRb was enhanced in the combination treatment. The enhanced downregulation of Rb and pRb was stronger in combination with XVir-N-31 compared to WT Adenovirus, probably due to E1A13S which is known to stabilise Rb upon WT infection. Expression of p107 was slightly increased by CDK4/6 inhibition but downregulated in combination with Adenovirus infection. p130 was upregulated upon CDK4/6 inhibition alone and in the combination treatment. Expression of DP1 was not changed by CDK4/6 inhibition and/or virus infection. p21 was not changed by CDK4/6 inhibition or virus infection alone but expres-

sion was strongly upregulated upon time. p27 was upregulated by monotherapy with CDK4/6 inhibition or virus infection. However, in the combination treatment, p27 was downregulated. Expression of CDK2 was slightly upregulated by CDK4/6 inhibition. Virus infection alone caused a downregulation in CDK2 expression and this effect was reversed in the combination treatment. Cyclin D1 was strongly upregulated by CDK4/6 inhibition. However, Adenovirus infection alone and in combination with CDK4/6 inhibition strongly downregulated cyclin D1 expression. Cyclin E2 was downregulated by monotherapy with CDK4/6 inhibition or virus infection. However, in the combination treatment, cyclin E2 expression was strongly increased. Expression of the oncoprotein Myc was not majorly affected by CDK4/6 inhibition but Adenovirus infection alone and in combination with CDK4/6 inhibition increased Myc expression. The expression of Erk was not affected by CDK4/6 inhibition and/or virus infection. pErk was upregulated upon CDK4/6 inhibition but downregulated upon time and virus infection did not change this expression pattern. Expression of Akt was not changed by CDK4/6 inhibition and/or Adenovirus infection. However, expression of pAkt Ser and pAkt Thr was upregulated by CDK4/6 inhibition alone and in combination with the virus. This shows that Adenoviruses can strongly interfere with the expression of several cell cycle proteins such as E2F1, p107, p27, cyclin D1, and cyclin E2 of which the expression was inverted in combination with the virus.

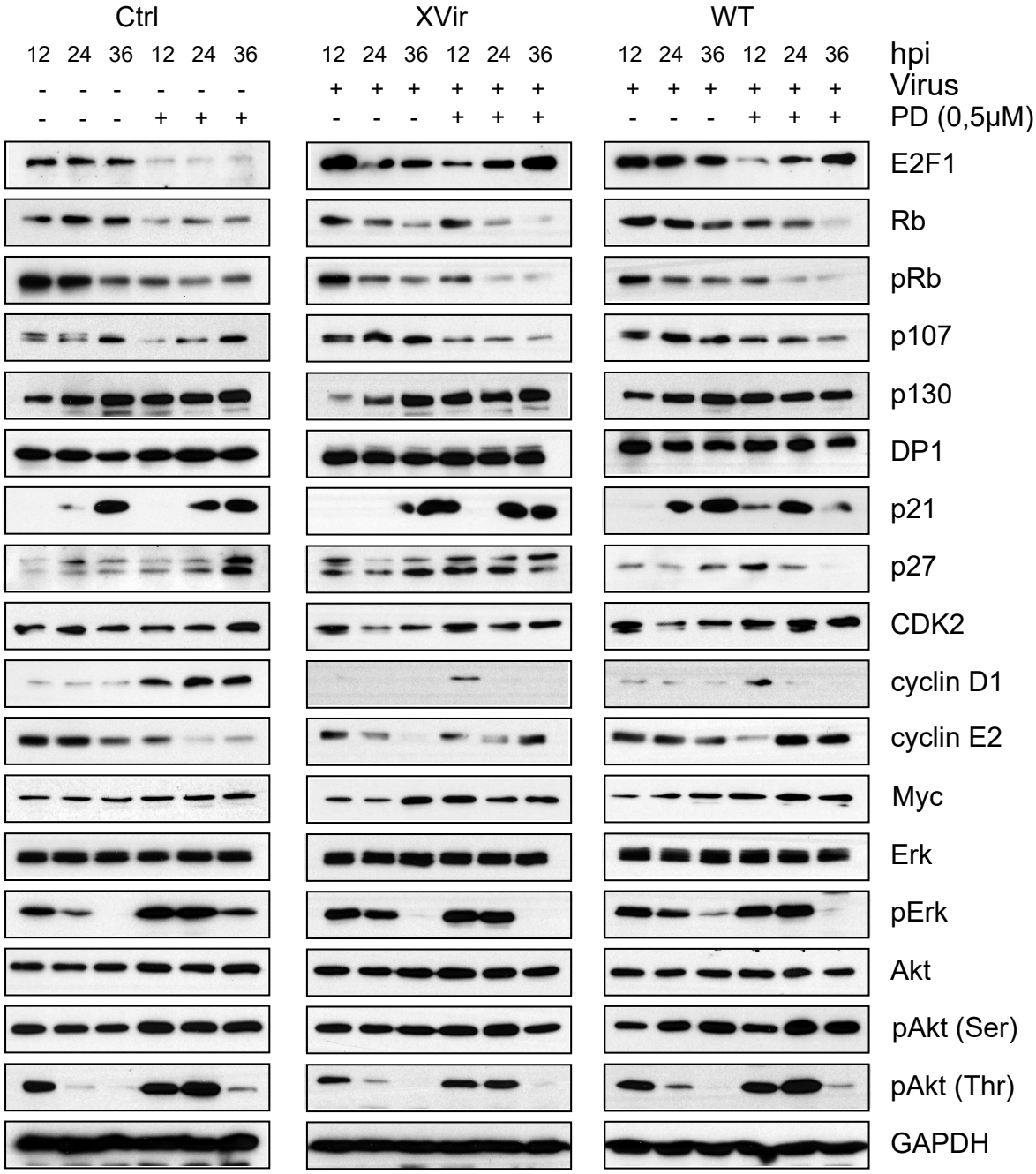

Figure 3.26.: **Adenoviruses Interfere with the Expression of Cell Cycle Proteins.** T24 cells were treated with PD-0332991 (500nM) and infected with the indicated viruses (MOI 50). Protein expression was analysed at indicated time points.

3.5. Analysis of Different Pretreatment Regimens on Combination Therapy with CDK4/6 Inhibition

As shown before, virus induced cell death was dramatically enhanced upon pretreatment with CDK4/6 inhibition for 24h. Furthermore, E2F1 protein expression was downregulated upon treatment with PD-0332991 500nM for up to three days (Figure 3.9) and therefore we wanted to investigate whether different CDK4/6 pretreatment regimens would affect virus induced cell death. For this, T24 cells were treated with 500nM PD-0332991 for up to seven days and

infected with XVir-N-31 or WT Adenovirus. As shown in Figure 3.27a, CDK4/6 inhibition greatly enhanced virus induced cell death by >90% independent of pretreatment time. Analysis of E2F1 and Rb protein expression showed a durable downregulation of E2F1 and Rb for up to seven days (Figure 3.27b).

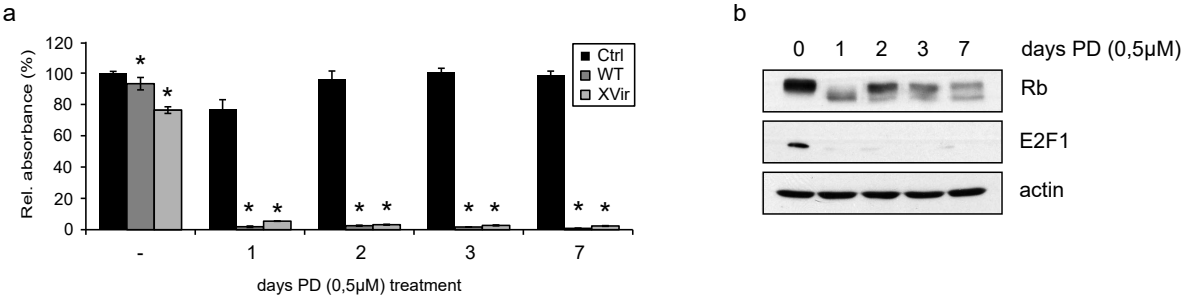

Figure 3.27.: **Long Term CDK4/6 Inhibition Enhances Virus Induced Cell Death.** T24 cells were treated daily with PD-0332991 (500nM) for up to 7 days and infected with XVir-N-31 (MOI 80) or WT Adenovirus (MOI 150). Cell viability was assessed at 4dpi (a). Error bars S.D., $p<0.05$. (b) T24 cells were treated as described in (a) and Rb and E2F1 protein expression was analysed at indicated time points.

In a next step, we analysed whether the duration of pretreatment time was important for enhanced virus induced cell death and whether CDK4/6 inhibition could enhance virus induced cell death even when the inhibitor was added after infection. For this, cells were treated with PD-0332991 24 or 6h before (1dai or 6hai, respectively) or one hour after infection (1hpi) and cell viability was assessed at 4dpi. As shown in Figure 3.28, CDK4/6 inhibition enhanced virus induced cell death by >75%, independent of pretreatment time and even when the inhibitor was added after infection.

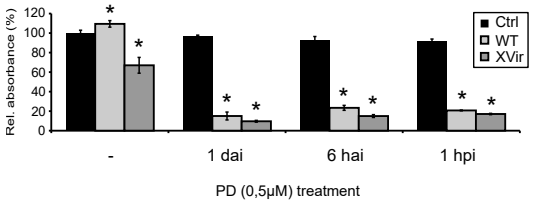

Figure 3.28.: **Short Term CDK4/6 Inhibition Enhances Virus Induced Cell Death.** T24 cells were pretreated with PD-0332991 (500nM) for indicated time points and infected with XVir-N-31 (MOI 80) or WT Adenovirus (MOI 150). Cell viability was assessed at 4dpi. Error bars S.D., $p<0.05$.

In order to rule out that the enhanced cell death in the combination therapy was due to ehanced virus entry into the cells, we used Fibre qPCR to analyse the entry level of viral DNA before viral DNA replication had started. For this, T24 cells were pretreated with CDK4/6 inhibition for 24h, infected with XVir-N-31 or WT Adenovirus, and viral Fibre DNA was analysed at 4hpi. As shown in Figure 3.29, pretreatment with CDK4/6 inhibition did not affect entry levels of viral Fibre DNA at 4hpi.

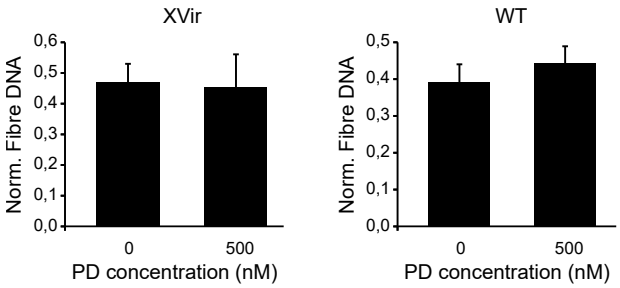

Figure 3.29.: **CDK4/6 Inhibition Does not Affect Viral Infectivity Rates.** T24 cells were pretreated with PD-0332991 for 24h and infected with the indicated viruses (MOI 50). Viral replication was analysed at 4hpi. Error bars S.D., $p<0.05$.

3.6. Analysis of Gene and Protein Expression of Viral Mutants in Combination with CDK4/6 Inhibition

Adenoviruses interfere with cellular signalling pathways at multiple sites. To analyse which viral proteins or transcription factor binding sites were important for the enhanced effects in combination with CDK4/6 inhibition, we analysed viral gene and protein expression of different viral mutants in combination with CDK4/6 inhibition. Figure 3.30 shows an overview of all viral mutants used in the following experiments (kindly provided by PD Dr. P. S. Holm, Klinikum rechts der Isar der TUM, Germany).

The genome of WT Adenovirus, as shown in Figure 3.30a, was described in detail in Chapter 1.2.1. For Adenoviral mutants (Figure 3.30b-g) only regions differing from WT genome are shown.

The oncolytic Adenovirus XVir-N-31 (Figure 3.30b) lacks the transactivating E1A13S protein and thus relies on nuclear YB-1 for activation of viral E2 gene transcription. Moreover, XVir-N-31 lacks the antiapoptotic E1B19k protein leading to enhanced apoptosis and tumour cell death. A full description of XVir-N-31 can be found in Chapter 1.2.3.

The Adenoviral CMV E1B55k RSV E4 mutant (Figure 3.30c) lacks the complete E1A region and does therefore not encode the transactivating E1A13S nor the Rb binding E1A12S [12, 51]. However, CMV E1B55k RSV E4 encodes the E1B55k, but not the E1B19k protein, under control of a CMV promoter. The E4 region is controlled by a RSV promoter instead of the E4 promoter. As E1A13S can not transactivate E1B and E4 expression in this virus, expression of E1B55k and E4 is controlled by two strong external promoters. By this, E1B55k and E4orf6 are expressed E1A-independently leading to enhanced E1B55k and E4orf6 protein expression, E1B55k-E4orf6 complex formation, nuclear translocation of YB-1, and finally E2 gene transcription [33].

The oncolytic Adenovirus delta24 is shown in Figure 3.30d. The Adenoviral E1A region possesses three conserved regions (CR1/2/3) of which the CR1/2 domains are required for the interaction with Rb [12]. Through this interaction, transcription factors such as E2Fs are released from the binding with Rb leading to cell cycle progression and DNA replication. In delta24, the CR2 domain is deleted and therefore this virus can only replicate in cells with mutated Rb [12]. The delta24 CMV virus in which the remaining E1A region is controlled by a CMV promoter (Figure 3.30e) was used in order to analyse whether the enhanced effects in combination with CDK4/6 inhibition were due to enhanced E1A promoter activity.

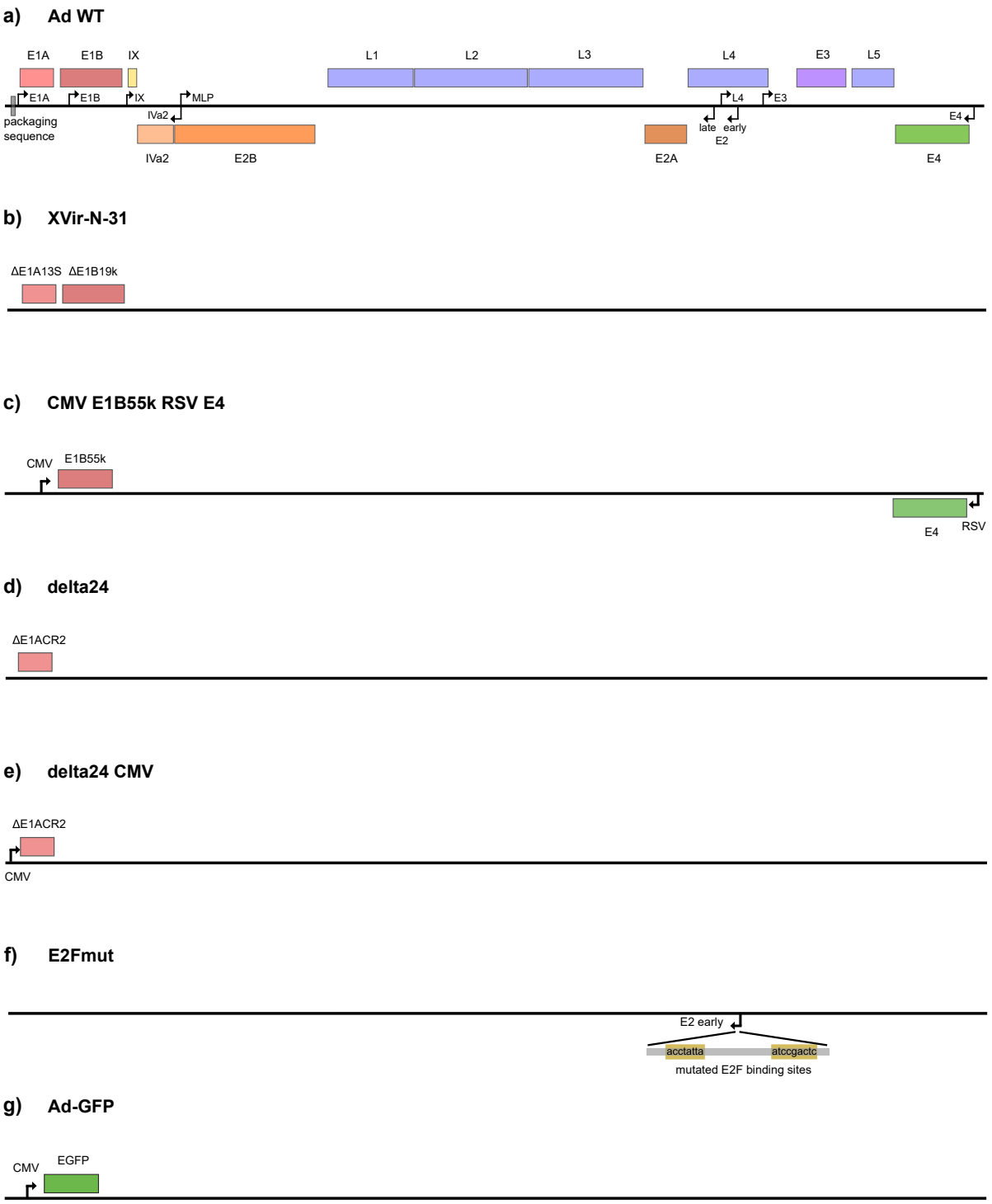

Figure 3.30.: **Genomes of Adenovirus Mutants.** Genomes of WT Adenovirus and Adenoviral mutants used in the following experiments. For (b)-(g) only regions differing from WT Adenovirus are shown. For full details, see text.

Adenoviral E2 gene transcription is controlled by the transactivating E1A13S protein and by E2F1 for which the E2 early promoter possesses two binding sites (see Chapter 1.2.1). As E2F1 is reported to be an activator of E2 transcription [62] and as E2F1 protein expression was downregulated upon CDK4/6 inhibition, we sought to analyse gene expression upon deletion of

E2F binding sites in the E2 early promoter (Figure 3.30f) to see whether CDK4/6 inhibition could also increase E2 gene expression in this virus.

To analyse whether the enhanced effects in combination with CDK4/6 inhibition were E1A- and E1B-independent, the E1-deleted virus Ad-GFP (Figure 3.30g) was used. This virus does not encode E1A nor E1B but instead possesses a EGFP protein under control of a CMV promoter.

CDK4/6 Inhibition Increases Viral Protein Expression

As viral DNA replication and viral particle formation were strongly increased upon CDK4/6 inhibition, we next investigated whether viral protein expression was enhanced in combination with CDK4/6 inhibition. As shown in Figure 3.31, CDK4/6 inhibition by PD-0332991 increased the expression of viral early and late proteins of XVir-N-31 and WT Adenovirus. The viral E1A protein was first detectable at 12hpi in combination with CDK4/6 inhibition and further increased from 12 to 36hpi. At all time points, the expression was stronger in the combination therapy. The early proteins E2A and E1B55k were first detectable at 24 and 36hpi for monotherapy with WT and XVir-N-3, respectively. However, these proteins were detected earlier and stronger in the combination treatment. The late Hexon protein was detectable at 24 and 48hpi for monotherapy with WT and XVir-N-31, respectively but in the combination the expression for XVir-N-31 was already detectable at 24hpi.

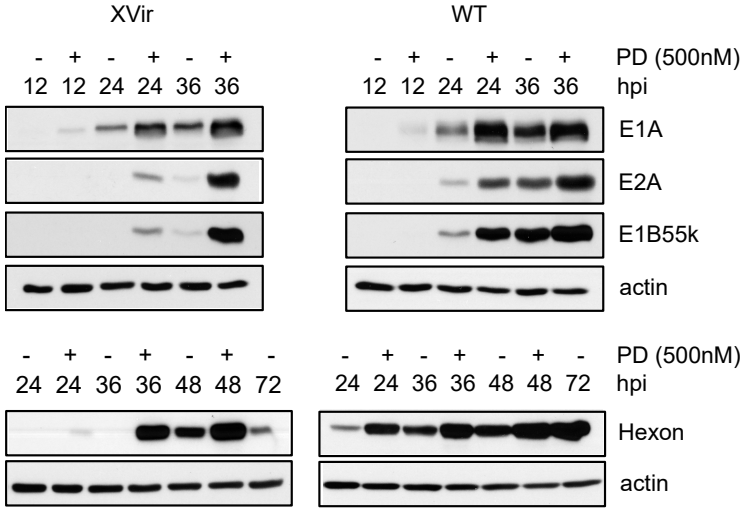

Figure 3.31.: **CDK4/6 Inhibition Enhances Viral Protein Expression.** T24 cells were treated with PD-0332991 (500nM) and infected with the indicated viruses (MOI 50). At indicated time points, protein expression was analysed by immunoblotting.

3.6.1. Enhanced Gene Expression upon CDK4/6 Inhibition Is E1A-Independent

XVir-N-31 lacks the E1A13S protein and thus transactivation of viral promoters by E1A [51]. To investigate whether CDK4/6 inhibition could increase viral gene expression as suggested by viral replication, viral titre, and viral protein expression analyses, we next assessed the expression of viral E1A and E4orf6 genes by RT-qPCR. As shown in Figure 3.32a, combination with CDK4/6 inhibition increased viral E1A12S expression 3- and 8-fold for WT and XVir-N-31, respectively.

Expression of viral E4orf6 was increased 5- and 25-fold for WT and XVir-N-31, respectively (Figure 3.32b).

To test whether CDK4/6 inhibition triggers a general mechanism in Adenoviral gene expression, the well established oncolytic Adenovirus delta24 which has a deletion in the Rb binding region of E1A was used (Figure 3.30d) [12]. As shown in Figure 3.32, upon CDK4/6 inhibition expression of E1A13S and E4orf6 genes was increased 6-fold for delta24 and even when E1A was placed under control of a CMV promoter (delta24 CMV, Figure 3.30e), E1A13S and E4orf6 expressions were increased 5-fold in the combination.

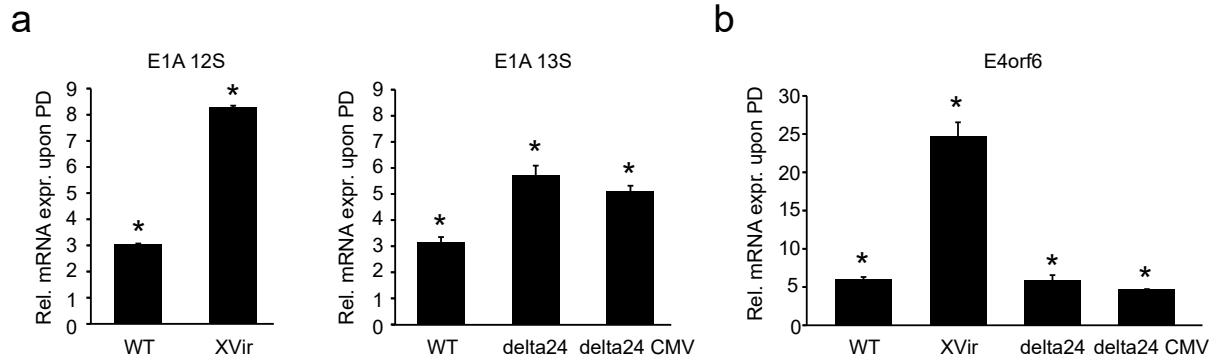

Figure 3.32.: **CDK4/6 Inhibition Enhances Viral E1A and E4 Gene Expression.** T24 cells were treated with PD-0332991 (500nM) and infected with the indicated viruses (MOI 50). At 24hpi, RNA was extracted and analysed by RT-qPCR. Values were normalised to GAPDH and values of virus infected samples only (without CDK4/6 inhibition). Error bars S.D., $p<0.05$.

3.6.2. Enhanced Gene Expression upon CDK4/6 Inhibition Is Independent of E2F1 Binding Sites in the E2 Early Promoter

The viral E1A protein and the cellular transcription factor E2F1 both stimulate the viral E2 early promoter [5, 41, 62]. Thus, we wanted to anlyse whether these two proteins were essential for the synergistic effects in combination with CDK4/6 inhibition. For this, E1A-deleted and E2 early promoter mutants were tested in combination with CDK4/6 inhibition and transcription from the E2 early and E2 late promoter were analysed (Figure 3.33). CMV E1B55k RSV E4 is E1A-depleted, thus lacking E1A transactivation of the E2 early promoter (Figure 3.30c) [5] . The E2F mutant virus has mutated E2F1 binding sites in the E2 early promoter (Figure 3.30f). Thus, for efficient replication and viral E2 gene expression these two viruses depend on the viral E2 late promoter which is E1A- and E2F1-independent. Transcript expression from the E2 early and E2 late promoter upon combination with CDK4/6 inhibition was analysed by RT-qPCR. As shown in Figure 3.33, CDK4/6 inhibition increased the expression from both E2 early and E2 late promoters by >40-fold for XVir-N-31, WT Adenovirus, and the E2 mutant virus. For CMV E1B55k RSV E4, expression of the early promoter was increased by 50%. Thus, CDK4/6 inhibition enhanced E2 gene transcription from the E2 early and the E2 late promoter independent of the viral E1A protein or the E2F1 binding sites in the E2 early promoter.

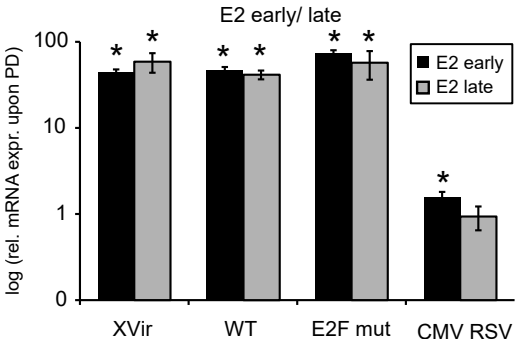

Figure 3.33.: **CDK4/6 Inhibition Enhances Viral E2 Gene Transcription.** T24 cells were treated with PD-0332991 (500nM) and infected with the indicated viruses (MOI 50). At 24hpi, RNA was extracted and analysed by RT-qPCR. Values were normalised to GAPDH and values of virus infected samples only (without CDK4/6 inhibition). Error bars S.D., $p<0.05$.

3.6.3. Enhanced Replication upon CDK4/6 Is E1-Independent

According to the gene expression results of viral E1A mutants, E1A12S and E1A13S are not essential for the enhanced effect in combination with CDK4/6 inhibition. Therefore, we wanted to go one step further, analysing whether replication of a E1-deficient virus could be increased by CDK4/6 inhibition. For this, viral replication of the E1-deleted Ad-GFP virus (Figure 3.30g) upon CDK4/6 and MDM-2 inhibition (Chapter 3.8) was analysed in the three Rb positive cell lines 253J, T24, and UMUC3 and in the Rb negative cell line 639V. In 253J cells, MDM-2 inhibition by Nutlin-3a increased viral replication 1.8-fold (Figure 3.34b). CDK4/6 inhibition by PD-0332991 and LEE011 increased replication 1.4-fold and LY2835219 increased replication 4-fold which was accompanied by an increase in GFP-expression of virus infected cells as shown in Figure 3.34a. In T24 cells, MDM-2 inhibition by Nutlin-3a increased viral replication 32-fold and CDK4/6 inhibition by PD-0332991 and LEE011 increased replication 8-fold. LY2835219 increased replication 5-fold in T24 cells (Figure 3.34c). In UMUC3 cells, MDM-2 inhibition by Nutlin-3a and CDK4/6 inhibition by PD-0332991 increased replication 2- and 2.5-fold, respectively. LY2835219 and LEE011 increased replication 8- and 3.5-fold, respectively (Figure 3.34d). In contrast to Rb positive cell lines, CDK4/6 inhibition did not increase viral replication in Rb negative cells (Figure 3.34e). In 639V cells, replication was reduced by approximately 30% in combination with PD-0332991 or LY2835219. In combination with LEE011, replication was decreased by 64% in these cells. However, MDM-2 inhibition could increase replication 5.5-fold in Rb negative cells.

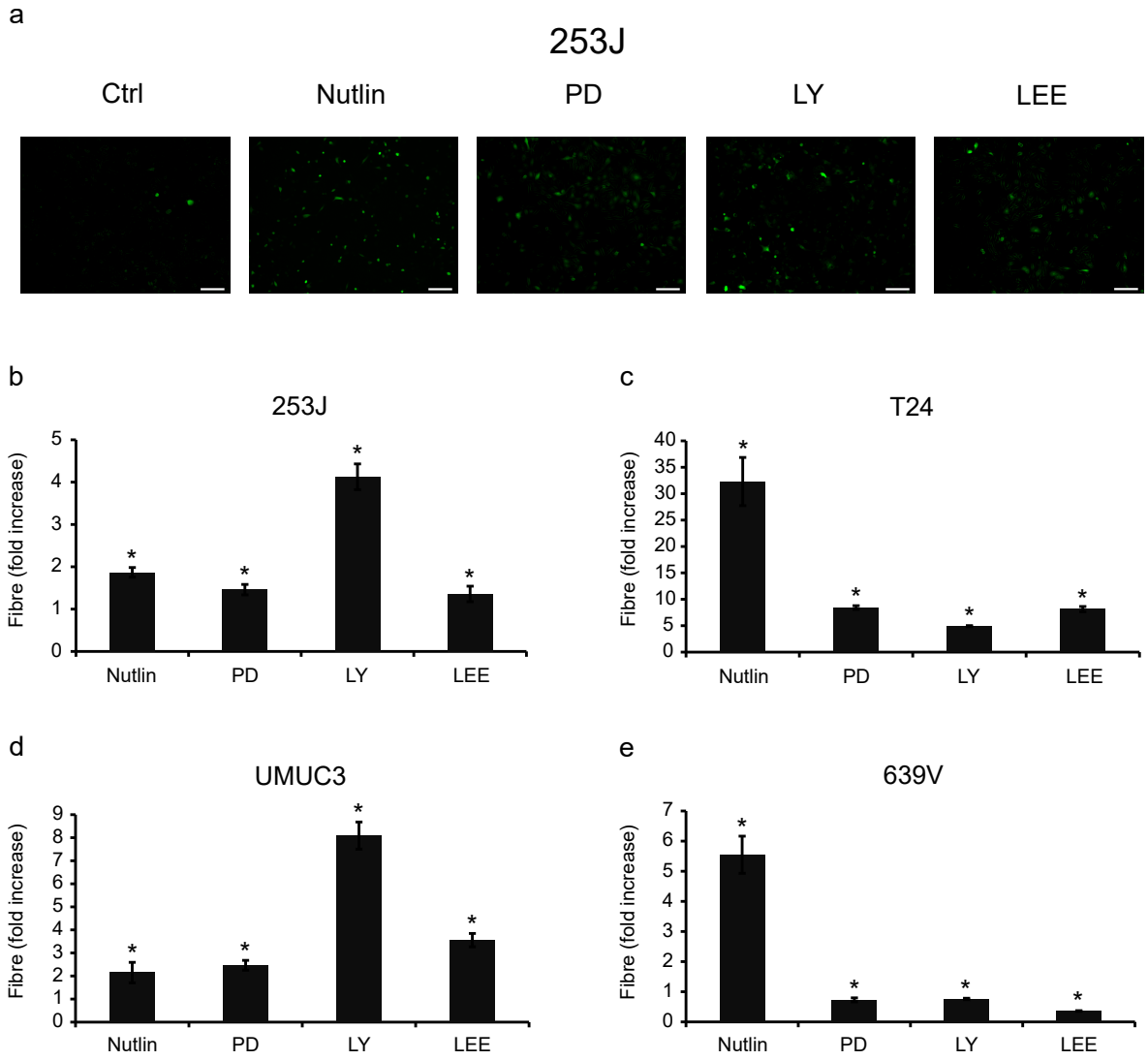

Figure 3.34.: **CDK4/6 or MDM-2 Inhibition Enhances Replication of E1-Deleted Virus in Rb Positive Cell Lines.** (a) 253J cells were treated with Nutlin-3a (30μM), PD-0332991/LY2835219 (500nM) or LEE011 (10μM) and infected with Ad-GFP (MOI 25). Virus infected cells express GFP and pictures were taken at 3dpi. Scale bar 10μm. (b) 253J cells were treated and infected as described in (a). (c) T24 cells were treated with Nutlin-3a (30μM), PD-0332991/LY2835219 (500nM) or LEE011 (10μM) and infected with Ad-GFP (MOI 50). (d) UMUC3 cells were treated with Nutlin-3a (30μM), PD-0332991/LY2835219 (1000nM) or LEE011 (10μM) and infected with Ad-GFP (MOI 25). (e) 639V cells were treated with Nutlin-3a (30μM), PD-0332991/LY2835219 (1000nM) or LEE011 (10μM) and infected with Ad-GFP (MOI 500). Viral replication was analysed at 72hpi. Values show the increase in replication upon treatment. Error bars S.D., $p<0.05$.

3.7. The Role of E2F1 upon Combination with CDK4/6 Inhibition

The results so far showed that (1st) E2F1 gene and protein expression were downregulated upon CDK4/6 inhibition, that (2nd) E2 gene expression was independent of the E1A region or the E2F1 binding sites in the E2 early promoter, and that (3rd) CDK4/6 inhibition could even increase transcription from the E2 early promoter in these viruses (Figure 3.33). These results led us to the hypothesis that E2F1 might be a negative regulator of viral replication which is in contrast to the current view that E1A and E2F1 stimulate the viral E2 early promoter [5, 41, 62].

3.7.1. Efficient Knockdown of E2F1 using siRNA Pool

To further investigate the role of E2F1 on virus induced cell death, viral replication, and viral particle formation, E2F1 was knocked down by a siRNA Pool and the effects on oncolytic virotherapy in combination with CDK4/6 inhibition were analysed. As shown in Figure 3.35a, E2F1 siRNA efficiently decreased E2F1 protein expression. CDK4/6 inhibition also decreased E2F1 protein expression in untransfected and control transfected cells but less efficiently than E2F1 siRNA. E2F1 gene expression levels were knocked down by >90% upon E2F1 siRNA transfection (Figure 3.35b) and CDK4/6 inhibition further decreased E2F1 gene expression levels by >60% in untreated cells as well as in siRNA transfected cells.

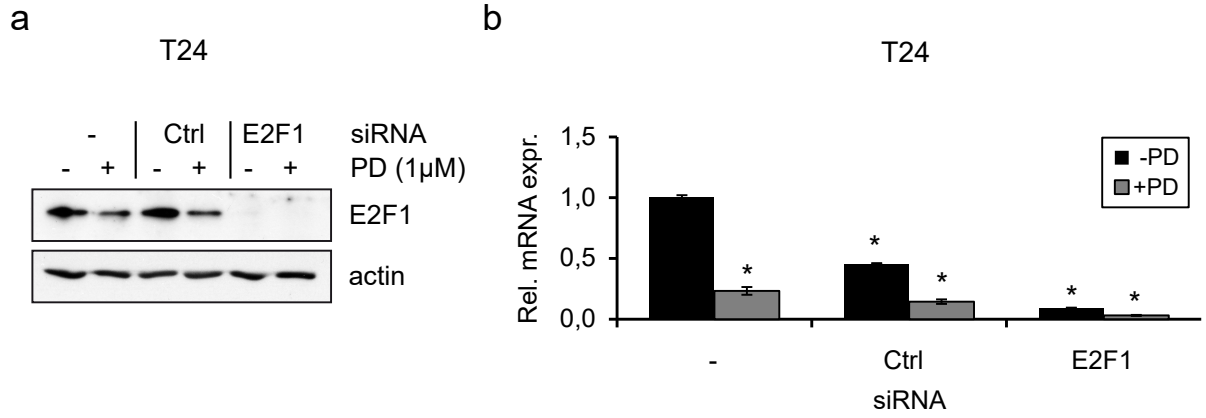

Figure 3.35.: **Efficient Knockdown of E2F1 using siRNA.** T24 were transfected with E2F1 or control siPOOL (1nM) and treated with PD-0332991 (1μM). After 24h, E2F1 protein (a) and E2F1 gene expression levels (b) were analysed. Values were normalised to GAPDH and values of untreated samples. Error bars S.D., p<0.05.

3.7.2. E2F1 Knockdown Increases Viral Replication in Rb Positive Cells

In a next step, viral replication upon E2F1 knockdown alone and in combination with CDK4/6 inhibition was analysed. As shown in Figure 3.36, E2F1 knockdown increased viral replication 3- and 1.5-fold for XVir-N-31 and WT, respectively. However, PD-0332991 treatment enhanced viral replication 7-16-fold for XVir-N-31 and 12-35-fold for WT.

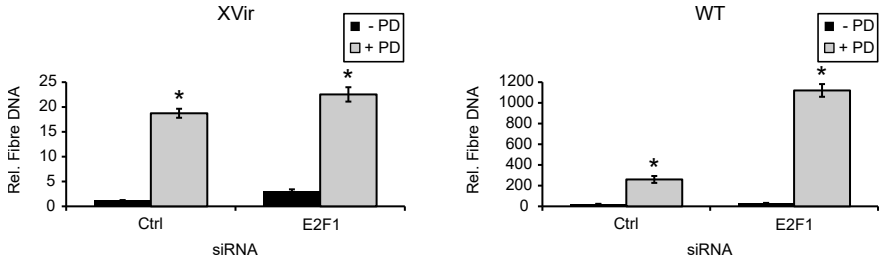

Figure 3.36.: **Viral Replication Is Enhanced upon E2F1 Knockdown and CDK4/6 Inhibition in Rb Positive Cells.** T24 were transfected with E2F1 or control siPOOL (1nM), where indicated treated with PD-0332991 (1μM), and infected with the indicated viruses (MOI 50). Viral replication was analysed at 24hpi. Error bars S.D., p<0.05.

3.7.3. In Rb Negative Cells E2F1 Knockdown Enhances Viral Replication of XVir-N-31 but not WT Adenovirus

To further analyse the role of Rb and E2F1 on viral replication, we analysed whether E2F1 knockdown could also increase viral replication in Rb negative cells in which CDK4/6 inhibition did not decrease E2F1 protein expression. As shown in Figure 3.37a, E2F1 siRNA efficiently decreased cellular E2F1 protein expression also in Rb negative 639V cells. Next, 639V cells were infected with XVir-N-31 or WT Adenovirus and viral replication upon E2F1 knockdown and/or CDK4/6 inhibition was analysed. As shown in Figure 3.37b, E2F1 knockdown increased viral replication of XVir-N-31 by 34-46%. However, CDK4/6 inhibition decreased viral replication of XVir-N-31 by 60% (compare Figure 3.21). In contrast to this, viral replication of WT Adenovirus was not significantly affected neither by E2F1 knockdown nor by CDK4/6 inhibition.

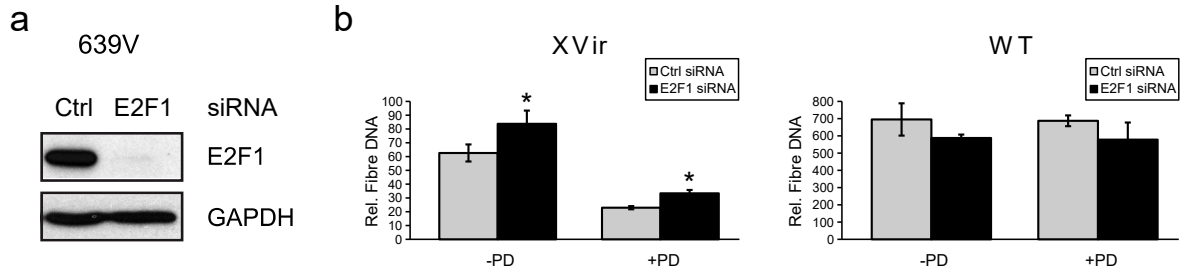

Figure 3.37.: **In Rb Negative Cells E2F1 Knockdown Enhances Viral Replication of XVir-N-31 but not WT Adenovirus.** (a) 639V cells were transfected with E2F1 or control siPOOL (1nM) and E2F1 protein expression was analysed after 24h. (b) 639V cells were transfected with E2F1 or control siPOOL (1nM), where indicated treated with PD-0332991 (1μM), and infected with the indicated viruses (MOI 50). Viral replication was analysed at 24hpi. Error bars S.D., $p<0.05$.

In a next step, we sought to analyse the effects of E2F1 knockdown in Rb negative T24 cells (T24 shRb1). As shown in Figure 3.38, E2F1 knockdown enhanced viral replication of XVir-N-31 2.5-fold in T24 shCtrl and 82% in T24 shRb1 cells. In T24 shCtrl cells, this effect was further enhanced in combination with CDK4/6 inhibition which increased viral replication 2-10-fold. For WT Adenovirus, E2F1 knockdown enhanced viral replication 10-fold in T24 shCtrl cells but decreased replication by 30% in T24 shRb1 cells. Moreover, viral replication of WT Adenovirus was enhanced 10-fold upon CDK4/6 inhibition in T24 shCtrl cells.

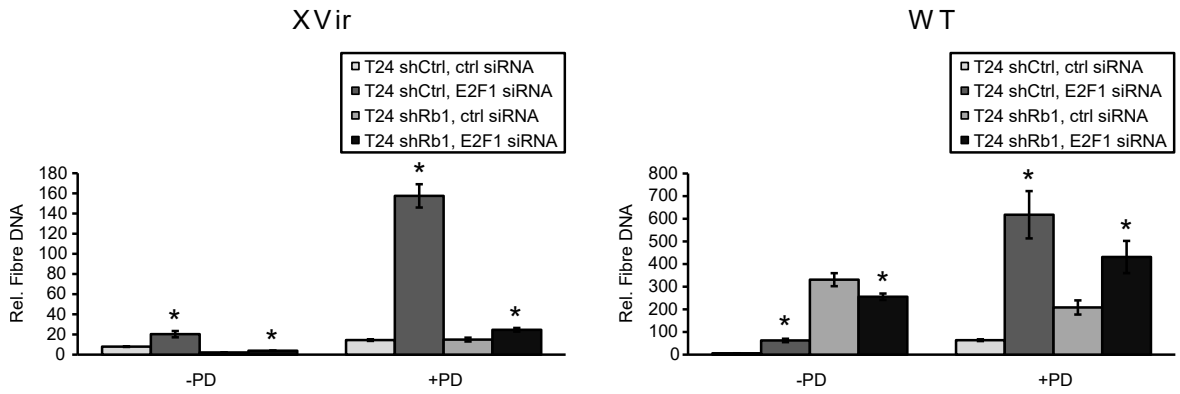

Figure 3.38.: **In T24 shRb1 cells E2F1 Knockdown Enhances Viral Replication of XVir-N-31 but not WT Adenovirus.** T24 shCtrl and T24 shRb1 cells were transfected with E2F1 or control siPOOL (1nM), where indicated treated with PD-0332991 (1μM), and infected with the indicated viruses (MOI 50). Viral replication was analysed at 24hpi. Error bars S.D., p<0.05.

3.7.4. E1-Independent Replication Is Decreased upon E2F1 Knockdown

In a next step, we analysed whether E2F1 knockdown could increase viral replication independent of the viral E1 or the cellular Rb protein. For this, T24 shCtrl and T24 shRb1 cells were transfected with E2F1 siRNA and infected with the E1-deleted Adenovirus Ad-GFP (Figure 3.30g). As shown in Figure 3.39, E2F1 knockdown decreased viral replication of Ad-GFP by 54-64% in both T24 shCtrl and T24 shRb1 cells. CDK4/6 inhibition by PD-0332991 could increase viral replication 2.4-2.7-fold in T24 shCtrl but not in T24 shRb1 cells. However, viral replication was still decreased upon E2F1 knockdown compared to control transfected cells.

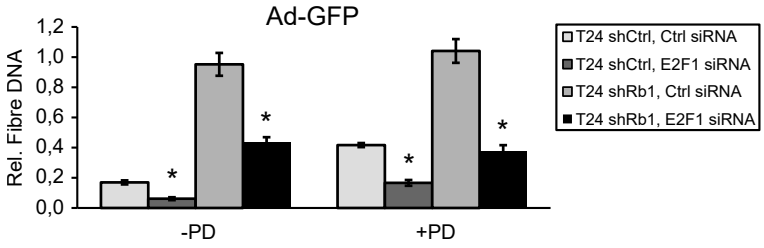

Figure 3.39.: **E1-Independent Replication Is Decreased upon E2F1 Knockdown.** T24 shCtrl or T24 shRb1 cells were transfected with E2F1 or control siPOOL (1nM), where indicated treated with PD-0332991 (1μM), and infected with Ad-GFP (MOI 100). Viral replication was analysed at 24hpi. Error bars S.D., p<0.05.

3.7.5. E2F1 Knockdown Does not Increase Virus Induced Cell Death nor Viral Particle Formation in Rb Positive Cells

Cell viability and viral particle formation were then analysed to see whether the increased replication upon E2F1 knockdown also led to an enhanced virus induced cell death and enhanced viral particle formation.

In contrast to viral replication, virus induced cell death was not increased by E2F1 knockdown. Figure 3.40 shows that there was no additional effect on cell viability for XVir-N-31 compared to

control treatment. For WT Adenovirus, E2F1 knockdown led to a 14% reduction in cell viability compared to control treatment. However, this effect was not as strong as with CDK4/6 inhibition which caused a >90% reduction in cell viability in all conditions.

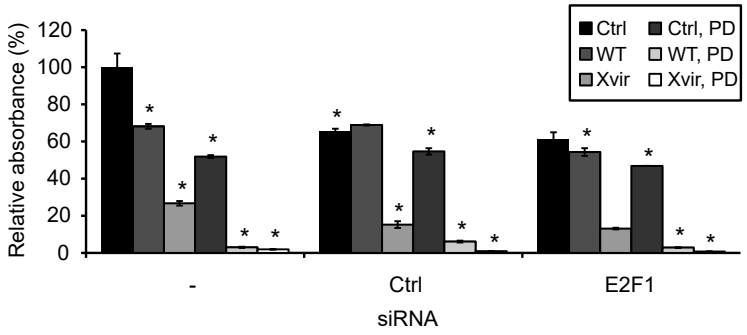

Figure 3.40.: **Knockdown of E2F1 Does not Enhance Virus Induced Cell Death.** T24 cells were transfected with E2F1 or control siPOOL (1nM), where indicated treated with PD-0332991 (1μM), and infected with the indicated viruses (MOI 50). Cell viability was analysed at 4dpi. Error bars S.E., p<0.05.

Next, viral particle formation upon E2F1 knockdown alone and in combination with CDK4/6 inhibition was analysed. As shown in Figure 3.41, knockdown of E2F1 did not increase infectious viral particle formation. However, CDK4/6 inhibition enhanced viral particle formation 1.4-fold for XVir-N-31 and 8-11-fold for WT Adenovirus.

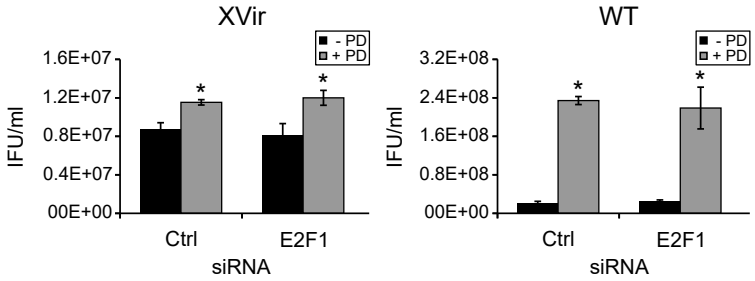

Figure 3.41.: **Knockdown of E2F1 Does not Enhance Infectious Viral Particle Production.** T24 cells were transfected with E2F1 or control siPOOL (1nM), where indicated treated with PD-0332991 (1μM), and infected with the indicated viruses (MOI 50). Viral titre is shown in infectious units/ml (IFU/ml). Values are averages of at least two independent experiments. Error bars S.E., p<0.05.

3.7.6. Ectopic E2F1 Expression Does not Influence Viral Replication

Knockdown of E2F1 induced an increase in viral replication and we next wanted to analyse whether viral replication was changed in E2F1 overexpressing cells. Therefore, E2F1 was cloned into a plasmid controlling gene expression under a CMV promoter and Hek293T cells were transiently transfected with this plasmid. As shown in Figure 3.42a, Hek293T cells transfected with the E2F1 plasmid showed increased E2F1 protein expression compared to control transfected cells (empty vector). Next, T24 cells were stably transfected with this plasmid by Lentivirus infection. Cells were infected with XVir-N-31 or WT Adenovirus and viral replication was analysed. Figure 3.42b shows that viral replication was not significantly changed in E2F1 overexpressing cells compared to control.

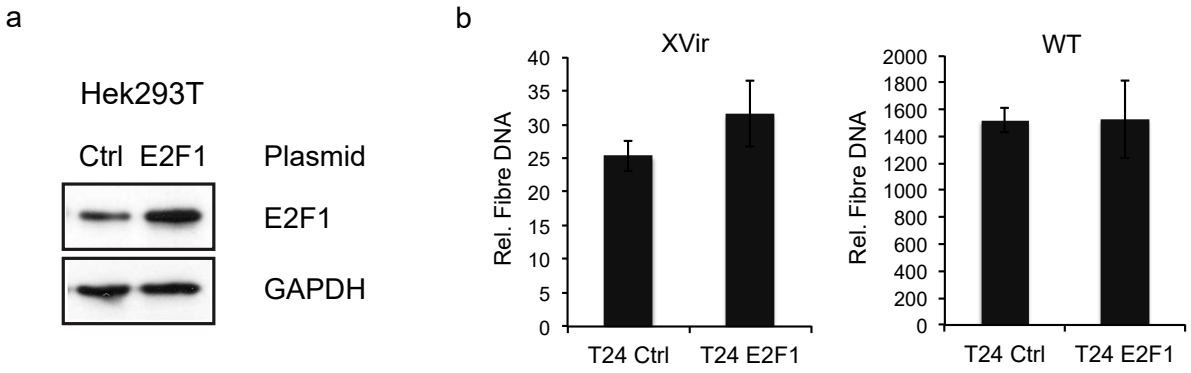

Figure 3.42.: **E2F1 Overexpression Does not Affect Viral Replication.** Hek293T cells were transiently transfected with E2F1 or control plasmid (empty vector) and protein expression was analysed 48h after transfection (a). T24 cells were stably transfected with the plasmid and infected with the indicated viruses (MOI 50). Viral replication was analysed at 48hpi. Error bars S.D., $p<0.05$.

3.8. The Role of MDM2 on Viral Replication

MDM2 was reported to bind to hypophosphorylated Rb thereby disrupting the interaction with E2F1 which leads to activation of E2F1 and subsquently cell cylce progression [10]. Moreover, MDM2 was shown to regulate Rb stability on the one hand by inducing ubiquitination of Rb and on the other hand by inducing E2F1 activity [10]. Furthermore, unpublished data from our group showed that the initial response to CDK4/6 inhibition by PD-0332991 was impaired by siRNA knockdown of MDM2 indicating a role for MDM2 in the CDK4/6 pathway (personal communication, AG Nawroth). Thus, we sought to analye viral replication upon MDM2 inhibition, first in combination with the MDM2 inhibitor Nutlin-3a and second upon siRNA mediated knockdown of MDM2.

3.8.1. Nutlin-3a Decreases E2F1 Protein Expression

Nutlin-3a is a MDM2 inhibitor which was first tested for its activity by analysis of E2F1 and Rb protein expression upon treatment. As shown in Figure 3.43, Nutlin-3a treatment strongly reduced E2F1, Rb, and pRb expression.

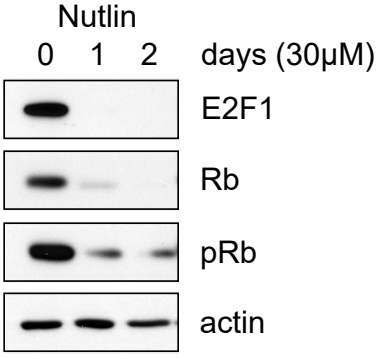

Figure 3.43.: **Nutlin-3a Reduces E2F1 and Rb Expression.** T24 cells were treated with Nutlin-3a (30μM) and E2F1, Rb, and pRb expression was analysed at indicated time points.

3.8.2. Nutlin-3a Treatment Increases Viral Replication

E2F1 expression was downregulated upon Nutlin-3a treatment and we therefore sought to investigate whether Nutlin-3a could increase viral replication of XVir-N-31 and WT Adenovirus. As shown in Figure 3.44, MDM2 inhibition increased viral replication 13- and 2-fold for XVir-N-31 and WT, respectively.

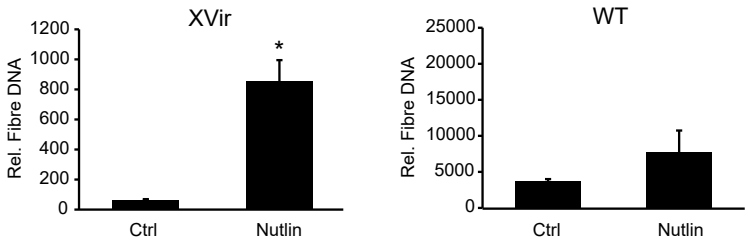

Figure 3.44.: **Nutlin-3a Increases Viral Replication** T24 cells were infected with the indicated viruses (MOI 50) and where indicated treated with Nutlin-3a (30μM). Viral replication was analysed at 48hpi. Error bars S.D., p<0.05.

3.8.3. Combined MDM2 Knockdown and CDK4/6 Inhibition Increase Viral Replication

As mentioned before, data from our group showed that MDM2 knockdown by siRNA reduced the cellular response to CDK4/6 inhibition (personal communication, AG Nawroth) and we therefore wanted to analyse viral replication upon combined MDM2 knockdown and CDK4/6 inhibition to see whether CDK4/6 inhibition could still enhance viral replication under these conditions. As shown in Figure 3.45a, CDK4/6 inhibition by PD-0332991 increased viral replication of XVir-N-31 2.8-fold in control transfected cells. Upon MDM2 knockdown by three different siRNAs, CDK4/6 inhibition increased viral replication 15-, 3.3-, and 239-fold, respectively. For WT Adenovirus, CDK4/6 inhibition increased viral replication 59-fold in control transfected cells. Upon MDM2 knockdown, CDK4/6 inhibition increased viral replication 10-, 13-, and 18-fold, respectively. Thus, CDK4/6 inhibition could still increase viral replication upon MDM2 knockdown.

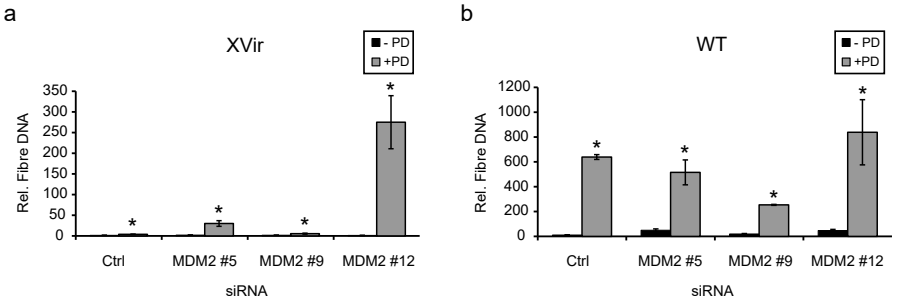

Figure 3.45.: **Combined MDM2 and CDK4/6 Inhibition Increases Viral Replication.** T24 were treated with MDM2 or control siRNA (1nM) and PD-0332991 (1000nM) for one day and infected with the indicated viruses (MOI 50). Viral replication was analysed at 24hpi. Error bars S.D., p<0.05.

3.9. The Role of Myc on Oncolytic Virotherapy

The Myc oncoprotein is a transcription factor that is involved in many signalling pathways during tumourigenesis. The Adenoviral E1A protein is known to stabilise Myc during viral infection and the E1A-Myc interaction is important for E1A activity [15]. Moreover, the induction of Myc and its downstream targets is a direct consequence of CDK4/6 inhibition which confers resistance to CDK4/6 inhibition as reported by Tarrado-Castellarnau et al [64]. Unpublished data from our group also showed that cells overexpressing Myc were partially resistant to CDK4/6 inhbition (personal communication, AG Nawroth). To further analyse the molecular mechanisms of CDK4/6 inhibition on oncolytic virotherapy, we sought to investigate the role of Myc by analysing viral replication in Myc overexpressing cells to see whether CDK4/6 inhibition could still enhance viral replication in these partially resistant cells.

3.9.1. Overexpression of Myc Decreases Viral Replication

Myc was stably overexpressed in T24 cells. For this, Myc was cloned into a plasmid controlling gene expression by a CMV promoter and T24 cells were transfected with this plasmid by Lentiviral gene transfer. As shown in Figure 3.46, T24 Myc cells showed increased protein expression compared to control cells. However, CDK4/6 inhibition could not decrease Myc protein expression in T24 Myc cells but in control cells indicating partial resistance of these cells to CDK4/6 inhibition.

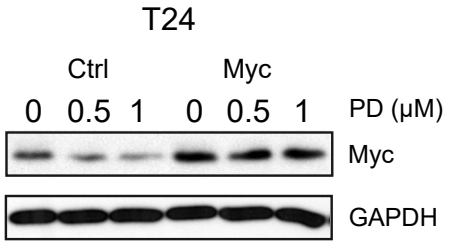

Figure 3.46.: **Upon CDK4/6 Inhibition Myc Protein Expression Is not Downregulated in T24 Myc Cells.** T24 cells overexpressing Myc or control cells were treated with PD-0332991 at indicated concentrations and protein expression was analysed at 24h. Data were kindly provided by Pan Qi.

In a next step, we analysed whether CDK4/6 inhibition could still increase viral replication in these partially resistant T24 Myc cells. As shown in Figure 3.47, viral replication upon PD-0332991 treatment was reduced in T24 Myc cells compared to control. For XVir-N-31, replication was reduced by 50 and >60% at 24 and 48hpi, respectively. Replication of WT Adenovirus was reduced by 40 and 14% at 24 and 48hpi, respectively. Thus, upon CDK4/6 inhibition viral replication was diminished in Myc overexpresing cells compared to control cells.

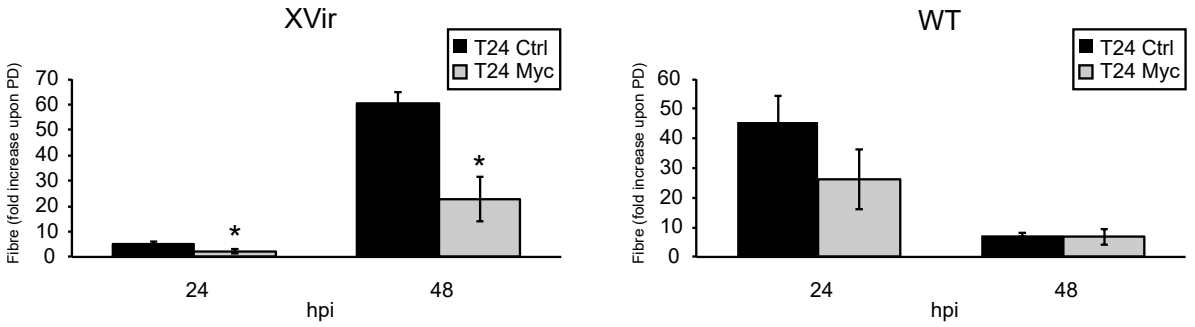

Figure 3.47.: **In Myc Overexpressing Cells Viral Replication Is Reduced upon CDK4/6 Inhibition.** T24 cells overexpressing Myc or control cells were treated with PD-0332991 (1μM) and infected with the indicated viruses (MOI 50). Viral replication was analysed at 24 and 48hpi. Values show the increase in replication upon treatment. Error bars S.D., $p<0.05$.

4. Discussion

The aim of this study was to improve oncolytic virotherapy in BC by combining the oncolytic Adenovirus XVir-N-31 with small molecule inhibitors and to examine the molecular mechanisms underlying these combination therapies. Oncolytic virotherapy makes use of tumour specific viruses which specifically replicate in tumour cells thereby causing tumour cell death, viral release from, and viral spread within the tumour. So far, it is well established that oncolytic viruses rely on the cellular cell cycle machinery, cellular transcription factors, and cell cycle progression for proper DNA replication and viral particle formation.

In this study, we combined several small molecule inhibitors with oncolytic virotherapy and investigated the effects of these combination therapies on virus induced cell death, viral replication, viral particle formation as well as on cellular and viral gene and protein expression. In contrast to the common view, we here showed that cell cycle inhibitors, which induce a G1-arrest, strongly enhanced virus induced cell death, viral replication, and viral particle formation. These effects were partially attributed to a downregulation of the cellular transcription factor E2F1 which, in contrast to current literature, was shown to be a negative regulator of viral replication.

4.1. The Oncolytic Adenovirus XVir-N-31 Is Effective in Human BC Cell Lines

In a first step, we examined the oncolytic efficacy of XVir-N-31 on a panel of BC cell lines. For this purpose, a dose-response assay upon infection with increasig MOIs of the virus was performed and cell viability was assessed after two cycles of viral replication (4dpi). We observed that different BC cell lines were differentially susceptible to virus induced cell killing by XVir-N-31: some cells showed a decrease in cell viability upon infection with MOIs <15 while others only showed a decrease in cell viability upon infection with MOIs >100.

During Adenoviral infection, the viral Fibre protein interacts with the cellular CAR receptor which is the most important receptor during Adenoviral infection. After initial attachment, the RGD motif in the viral Penton base binds to cellular αvβ3/αvβ5-integrins which finally leads to virus internalisation [52]. The oncolytic Adenovirus XVir-N-31 encodes an additional RGD motif in the viral Fibre protein so that the Fibre protein can also interact with cellular αvβ3/αvβ5-integrins thereby leading to a better infectivity of tumour cells which often show a downregulation in CAR expression levels [34].

Thus, the different susceptibilities of BC cell lines to infection with XVir-N-31 were accounted to differences in CAR expression levels as unpublished data from the group confirmed that the three most resistant cell lines T24, 639V, and RT112 express low to almost no CAR (personal communication, AG Holm). Therefore, infection of tumour cells might be enhanced by an additional RGD motif in the viral Fibre protein but still it seems that CAR expression levels determine the sensitivity of cells to Adenoviral infection.

4.2. Chk1 Inhibition Does not Improve Oncolytic Virotherapy

In 2011, Connell et al showed that the Chk1 inhibitor UCN-01 could increase the effects of WT and the oncolytic Adenovirus dl-922-947 in ovarian cancer cell lines [21]. According to this study, UCN-01 inhibits the ATR-Chk1 pathway, leading to increased cellular DNA damage and an impaired DNA repair response thereby potentiating the effects of virus induced host cell DNA damage. Thus, the authors concluded that the cellular DNA damage signalling and repair

pathway was a key determinant of oncolytic virus activity and that inhibition of this pathway by UCN-01 would lead to viral DNA over-replication and an increased virus induced cell death in the combination therapy [21]. Based on these data, we asked whether Chk1 inhibition could also increase the effects of XVir-N-31 in BC.

First, the two Chk1 inhibitors UCN-01 and AZD7762 (as described in Chapter 1.4.1) were tested in monotherapy for their effects on cell viability and on molecular downstream targets. Both inhibitors efficiently decreased cell viability of BC cell lines in the monotherapy setting. This experiment was performed in order to determine the IC_{50} values for further combination therapies as we wanted to use concentrations with low toxicities but biochemical activity in the combination therapy.

Similar to the described data [21], UCN-01 enhanced the oncolytic effects of XVir-N-31 on virus induced cell death in all BC cell lines tested. However, combination with AZD7762 could not enhance virus induced cell death. We therefore concluded that the effects responsible for the enhanced virus induced cell death upon combination with UCN-01 were probably not due to Chk1 inhibition but might be accounted to inhibition of other targets besides Chk1. In addition, the effects observed in the study by Connell et al could also be explained by non-specific effects of UCN-01 as high doses of the inhibitor (up to 300nM) were used. It was shown before that at these concentrations, UCN-01 inhibits several other targets besides Chk1 including cyclins, other CDKs, Akt, and protein kinase C [1, 26, 59, 61]. AZD7762 on the other hand, is known to specifically inhibit Chk1 and Chk2 [2] and therefore it is likely that the enhanced effects in combination with UCN-01 were not due to Chk1 inhibition as suggested by Connell et al [21] but rather due to unspecific effects on other targets.

In a next step, we investigated the biochemical effects of UCN-01 and AZD7762 on targets of the Chk1 and CDK4/6-Rb pathway as UCN-01 was described to be a potent inhibitor of the latter [1, 2, 61]. Here, we could show that UCN-01 but not AZD7762 strongly downregulated Rb and pRb protein expression (Figure 3.3) which is in line with previous studies [1, 61]. In addition, we and others have shown that downregulation of Rb and pRb expression is a common feature of CDK4/6 inhibition [55] and therefore the effects observed in combination with UCN-01 might be due to CDK4/6 rather than Chk1 inhibition. Moreover, it was reported before that UCN-01, but not AZD7762, arrests cells in G1-phase [1, 24, 61] probably due to CDK4/6 inhibition and Rb downregulation.

So far, it is well established that for optimal viral replication Adenoviruses require the activation of cellular transcription factors as well as the induction of S-phase [11]. Therefore, a combination with cell cycle inhibitors should, at least in theory, have antagonistic effects on oncolytic virotherapy. However, this model was already questioned by two publications: in 1997, Goodrum et al investigated whether the amount of viral particles produced by cells differed when cells were infected during G1- or S-phase. This study showed that cells infected with WT Adenovirus during G1-phase produced three times more virus than cells infected during S-phase [28]. The molecular mechanisms underlying these effects were however not investigated in this study. In addition, another study by Bagheri et al showed that MEK inhibition by CI1040 led to cell cycle arrest in G1-phase which was accompanied by an enhanced virus induced cell death in the combination therapy [4]. However, the enhanced effects in combination with G1-arresting drugs have not been explained to date, probably also because these observations were overlooked or ignored by the community as they stand in clear contrast to the current model of how Adenovirus biology and replication work.

4.3. CDK4/6 Inhibition Improves Oncolytic Virotherapy

As UCN-01 showed effects on Rb and pRb protein expression similar to other CDK4/6 inhibitors [1, 2, 55, 61], we next investigated whether the specific CDK4/6 inhibitors PD-0332991, LY2835219, and LEE011 had similar effects in combination with oncolytic virotherapy. Alike UCN-01, the combination of oncolytic virotherapy with specific CDK4/6 inhibitors strongly increased the effects of oncolytic virotherapy as observed by a strong synergistic effect on virus induced cell death, viral replication, and viral particle formation in all four Rb positive BC cell lines tested.

Moreover, we could show here that CDK4/6 inhibitors, which arrest cells in G1-phase [55], could strongly improve oncolytic virotherapy thereby further supporting the data of Bagheri and Goodrum et al that G1-arrest, but not S-phase induction, is beneficial for Adenovirus replication. In addition, we observed that CDK4/6 inhibitors decreased E2F1 protein expression which is an important transcription factor required for S-phase induction [26, 47]. Furthermore, E2F1 is thought to play a major role during Adenovirus replication because it was reported to be an important activator of viral E2 gene expression and DNA replication (see Chapter 1.2.1) [57, 62]. Thus, the findings presented here are especially striking as E2F1, which is thought to activate viral E2 gene expression [57, 62], was downregulated upon CDK4/6 inhibition and at the same time CDK4/6 inhibition strongly increased viral replication. In summary, our findings indicate that G1-arrest, but not S-phase induction, enhances viral replication and that downregulation of E2F1 is beneficial for viral replication.

4.3.1. CDK4/6 Inhibition Improves Oncolytic Virotherapy Independent of Pretreatment Regimen

Previous studies combining oncolytic virotherapy with small molecule inhibitors have shown that these inhibitors could alter the expression levels of CAR and thus influence viral infectivity [4, 7, 53, 56]. The MEK inhibitor CI1040 for example was shown to upregulate cellular CAR expression and improve oncolytic virotherapy [4]. To rule out the possibility that the enhanced effects observed in combination of oncolytic virotherapy with CDK4/6 inhibitors were due to a better infectivity of the cells and an enhanced virus entry into the cell, cells were treated with PD-0332991 at different time points before (24h and 6h) and after infection (1hpi) to see whether different pretreatment regiments had any effects on virus induced cell death. However, we could not observe any differences between theses pretreatment regimens. In addition, CAR expression levels were not changed upon CDK4/6 inhibition in T24 and UMUC3 cells (personal communication, AG Holm) which is in line with previous studies showing that CDK4/6 inhibition by PD-0332991 did not affect CAR expression levels [37]. Moreover, RT-qPCR data confirmed that the entry level of viral DNA into the cell was not changed upon CDK4/6 inhibition (Figure 3.29). Thus, we could rule out that the improved oncolytic virotherapy upon CDK4/6 inhibition was due to an enhanced viral entry into the cells or due to a technical artefact. These effects were rather attributed to changes in cell cycle progression and expression of transcription factors, such as E2F1, upon CDK4/6 inhibition.

4.3.2. CDK4/6 Inhibition Does not Improve Oncolytic Virotherapy in Rb Negative Cell Lines

As reported before by others and our group, CDK4/6 inhibitors are only effective in vitro in Rb positive cell lines [26, 47]. Therefore, we asked whether CDK4/6 inhibition could also improve oncolytic virotherapy in Rb negative, therapy resistant cell lines. Importantly, oncolytic virotherapy

was not enhanced in the Rb negative cell lines 639V and 647V nor in the Rb knockout cell line T24 shRb1 indicating that response to therapy directly correlated with effects on oncolytic virotherapy.

In contrast to Rb positive cells, Rb negative cells do not rely on Rb for cell cycle progression resulting in an Rb-independent regulation of S-phase induction [54] and resistance to CDK4/6 inhibition [26, 47]. As a consequence, CDK4/6 inhibitors do not cause any G1-arrest in these cell lines as shown previously by our group [55]. However, G1-arrest was associated with increased viral replication in previous and our studies (see above) [4, 28] and therefore the lack of G1-arrest upon CDK4/6 inhibition in Rb negative cells could explain why oncolytic virotherapy was not improved in these cells. This implies that oncolytic virotherapy is only improved in cell lines that are responsive to CDK4/6 inhibition and in which the latter causes cell cycle arrest in G1-phase.

4.3.3. E2F1 Is a Negative Regulator of Viral Replication

As reported before, the cellular transcription factor E2F1 plays an important role in Adenovirus biology and it is considered to be an activator for viral E2 gene transcription and viral replication [57, 62].

In this study, the cellular response to CDK4/6 inhibition was associated with a downregulation of E2F1 expression (Figure 3.9) which directly correlated with an enhanced virus induced cell death, viral replication, and viral particle formation. Rb negative cells in contrast, did not respond to CDK4/6 inhibition: in these cells, E2F1 protein expression was not affected upon CDK4/6 inhibition and oncolytic virotherapy could not be improved in the combination therapy. Thus, response to CDK4/6 inhibition was associated with decreased E2F1 levels and improved oncolytic virotherapy in the combination treatment. In Rb positive cells, the expression of transcription factors such as E2F1 is tightly controlled during cell cycle progression. It is known that E2F1 can stimulate its own transcription and expression leading to a positive feedback loop and finally cell cycle progression [66]. Moreover, Rb can stabilise E2F1 transcription factors [44] and thus the downregulation of Rb upon CDK4/6 inhibition might correlate with downregulation of E2F1 and finally cell cycle arrest in G1-phase. In contrast to this, transcription factors such as E2F1 can not be stabilised by Rb in Rb negative cells [44] leading to a differentially regulated expression of E2F1 in these cells. This could explain why E2F1 expression was not affected by CDK4/6 inhibition in Rb negative cells which in turn were not arrested in G1-phase upon CDK4/6 inhibition.

So far, E2F1 is considered to be an activator for viral E2 gene transcription and viral replication [57, 62]. In 2011, Pelka et al showed that E2F1 activated a E2F-responsive promoter in a luciferase plasmid [48]. Moreover, our group was able to reproduce these data showing that E2F1 could indeed activate the promoter of a luciferase plasmid (personal communication, AG Holm). In contrast to this, we here showed that decreased E2F1 levels upon CDK4/6 inhibition were associated with increased viral replication thereby providing evidence that E2F1 was rather a repressor of viral E2 gene expression and replication instead of an activator. The discrepacies between this study and the results presented by Pelka et al could be explained by the difference that in this study the replication of intact viruses was analysed while Pelka et al investigated the promoter activity of a luciferase plasmid [48]. It is likely that the promoter activity of a simple plasmid can not reflect the complex interplay of transcription factors and transcription factor binding sites during viral replication. In contrast to plasmids, Adenoviruses possess various binding sites for transcription factors including two E2F1 binding sites in the E2 early promoter. In addition, whole viruses encode various proteins, such as E1A, which are capable of manipulating a variety of cellular processes. Thus, E2F1 seems to have different activities on promoters leading to activation in plasmids while repressing promoter activities of intact viruses.

Based on these results, our group constructed a virus with mutated E2F1 binding sites in the E2 early promoter (E2F mut). In line with the results presented in this study, E2F mut replicated stronger than WT Adenovirus with intact E2F1 binding sites in the E2 early promoter (personal communication, AG Holm) thereby supporting the hypothesis that, in contrast to the common view, E2F1 might be a repressor for viral E2 gene transcription and viral replication.

In the following, we further analysed the role of E2F1 on viral replication using siRNA mediated knockdown of E2F1. Knockdown of E2F1 slightly enhanced viral replication but not viral particle formation. However, CDK4/6 inhibition strongly increased viral replication and viral particle formation indicating that downregulation of E2F1 might be one but not the only factor contributing to the enhanced effects upon combination with CDK4/6 inhibition. In addition, in Rb negative cells E2F1 knockdown increased viral replication of XVir-N-31 but not WT Adenovirus suggesting that in these cells E2F1 knockdown enhanced viral replication only in the presence of E1A12S (XVir-N-31) but not in the presence of E1A13S (WT) which in previous studies was shown to also have repressive functions (see Chapter 4.3.4 and 4.4) [9, 30]. In conclusion, these results showed that downregulation of E2F1 was correlated with enhanced viral replication although these effects were not as strong as with CDK4/6 inhibitors. Thus, downregulation of E2F1 upon CDK4/6 inhibition might be one but not the only factor contributing to the enhanced effects upon CDK4/6 inhibition.

As CDK4/6 inhibition downregulated E2F1 protein levels, we next investigated the effects of combined CDK4/6 inhibition and Adenoviral infection on E2F1 expression levels (Figure 3.25 and 3.26). At early phases of infection, E2F1 gene and protein expressions were downregulated in the combination treatment. However, at later times of infection, Adenoviruses reversed the effect of CDK4/6 inhibition on E2F1 expression levels leading to an increased E2F1 gene and protein expression. Interestingly, increasing E2F1 levels parallelled with increasing E1A levels (Figure 3.31) thereby suggesting an effect of E1A on E2F1 expression at later time points. This kinetic can be explained with respect to the Adenoviral live cycle: during early times of infection E2F1 acts as a repressor for viral E2 gene expression and replication so that downregulated E2F1 levels are beneficial for viral replication. As E2F1 was also shown to be associated with apoptosis, upregulation of E2F1 at later times of infection could be induced by the virus in order to repress viral DNA replication and to ensure an efficient packaging, cell lysis, apoptosis, and viral release from the cell [23]. In summary, the expression of E2F1 is controlled by the virus, probably by E1A, in order to ensure proper DNA replication, packaging, and release from the cell.

4.3.4. CDK4/6 Inhibition Improves Oncolytic Viortherapy Independent of the Viral E1 Region or E2F1 Binding Sites

Adenoviruses have evolved several mechanisms to activate cellular genes and to interfere with cellular cell cycle pathways thereby leading to optimal conditions for viral replication and S-phase transition [11].

To further analyse the mechanisms underlying the enhanced effects of CDK4/6 inhibition on oncolytic virotherapy, we investigated the role of different viral genes and transcription factor binding sites using different viral mutants. In detail, we investigated the role of the viral E1A/E1 region as well as the two E2F1 binding sites in the viral E2 early promoter on viral gene and protein expression in combination with CDK4/6 inhibition. We could show that viral protein and gene expressions were strongly enhanced upon CDK4/6 inhibition independent of mutations in or deletions of the viral E1 region. Interestingly, gene expression was enhanced stronger for XVir-N-31 compared to WT Adenovirus. This could be explained by E1A13S which is mutated in XVir-N-31 and which was shown by Borrelli and Hen et al to also have repressive functions on

viral gene expression [9, 30]. Thus, WT E1A13S might attenuate the increase in gene expression levels upon CDK4/6 inhibition.

In addition, we showed that CDK4/6 inhibition strongly enhanced viral E2 gene transcription and viral replication independent of E1A mutations (CMV E1B55k RSV E4 virus) or E1-deletions (Ad-GFP virus) (Figure 3.33 and 3.34). This implies that the viral E1 proteins are not involved in the enhanced effects upon CDK4/6 inhibition. Nevertheless, these results also showed that E1A mutated and E1-deleted viruses replicated to a much lower extend than XVir-N-31 or WT Adenovirus. Thus, E1 proteins are needed for efficient viral DNA replication but they are not essential for the enhanced replication upon CDK4/6 inhibition.

Furthermore, our results showed that CDK4/6 inhibition could enhance E2 gene transcription from the E2 early and the E2 late promoter independent of E2F1 binding sites in the E2 early promoter (Figure 3.33). The result that mutations of E2F1 binding sites did not negatively affect E2 gene transcription further supports the hypothesis that E2F1 might be a repressor rather than an activator of viral E2 gene expression and viral replication (see Chapter 4.3.3). On the other hand, if E2F1 was an activator of E2 gene transcription, mutations in these binding sites would strongly suppress E2 gene transcription of this virus. In summary, these data give further evidence that E2F1 is a repressor instead of an activator of viral E2 gene expression and replication.

4.3.5. MDM2 Knockdown Confers Resistance to CDK4/6 Inhibition but Does not Attenuate Viral Replication upon CDK4/6 Inhibition

The oncoprotein MDM2 is a ubiquitin ligase which is frequently overexpressed or amplified in tumours. MDM2 plays an important role in the regulation of the tumour suppressor p53 leading to ubiquitination and degradation of the latter. However, recent findings indicate that MDM2 also plays a role in tumourigenesis independent of p53: it was shown that MDM2 directly promotes ubiquitination and destruction of Rb thereby leading to activation of E2F1 and cell cycle entry. Moreover, MDM2 overexpression was shown to result in increased E2F1 expression and E2F1-dependent transcriptional activity. Thus, MDM2 promotes cell cycle progression by inducing E2F1 activity and by simultaneously inhibiting Rb [10].

Nutlin-3a which was originally designed to inhibit the MDM2–p53 binding was also shown to disrupt the interaction of MDM2–E2F1 [10]. We were therefore interested in the effects of Nutlin-3a on E2F1 and Rb protein expression as well as in its role during viral replication. Here, we showed that Nutlin-3a decreased the expression of Rb, pRb, and E2F1 (Figure 3.43) which is in line with previous studies [67] as E2F1 can no longer be stabilised upon inhibition of MDM2 [10]. Furthermore, E2F1 downregulation upon Nutlin-3a treatment was associated with increased viral replication thereby showing the same association between E2F1 downregulation and increased viral replication as observed in combination with CDK4/6 inhibition.

Our group has recently shown that MDM2 is directly involved in the proteasome mediated degradation of Rb upon CDK4/6 inhibition and that knockdown of MDM2 partially prevents the initial degradation of Rb upon CDK4/6 inhibition (personal communication, AG Nawroth). Thus, MDM2 plays an important role in therapy response to CDK4/6 inhibitors and it is directly involved in the regulation of Rb and E2F1. Therefore, we analysed the role of combined MDM2 knockdown and CDK4/6 inhibition to see whether CDK4/6 inhibition could still increase viral replication even upon knockdown of MDM2.

However, siRNA mediated knockdown of MDM2 could not prevent the effects of CDK4/6 inhibition on viral replication as viral replication was strongly enhanced in combination with CDK4/6 inhibition and all three MDM2 siRNAs tested. This indicates that MDM2 knockdown plays

a role in resistance to CDK4/6 inhibition only at early times of treatment (personal communication, AG Nawroth). As viral replication was analysed at 24hpi, this initial resistance was probably overcome so that the effects of CDK4/6 inhibition on viral replication predominated.

4.3.6. Myc Overexpression Confers Resistance to CDK4/6 Inhibition and Attenuates Viral Replication upon CDK4/6 Inhibition

The transcription factor Myc is involved in many cellular signalling pathways and it also plays a role in Adenovirus biology. The Adenoviral E1A protein can stabilise Myc during viral infection and this E1A-Myc interaction is important for E1A activity [15]. Moreover, we and others could show that the induction of Myc was a direct consequence of CDK4/6 inhibition [64] and that Myc overexpressing cells were partially resistant to CDK4/6 inhibition. To further analyse the mechanisms involved in the enhanced effects of CDK4/6 inhibition on viral replication, we analysed viral replication in Myc overexpressing cells, which are resistant to CDK4/6 inhibition, to see whether CDK4/6 inhibition could enhance viral replication even in these partially resistant cells.

Here, we showed that viral replication of XVir-N-31 and WT Adenovirus was decreased upon CDK4/6 inhibition in Myc overexpressing cells compared to control cells (Figure 3.47). Thus, CDK4/6 inhibition could only improve viral replication in responding cell lines but not in cells that were (partially) resistant to CDK4/6 inhibition. This might imply that, apart from Rb, Myc is also involved in the resistance of cells to CDK4/6 inhibition and that Myc might also contribute to the enhanced effects on viral replication in the combination therapy. In summary, our results showed that Myc overexpression did not only confer resistance to CDK4/6 inhibition but also attenuated the enhanced replication upon CDK4/6 inhibition. This is in line with the results obtained in Rb negative cell lines which already implied that viral replication could only be improved in cell lines that are responsive to CDK4/6 inhibition.

4.4. Proposed Model for the Regulation of Viral Replication

According to the common view, Adenoviruses require S-phase entry and transcriptional activation by cellular transcription factors, such as E2F1, for proper E2 gene activation and DNA replication [11, 62]. During G1-phase of the cell cycle, E2F1 transcription factors are bound to pocket proteins such as Rb which thereby repress E2Fs' transcriptional activity and S-phase entry [26, 47]. In this stage, E2F1 can not activate cellular nor viral promoters including the viral E2 early promoter which possesses two E2F1 binding sites (see Figure 1.5) [57]. However, this promoter is needed for viral E2 gene transcription and viral DNA replication and thus, according to the common view, Adenoviruses require S-phase entry and transcriptional activation by E2F1 for proper DNA replication [57]. For this, Adenoviruses have evolved mechanisms to induce S-phase entry and to interfere with the Rb/E2F1 complex through the viral E1A protein which interacts with this complex by binding to Rb. In the following, E2F1 transcription factors are released from the complex to activate S-phase entry, viral E2 gene transcription, and viral replication [11].

In contrast to this, further studies revealed that the viral E1A protein was unable to disrupt the Rb/E2F1 complex but instead formed a stable complex with Rb and E2F1 [29, 48, 57]. Moreover, it was shown that E2F1, but not other E2F transcription factors, binds to the viral E2 early promoter only in complex with Rb and E1A thereby activating E2 gene transcription [57]. The two described activation models are illustrated schematically in Figure 4.1 (top).

On the contrary, we here provide evidence that E2F1 is not an activator but rather a repressor for E2 gene transcription and viral replication. This was shown by induction of G1-arrest and downregulation of E2F1 by CDK4/6 inhibition or E2F1 siRNA which both enhanced viral replication (Figure 4.1, bottom). Moreover, mutations of the two E2F1 binding sites in the viral E2 early promoter (E2F mut virus) revealed that replication of this virus was increased compared to WT Adenovirus (personal communication, AG Holm). If E2F1 was an activator of E2 gene transcription, as it is claimed by current literature, mutations in these binding sites would strongly suppress E2 gene transcription and viral replication of this virus.

In summary, all these data provide evidence that, in contrast to the current view, E2F1 is a repressor rather than an activator for E2 gene transcription and viral replication. The model provided here is probably a very simplified illustration of viral E2 gene transcription and promoter activation. Most likely, there are many more transcription factors involved which also bind to the viral E2 promoter in complex with Rb and/or E1A. To unravel these transcription factors and transcription factor complexes, additional promoter studies and immuno-precipitation (IP) assays would be needed. Nevertheless, our model could explain why CDK4/6 inhibition and knockdown of E2F1 enhanced viral replication of XVir-N-31 and WT Adenovirus in this study.

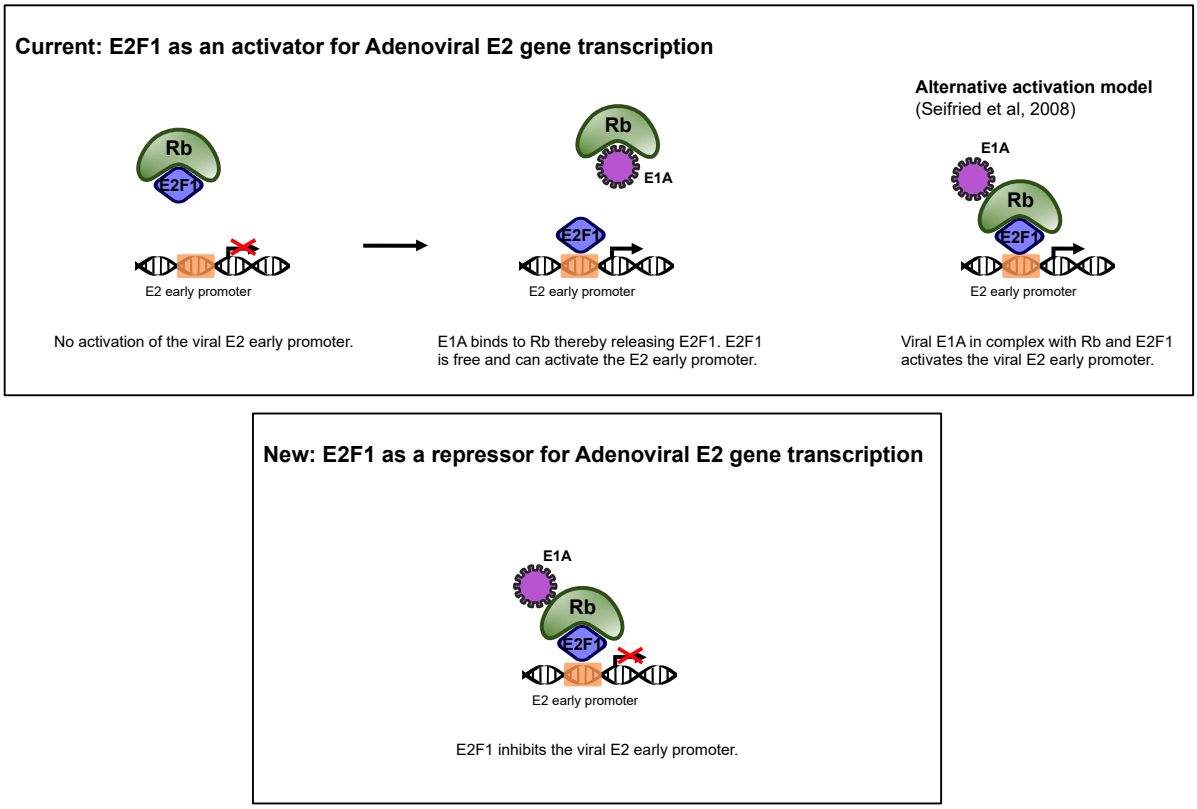

Figure 4.1.: **Proposed Model for E2 Early Promoter Activation Based on E2F1 Knockdown Studies. Top** Current view how E2F1 and Rb regulate viral E2 early promoter activity. On the right, an alternative model based on studies by Seifried et al is shown [57]. **Bottom** According to our studies, E2F1 is a repressor of E2 gene transcription. Therefore, binding of E2F1 to the E2 early promoter inhibits viral replication. For full details, see text.

4.5. Outlook

In this study we have shown that inhibition of cell cycle progression in G1-phase was beneficial for viral replication and that neither E2F1 transcription factors nor Rb pocket proteins are needed for viral replication. In addition, we provided evidence that, in contrast to the common view, E2F1 might be a repressor rather than an activator for viral replication. To further analyse transcription factors and transcription factor complexes which bind to the viral E2 early promoter in the absence of E2F1 and/or Rb, additional electrophoretic mobility shift assays (EMSA) and immuno-precipitation assays will be needed. These would help to identify viral proteins and transcription factor complexes which bind to the E2 early promoter to enhance viral replication in combination with CDK4/6 inhibitors. Importantly, these studies need to be performed using functional viruses but not plasmids.

Furthermore, proteomics and transcriptom sequencing analyses upon combination of oncolytic virotherapy with CDK4/6 inhibition will help to shed light into proteins and genes that are up- or downregulated upon this combination therapy. This would help to identify important players in this combination therapy which could be of functional importance for viral replication and Adenovirus biology in general. Moreover, these data could help to further understand the mechanism underlying the combination with CDK4/6 inhibitors which would be needed with respect to upcoming in vivo experiments and clinical trials.

In the future, in vivo experiments are planned to test the combination of XVir-N-31 with CDK4/6 inhibitors in a subcutaneous mouse model to analyse whether CDK4/6 inhibitors could improve viral effectiveness also in a 3D model. In addition, this combination therapy should then be tested in clinical trials with patients with BC and maybe also other tumour entities: XVir-N-31 is a YB-1-dependent oncolytic Adenovirus and YB-1 was shown to be associated with a poor clinical outcome in a variety of malignancies including breast, lung, prostate, liver, head and neck, and colon cancer [27, 40, 45, 68]. Moreover, the two CDK4/6 inhibitors palbociclib and ribociclib are already approved by the FDA for treatment of breast cancer [26, 47]. Thus, a combination therapy using a YB-1-dependent oncolytic Adenovirus in combination with CDK4/6 inhibitors could be a promising therapy approach for a variety of cancers.

A. Appendices

Table A.1.: Combination of Oncolytic Viruses with Standard Chemotherapeutic Drugs; reprinted from [12], Table 1, with permission from Elsevier.

Virus	Drug	Tumour origin	Viral replication	Synergy/ additivity	Mechanism other than oncolysis
Mitotic inhibitors					
Onyx-015	Paclitaxel	Lung	n.i.	Synergy	n.i.
CV787	Paclitaxel, Docetaxel	Prostate	Slightly increased	Synergy	n.i.; E1A-induced chemosensitisation?
OBP-401	Docetaxel, Vinorelbin	Different origin, lung	Unmodified	Synergy	n.i.
dl922-947	Paclitaxel	Ovary	Unmodified	n.i.	Abnormal mitosis leading to apoptosis
AdhTERT/E1A-HRE/E1B	Vincristine	Ocular	n.i.	Synergy	n.i.
Antibiotics					
Onyx-015	Doxorubicin	Thyroid	n.i.	Synergy	E1A-induced chemosensitisation?
CV980	Doxorubicin	Liver	n.i.	Synergy	n.i.
AddlE1B55	Mitomycine C	Esophagus	n.i.	Synergy	n.i.
Anti-metabolites					
Onyx-015	5-FU	Colon	n.i.	n.i.	n.i.
Onyx-015	5-FU + Leucovorin	Colon	Increased	n.a.	n.a.
OBP-301 (Telomelysin)	Gemcitabine	Lung	Unmodified	n.i.	Sensitisation to gemcitabine
Ad5/3Δ24	Gemcitabine	Ovary	Unmodified	Synergy	E1A-induced chemosensitisation?

Continued from Table A.1

Virus	Drug	Tumour origin	Viral replication	Synergy/ additivity	Mechanism other than oncolysis
AddlE1B55	5-FU	Esophagus	Unmodified	n.i.	n.i.
Platine salts					
Onyx-015	Cisplatin	Liver	n.i.	n.i.	n.a.
OBP-401 (Telomelysin)	Cisplatin	Ovary	n.i.	Additivity	n.i.
ΔE1B19K ΔE1B55K	Cisplatin	Diverse	Increased	n.i.	n.i.; E1A-induced chemosensitisation?
dl920-946-reverse-chk1, dl920-946-reverse-STAT3	Cisplatin	Diverse	n.i.	n.i.	n.i.
Alkylating agents					
Adsurvivin-E1-Fib-k7, OBP-405 or Δ24-fib-RGD	TMZ (RAD001)	Glia	Unmodified	n.i.	Autophagy, down-regulation of MGMT
Topoisomerase inhibitors					
Δ24	Irinotecan (CPT-11)	Glia	n.i.	n.i.	n.i.
ΔE1ACR2 ΔE1B19K	Irinotecan	Pancreas	Unmodified	Additivity	Apoptosis
Onyx-015	Irinotecan	Glia	Increased	n.i.	n.i.
AddlE1B55	Etoposide	Esophagus	Unmodified	Additivity	n.i.
Onyx-015	Mitoxantrone	Prostate	Unmodified	Synergy	CRAd-induced chemosensitisation

CRAd, Conditionally-replicative Adenovirus; n.a., not applicable; n.i., not investigated

Table A.2.: Combination of Oncolytic Viruses with Target Therapy; reprinted from [12], Table 2, with permission from Elsevier.

Virus	Drug	Tumour origin	Viral replication	Synergy/ additivity	Mechanism other than oncolysis
mTOR inhibitors					
Adtcf-E1AE1B	RAD001	Colon	Unmodified	n.i.	Angiogenesis inhibition
Δ24-FibRGD	RAD001	Glia	Unmodified	Synergy	Autophagy
OBP-405	Rapamycin	Glia	Unmodified	Synergy	Autophagy
Adcyc3-E1A (ΔE1B)	Rapamycin	Breast, lung	Increased	Synergy	Autophagy
dl922-947	Rapamycin	Glia	Reduced	n.a.	Autophagy inhibition
Inhibitors of other kinases					
Δ24-FibK7	Cetuximab (+5-FU + radiotherapy)	Lung	n.i.	n.i.	n.i.
AdS100A2-E1	Cetuximab	Lung, skin	n.i.	Additivity	n.i.
dl922-947	Bevacizumab	Thyroid	Increased	Additivity	Angiogenesis inhibition, drop of interstitial pressure
dl922-947	AZD1152	Thyroid	Increased	Additivity	Polyploidy, caspase-3 activation
Onyx-015	CI-1040	Colon	Reduced	n.i.	Cell cycle arrest
Inhibitors of histone deacetylases					
Telomelysin	Valproic acid, FK228	Lung	Increased	Synergy	Increased cell entry
Onyx-015	Trichostatin	Esophagus	Increased	Synergy	Increased cell entry
CN702	Valproic acid	Prostate, colon	Decreased	Antagonism	Cell cycle arrest
Δ24-FibRGD	Valproic acid	Glia	Unmodified	n.a.	n.a.
dl922-947	Valproic acid	Colon	Unmodified	n.i.	Induction of polyploidy

CRAd, Conditionally-replicative Adenovirus; n.a., not applicable; n.i., not investigated

List of Figures

List of Tables

Bibliography

[1] S. Abe, T. Kubota, Y. Otani, T. Furukawa, M. Watanabe, K. Kumai, T. Akiyama, S. Akinaga, and M. Kitajima. UCN-01 (7-hydoxystaurosporine) inhibits in vivo growth of human cancer cells through selective perturbation of G1 phase checkpoint machinery. *Jpn J Cancer Res*, 92(5):537–545, 2001.

[2] S. Ashwell and S. Zabludoff. DNA damage detection and repair pathways-recent advances with inhibitors of checkpoint kinases in cancer therapy. *Clinical Cancer Research*, 14(13):4032–4037, 2008.

[3] M. Babjuk, A. Böhle, M. Burger, E. Compérat, E. Kaasinen, J. Palou, Rouprêt M, B. van Rhijn, S. Shariat, R. Sylvester, and R. Zigeuner. Guidelines on Non-muscle invasive Bladder Cancer. *European Association of Urology*, 41(2):1–42, 2015.

[4] N. Bagheri, M. Shiina, D. A. Lauffenburger, and W. M. Korn. A Dynamical Systems Model for Combinatorial Cancer Therapy Enhances Oncolytic Adenovirus Efficacy by MEK- Inhibition. *PLOS Computational Biology*, 7(2):1–10, 2011.

[5] A. J. Berk. Adenovirus Promoters and E1A Transactivation. *Annual Review of Genetics*, 20(1):45–79, 1986.

[6] K. M. Bernt, D. S. Steinwaerder, S. Ni, Z.-y. Li, and S. R. Roffler. Enzyme-activated Prodrug Therapy Enhances Tumor-specific Replication of Adenovirus Vectors. *Cancer Research*, 62:6089–6098, 2002.

[7] A. Bieler, K. Mantwill, T. Dravits, A. Bernshausen, G. Glockzin, N. Köhler-vargas, H. Lage, B. Gansbacher, and P. S. Holm. Novel Three-Pronged Strategy to Enhance Cancer Cell Killing in Glioblastoma Cell Lines: Histone Deacetylase Inhibitor, Chemotherapy, and Oncolytic Adenovirus dl520. *Human Gene Therapy*, 17:55–70, 2006.

[8] A. Biosystems. Guide to Performing Relative Quantitation of Gene Expression Using Real-Time Quantitative PCR. pages 1–60, 2004.

[9] E. Borrelli, R. Hen, and P. Chambon. Adenovirus-2 E1A products repress enhancer-induced stimulation of transcription. *Nature*, 312:608–612, 1984.

[10] A. Bouska and C. M. Eischen. Murine double minute 2: p53-independent roads lead to genome instability or death. *Trends in Biochemical Sciences*, 34(6):279–286, 2009.

[11] A. W. Braithwaite and I. A. Russell. Induction of cell death by adenoviruses. *Apooptosis*, 6(1):359–370, 2001.

[12] C. Bressy and K. Benihoud. Association of oncolytic adenoviruses with chemotherapies: An overview and future directions. *Biochemical Pharmacology*, 90(2):97–106, 2014.

[13] M. Burger, J. W. F. Catto, G. Dalbagni, H. B. Grossman, H. Herr, P. Karakiewicz, W. Kassouf, L. A. Kiemeney, C. La Vecchia, S. Shariat, and Y. Lotan. Epidemiology and risk factors of urothelial bladder cancer. *European Urology*, 63(2):234–241, 2013.

[14] J. M. Burke, D. L. Lamm, M. V. Meng, J. J. Nemunaitis, J. J. Stephenson, J. C. Arseneau, J. Aimi, S. Lerner, A. W. Yeung, T. Kazarian, D. J. Maslyar, and J. M. McKiernan. A first in human phase 1 study of CG0070, a GM-CSF expressing oncolytic adenovirus, for the treatment of nonmuscle invasive bladder cancer. *Journal of Urology*, 188(6):2391–2397, 2012.

[15] A. A. Chakraborty and W. P. Tansey. Adenoviral E1A function through Myc. *Cancer Research*, 69(1):6–9, 2009.

[16] P.-h. Cheng, S. Lian, R. Zhao, X.-m. Rao, K. M. Mcmasters, and H. S. Zhou. Combination of autophagy inducer rapamycin and oncolytic adenovirus improves antitumor effect in cancer cells. *Virology Journal*, 10(293):1–13, 2013.

[17] G. Cheung, A. Sahai, M. Billia, P. Dasgupta, and M. S. Khan. Recent advances in the diagnosis and treatment of bladder cancer. *BMC Medicine*, 11(13):1–8, 2013.

[18] T.-c. Chou. Theoretical Basis, Experimental Design, and Computerized Simulation of Synergism and Antagonism in Drug Combination Studies. *Pharmacological Reviews*, 58(3):621–681, 2006.

[19] T. C. Chou. Drug combination studies and their synergy quantification using the chou-talalay method. *Cancer Research*, 70(2):440–446, 2010.

[20] M. Colombel, M. Soloway, H. Akaza, A. Böhle, J. Palou, R. Buckley, D. Lamm, M. Brausi, J. A. Witjes, and R. Persad. Epidemiology, Staging, Grading, and Risk Stratification of Bladder Cancer. *European Urology, Supplements*, 7(10):618–626, 2008.

[21] C. M. Connell, A. Shibata, L. A. Tookman, K. M. Archibald, M. B. Flak, K. J. Pirlo, M. Lockley, S. P. Wheatley, and I. A. McNeish. Genomic DNA damage and ATR-Chk1 signaling determine oncolytic adenoviral efficacy in human ovarian cancer cells. *Journal of Clinical Investigation*, 121(4):1283–1297, 2011.

[22] F. Dallaire, S. Schreiner, G. E. Blair, T. Dobner, P. E. Branton, and P. Blanchette. The Human Adenovirus Type 5 E4orf6/E1B55K E3 Ubiquitin Ligase Complex Enhances E1A Functional Activity. *mSphere*, 1(1):1–13, 2015.

[23] F. A. Dick and N. Dyson. pRB Contains an E2F1-Specific Binding Domain that Allows E2F1-Induced Apoptosis to Be Regulated Separately from Other E2F Activities. *Molecular Cell*, 12:639–649, 2003.

[24] M. M. Facchinetti, A. De Siervi, D. Toskos, and A. M. Senderowicz. UCN-01-Induced Cell Cycle Arrest Requires the Transcriptional Induction of p21 ^{waf1/cip1} by Activation of Mitogen-Activated Protein/Extracellular Signal-Regulated Kinase Kinase/Extracellular Signal-Regulated Kinase Pathway. *Cancer Research*, 64(10):3629–3637, 2004.

[25] J. Ferlay, I. Soerjomataram, R. Dikshit, S. Eser, C. Mathers, M. Rebelo, D. M. Parkin, D. Forman, and F. Bray. Cancer incidence and mortality worldwide: Sources, methods and major patterns in GLOBOCAN 2012. *International Journal of Cancer*, 136(5):E359–E386, 2015.

[26] R. S. Finn, A. Aleshin, and D. J. Slamon. Targeting the cyclin-dependent kinases (CDK) 4 6 in estrogen receptor-positive breast cancers. *Breast Cancer Research*, 18(1):1–11, 2016.

[27] O. Gluz, K. Mengele, M. Schmitt, R. Kates, R. Diallo-Danebrock, F. Neff, H. D. Royer, N. Eckstein, S. Mohrmann, E. Ting, M. Kiechle, C. Poremba, U. Nitz, and N. Harbeck. Y-box-binding protein YB-1 identifies high-risk patients with primary breast cancer benefiting from rapidly cycled tandem high-dose adjuvant chemotherapy. *Journal of Clinical Oncology*, 27(36):6144–6151, 2009.

[28] F. D. Goodrum and D. a. Ornelles. The early region 1B 55-kilodalton oncoprotein of adenovirus relieves growth restrictions imposed on viral replication by the cell cycle. *Journal of virology*, 71(1):548–61, 1997.

[29] G. V. Helgason, J. O. Prey, and K. M. Ryan. Oncogene induced sensitization to chemotherapy-induced death requires induction as well as de-regulation of E2F1. *Cancer Research*, 70(10):4074–4080, 2010.

[30] R. Hen, E. Borrelli, C. Fromental, P. Sassone-Corsi, and P. Chambon. A mutated polyoma virus enhancer which is active in undifferentiated embryonal carcinoma cells is not repressed by adenovirus-2 E1A products. *Nature*, 321:249–251, 1986.

[31] R. C. Hoeben and T. G. Uil. Adenovirus DNA replication. *Cold Spring Harbor perspectives in biology*, 5(3):1–11, 2013.

[32] P. S. Holm, S. Bergmann, K. Jürchott, H. Lage, K. Brand, A. Ladhoff, K. Mantwill, D. T. Curiel, M. Dobbelstein, M. Dietel, B. Gänsbacher, and H. D. Royer. YB-1 relocates to the nucleus in adenovirus-infected cells and facilitates viral replication by inducing E2 gene expression through the E2 late promoter. *Journal of Biological Chemistry*, 277(12):10427–10434, 2002.

[33] P. S. Holm, H. Lage, S. Bergmann, K. Ju, G. Glockzin, A. Bernshausen, K. Mantwill, A. Ladhoff, A. Wichert, J. S. Mymryk, T. Ritter, M. Dietel, B. Gänsbacher, and H.-D. Royer. Multidrug-resistant Cancer Cells Facilitate E1-independent Adenoviral Replication : Impact for Cancer Gene Therapy. *Cancer Research*, 64:322–328, 2004.

[34] R. Holzmüller, K. Mantwill, C. Haczek, E. Rognoni, M. Anton, A. Kasajima, W. Weichert, D. Treue, H. Lage, T. Schuster, J. Schlegel, B. Gänsbacher, and P. S. Holm. YB-1 dependent virotherapy in combination with temozolomide as a multimodal therapy approach to eradicate malignant glioma. *International Journal of Cancer*, 129(5):1265–1276, 2011.

[35] K. Homicsko, A. Lukashev, and R. D. Iggo. RAD001 (Everolimus) Improves the Efficacy of Replicating Adenoviruses that Target Colon Cancer. *Cancer Research*, 65(15):6882–6891, 2005.

[36] Human adenovirus c serotype 2, viralzone 2015, swiss institute of bioinformatics. `http://viralzone.expasy.org/3256`. last viewed 16.08.2018.

[37] C. K. Ingemarsdotter, L. A. Tookman, A. Browne, K. Pirlo, R. Cutts, C. Chelela, K. F. Khurrum, E. Y. L. Leung, S. Dowson, L. Webber, I. Khan, D. Ennis, N. Syed, T. R. Crook, J. D. Brenton, M. Lockley, and I. A. Mcneish. Paclitaxel resistance increases oncolytic adenovirus efficacy via upregulated CAR expression and dysfunctional cell cycle control. *Molecular Oncology*, 9(4):791–805, 2015.

[38] J. Kim. Immune checkpoint blockade therapy for bladder cancer treatment. *Investigative and clinical urology*, 57(1):98–105, 2016.

[39] M. A. Knowles and C. D. Hurst. Molecular biology of bladder cancer: new insights into pathogenesis and clinical diversity. *Nature Reviews Cancer*, 15(1):25–41, 2015.

[40] A. Kolk, N. Jubitz, K. Mengele, K. Mantwill, O. Bissinger, M. Schmitt, M. Kremer, and P. S. Holm. Expression of Y-box-binding protein YB-1 allows stratification into long-and short-term survivors of head and neck cancer patients. *British Journal of Cancer*, 105(12):1864–1873, 2011.

[41] I. Kovesdi, R. Reichel, and J. R. Nevins. Role of an adenovirus E2 promoter binding factor in E1A-mediated coordinate gene control. *Proceedings of the National Academy of Sciences of the United States of America*, 84(8):2180–4, 1987.

[42] S. Libertini, A. Abagnale, C. Passaro, G. Botta, S. Barbato, P. Chieffi, and G. Portella. AZD1152 negatively affects the growth of anaplastic thyroid carcinoma cells and enhances the effects of oncolytic virus dl922-947. *Endocrine-Related Cancer*, 18:129–141, 2011.

[43] K. Mantwill, N. Köhler-vargas, A. Bernshausen, K. Mantwill, N. Ko, A. Bernshausen, A. Bieler, H. Lage, A. Kaszubiak, P. Surowiak, T. Dravits, U. Treiber, and R. Hartung. Inhibition of the Multidrug-Resistant Phenotype by Targeting YB-1 with a Conditionally Oncolytic

Adenovirus : Implications for Combinatorial Treatment Regimen with Chemotherapeutic Agents. *Cacner Research*, 66:7195–7202, 2006.

[44] F. Martelli and D. M. Livingston. Regulation of endogenous E2F1 stability by the retinoblastoma family proteins. *Proceedings of the National Academy of Sciences of the United States of America*, 96(6):2858–2863, 1999.

[45] P. K. Maurya, A. Mishra, B. S. Yadav, S. Singh, P. Kumar, A. Chaudhary, S. Srivastava, S. N. Murugesan, and A. Mani. Role of Y box protein-1 in cancer: As potential biomarker and novel therapeutic target. *Journal of Cancer*, 8(10):1900–1907, 2017.

[46] R. Nawroth, F. Stellwagen, W. A. Schulz, R. Stoehr, A. Hartmann, B. J. Krause, J. E. Gschwend, and M. Retz. S6k1 and 4E-BP1 are independent regulated and control cellular growth in bladder cancer. *PLoS ONE*, 6(11):1–11, 2011.

[47] Q. Pan, A. Sathe, P. C. Black, P. J. Goebell, A. M. Kamat, B. Schmitz-Draeger, and R. Nawroth. CDK4 6 Inhibitors in Cancer Therapy A Novel Treatement Strategy for Bladder Cancer. *Bladder Cancer*, 3(2):79–88, 2017.

[48] P. Pelka, M. S. Miller, M. Cecchini, A. F. Yousef, D. M. Bowdish, F. Dick, P. Whyte, and J. S. Mymryk. Adenovirus E1A Directly Targets the E2F/DP-1 Complex. *Journal of Virology*, 85(17):8841–8851, 2011.

[49] M. W. Pfaffl. A new mathematical model for relative quantification in real-time RT-PCR. *Nucleic Acids Research*, 29(9):2002–2007, 2001.

[50] N. Ramesh, Y. Ge, D. L. Ennist, M. Zhu, M. Mina, S. Ganesh, P. S. Reddy, and D. C. Yu. CG0070, a conditionally replicating granulocyte macrophage colony-stimulating factor - Armed oncolytic adenovirus for the treatment of bladder cancer. *Clinical Cancer Research*, 12(1):305–313, 2006.

[51] E. Rognoni, M. Widmaier, C. Haczek, K. Mantwill, R. Holzmüller, B. Gansbacher, A. Kolk, T. Schuster, R. M. Schmid, D. Saur, A. Kaszubiak, H. Lage, and P. S. Holm. Adenovirus-based virotherapy enabled by cellular YB-1 expression in vitro and in vivo. *Cancer Gene Therapy*, 16(10):753–763, 2009.

[52] W. C. Russell. Adenoviruses: Update on structure and function. *Journal of General Virology*, 90(1):1–20, 2009.

[53] M. D. Sachs, M. Ramamurthy, H. Van Der Poel, T. J. Wickham, M. Lamfers, W. Gerritsen, W. Chowdhury, Y. Li, M. P. Schoenberg, and R. Rodriguez. Histone deacetylase inhibitors upregulate expression of the coxsackie adenovirus receptor (CAR) preferentially in bladder cancer cells. *Cancer Gene Therapy*, 11(7):477–486, 2004.

[54] M. Santamariña, G. Hernández, and J. Zalvide. CDK redundancy guarantees cell cycle progression in Rb-negative tumor cells independently of their p16 status. *Cell Cycle*, 7(13):1962–1972, 2008.

[55] A. Sathe, N. Koshy, S. C. Schmid, M. Thalgott, S. M. Schwarzenböck, B. J. Krause, P. S. Holm, J. E. Gschwend, M. Retz, and R. Nawroth. CDK4/6 Inhibition Controls Proliferation of Bladder Cancer and Transcription of RB1. *Journal of Urology*, 195(3):771–779, 2016.

[56] B. Segura-Pacheco, B. Avalos, E. Rangel, D. Velazquez, and G. Cabrera. HDAC inhibitor valproic acid upregulates CAR in vitro and in vivo. *Genetic Vaccines and Therapy*, 5(10):6–13, 2007.

[57] L. a. Seifried, S. Talluri, M. Cecchini, L. M. Julian, J. S. Mymryk, and F. a. Dick. pRB-E2F1 complexes are resistant to adenovirus E1A-mediated disruption. *Journal of virology*, 82(9):4511–20, 2008.

[58] J. B. Shah, D. J. McConkey, and C. P. Dinney. New strategies in muscle-invasive bladder cancer: On the road to personalized medicine. *Clinical Cancer Research*, 17(9):2608–2612, 2011.

[59] S. L. Shankar, M. Krupski, B. Parashar, C. Okwuaka, K. O'Guin, S. Mani, and B. Shafit-Zagardo. UCN-01 alters phosphorylation of Akt and GSK3-beta and induces apoptosis in six independent human neuroblastoma cell lines. *Journal of Neurochemistry*, 90(3):702–711, 2004.

[60] S. G. Smith and D. A. Zaharoff. Future directions in bladder cancer immunotherapy: towards adaptive immunity. *Immunotherapy*, 8(3):351–365, 2016.

[61] K. Sugiyama, T. Akiyama, M. Shimizu, T. Tamaoki, C. Courage, A. Gescher, and S. Akinaga. Decrease in susceptibility toward induction of apoptosis and alteration G1 in checkpoint function as determinants of resistance of human lung cancer cells against the antisignaling drug UCN-01 (7-hydroxystaurosporine). *Cancer Research*, 59(17):4406–4412, 1999.

[62] S. Swaminathan and B. Thimmapaya. Transactivation of adenovirus E2-early promoter by E1A and E4 6/7 in the context of viral chromosome. *Journal of molecular biology*, 258(5):736–46, 1996.

[63] S. Taguchi, H. Fukuhara, Y. Homma, and T. Todo. Current status of clinical trials assessing oncolytic virus therapy for urological cancers. *International Journal of Urology*, 24(5):1–10, 2017.

[64] M. Tarrado-Castellarnau, P. de Atauri, J. Tarrago-Celada, J. Perarnau, M. Yuneva, T. M. Thomson, and M. Cascante. De novo MYC addiction as an adaptive response of cancer cells to CDK4/6 inhibition. *Molecular Systems Biology*, 13(94):1–15, 2017.

[65] B. Täuber and T. Dobner. Molecular regulation and biological function of adenovirus early genes: The E4 ORFs. *Gene*, 278(1-2):1–23, 2001.

[66] H. E. Wade, S. Kobayashi, M. L. Eaton, M. S. Jansen, E. K. Lobenhofer, M. Lupien, T. R. Geistlinger, W. Zhu, J. R. Nevins, M. Brown, D. C. Otteson, and D. P. McDonnell. Multimodal Regulation of E2F1 Gene Expression by Progestins. *Molecular and Cellular Biology*, 30(8):1866–1877, 2010.

[67] E. M. Walsh, M. Niu, J. Bergholz, and Z.-X. Jim Xiao. Nutlin-3 down-regulates Retinoblastoma protein expression and inhibits muscle cell differentiation. *Biochemical and Biophysical Research Communications*, 461(2):293–299, 2015.

[68] X. Wang, X.-B. Guo, X.-C. Shen, H. Zhou, D.-W. Wan, X.-F. Xue, Y. Han, B. Yuan, J. Zhou, H. Zhao, Q.-M. Zhi, and Y.-T. Kuang. Prognostic role of YB-1 expression in breast cancer: a meta-analysis. *International journal of clinical and experimental medicine*, 8(2):1780–91, 2015.